Channel Access Management in Data Intensive Sensor Networks

by

Chih-Kuang Lin

B.S. of Computer Information System, San Francisco State University, 1998

M.S. of Telecommunications, University of Colorado (Boulder), 2000

Submitted to the Graduate Faculty of

the School of Information Science in partial fulfillment

of the requirements for the degree of

Doctor of Philosophy

University of Pittsburgh

2008

UNIVERSITY OF PITTSBURGH

THE SCHOOL of INFORMATION SCIENCE

This dissertation was presented

by

Chih-Kuang Lin

It was defended on

July 23, 2008

and approved by

Prof. Richard A. Thompson, Telecommunications Program

Prof. Martin B.H. Weiss, Telecommunications Program

Prof. Vladimir Oleshchuk, Department of Information and Communication Technology

Co-advisor: Prof. Vladimir Zadorozhny, Department of Information Science

Dissertation Proposal Director/Co-advisor: Prof. Prashant Krishnamurthy,

Telecommunications Program

Copyright © by Chih-Kuang Lin

2008

Channel Access Management in Data Intensive Sensor Networks

Chih-Kuang Lin

University of Pittsburgh, 2008

There are considerable challenges for channel access in Data Intensive Sensor Networks – DISN, supporting Data Intensive Applications like Structural Health Monitoring. As the data load increases, considerable degradation of the key performance parameters of such sensor networks is observed. Successful packet delivery ratio drops due to frequent collisions and retransmissions. The data glut results in increased latency and energy consumption overall. With the considerable limitations on sensor node resources like battery power, this implies that excessive transmissions in response to sensor queries can lead to premature network death. After a certain load threshold the performance characteristics of traditional WSNs become unacceptable. Research work indicates that successful packet delivery ratio in 802.15.4 networks can drop from 95% to 55% as the offered network load increases from 1 packet/sec to 10 packets/sec. This result in conjunction with the fact that it is common for sensors in an SHM system to generate 6-8 packets/sec of vibration data makes it important to design appropriate channel access schemes for such data intensive applications.

In this work, we address the problem of significant performance degradation in a special-purpose DISN. Our specific focus is on the medium access control layer since it gives a fine-grained control on managing channel access and reducing energy waste. The goal of this dissertation is to design and evaluate a suite of channel access schemes that ensure graceful performance degradation in special-purpose DISNs as the network traffic load increases.

First, we present a case study that investigates two distinct MAC proposals based on random access and scheduling access. The results of the case study provide the motivation to develop hybrid access schemes. Next, we introduce novel hybrid channel access protocols for DISNs ranging from a simple randomized transmission scheme that is robust under channel and topology dynamics to one that utilizes limited topological information about neighboring sensors to minimize collisions and energy waste. The protocols combine randomized transmission with heuristic scheduling to alleviate network performance degradation due to excessive collisions and retransmissions. We then propose a grid-based access scheduling protocol for a mobile DISN that is scalable and decentralized. The grid-based protocol efficiently handles sensor mobility with acceptable data loss and limited overhead. Finally, we extend the randomized transmission protocol from the hybrid approaches to develop an adaptable probability-based data transmission method. This work combines probabilistic transmission with heuristics, i.e., Latin Squares and a grid network, to tune transmission probabilities of sensors, thus meeting specific performance objectives in DISNs. We perform analytical evaluations and run simulation-based examinations to test all of the proposed protocols.

TABLE OF CONTENTS

LIST OF TABLES

LIST OF FIGURES

LIST OF ABBREVIATIONS

APT	Adaptable Probabilistic Transmission
BCD	Blind Concurrent Transmission Degree
BS	Base Station
CAIG	Collision Avoidance near Intersection of Grid Cells
CAP	Contention Access Period
CBR	Constant Bit Rate
CD	Collision Degree
CDMA	Code Division Multiple Access
CPT	Cyclic Probabilistic Transmission
CSMA/CA	Carrier Sense Multiple Access / Collision Avoidance
DF	Delay Factor
DIA	Data Intensive Application
DISN	Data Intensive Sensor Network
DRAND	Distributed Randomized TDMA Scheduling Algorithm
DTA	Data Transmission Algebra
DTMC	Discrete Time Markov Chain
ECSP	Energy Consumption for a Successful Packet
EF	Energy Factor

FDMA	Frequency Division Multiple Access
GS	Grid Search
GLASS	Grid-based Latin Square Scheduling Access
HC	Hop count
LS	Latin Square
LSM	Latin Square Matrix
M2M	Machine-to-Machine
MEMS	Micro-electro Mechanical Systems
NAPT	Neighbor Aware Probabilistic Transmission
ND	Neighbor Discovery
PP	Probabilistic Process
PR	Packet Reliability
RT	Response Time
SHM	Structural Health Monitoring
SPT	Successful Percentage of Transmission
STF	Sub Transmission Frame
STGR	Supported Traffic Generation Rate
TDMA	Time Division Multiple Access
TF	Transmission Frame
TPM	Transmission Probability Matrix
TS	Time Slot
TSSD	Time Slot Schedule and Dissemination
VLS	Value of a Cell of Latin Square Matrix

WLAN	Wireless Local Area Network
WSN	Wireless Sensor Network

PREFACE

First and foremost, I earnestly thank my co-advisors, Prof. Prashant Krishnamurthy and Prof. Vladimir Zadorozhny, for accepting me as their doctoral student and guiding me through all these years. I learned how to do research from them. Specifically, Prof. Zadorozhny has guided, encouraged and inspired me throughout the course of my doctoral research. Without his continuous and valuable support, this dissertation would not have been completed. Prof. Krishnamurthy always spent the time to consult with me, offering important comments and suggestions on my study, research, and other aspects of life. I truly appreciate his kindness for academic and financial support and his inspiration for further improving my research. With such endearing and encouraging mentors, I find the pursuit for the Ph.D. more rewarding than I thought, and has even significantly broadened my view of satisfaction while considering a career.

Prof. Vladimir Oleshchuk, Prof. Richard Thompson, and Prof. Martin Weiss have kindly served on my dissertation committee and provided insightful comments and advice on various aspects of the dissertation.

I am also very thankful for the support of the Graduate Telecommunication Program at the University of Pittsburgh. I have profoundly learned the different subjects related to Telecommunications from foundations to system prospects. In addition, I would like to thank Prof. Thompson and Prof. Weiss for the financial support during my study in the program.

My thanks to fellows in the *Network-Aware Data Management* group (NADM) and to all friends in Pittsburgh: your valuable feedback and friendship enrich my work and life here. Thank you!

Last but not least, I would like to extend my appreciation to my parents and to my brothers in Taiwan. Their faith and constant support have accompanied me in each and every step of my graduate study. Thank You!

1.0 INTRODUCTION

With the emergence of *micro-electro mechanical systems* (MEMS)[1] technology over the last two decades, a smart device such as a sensor or actuator has seen reductions in cost even as the hardware components (processor, memory and transceiver) get smaller in size to the point where they can now be embedded in a single chip. These developments make sensors light-weight and possibly mobile while maintaining an adequate computing and communications capability. A cost-effective and realistic *Wireless Sensor Network* (WSN) thus can now be utilized for a wide range of applications such as environmental monitoring, habitat sensing, health care assistance, structural health monitoring…, etc [2] [3] [5]. These applications apply *machine-to-machine* (M2M) communications, i.e., sensor-to-sensor communications, to assist the application objective or scientific research so that they will considerably impact future human society. IBM's Zurich Research Laboratory perceives that "in a few years, PC, PDAs, and cell phones will be outnumbered by sensor and actuators. New forms of M2M communication will emerge and enable a plethora of new services and applications [4]". Statistics from the Wireless Data Research Group shows that the market for hardware, software, and professional and wireless network services for M2M communications will grow at a 27% annual rate, expanding from $9.3 billion in 2004 to $31 billion in 2008 [6]. FocalPoint Group's

[1] MEMS device is a miniature structure fabricated on silicon substrates in a similar manner to silicon integrated circuits. However, unlike electronic circuits, these are mechanical devices. [1]

research [7] revealed a survey about expected growth of M2M adoption in 2003. North American innovators of M2M technology who were surveyed foresaw a 40% growth rate in their customers' device deployments over the next 18 months. Over 60% of these innovators anticipated over 50% growth in their revenues in the next six months. Some market forecasts [3] [6] [7] report that the M2M communication using sensor networks is the next wave of technology expansion after the success of the PC and cell phone.

While the increasing popularity of WSNs is highly anticipated, many of these wireless sensor applications need to support high traffic loads during their operations (e.g., *Structural Health Monitoring* (SHM) [19] is one such data intensive application). This dissertation aims to investigate the challenges in channel access that are posted by special-purpose data intensive sensor networks, to develop novel channel access mechanisms, and to methodically demonstrate the feasibility and benefits of the proposed work.

The rest of this dissertation is organized as follows. Chapter 1 covers some background and challenges of data intensive wireless sensor networks. In addition, the research goal and contributions of this dissertation are explained here. Chapter 2 presents a review of previous literature which covers the medium access schemes of wireless sensor networks. A taxonomy of MAC alternatives is included in this chapter and used to explain the background material necessary for the rest of the dissertation. In Chapter 3, exploratory analysis of existing channel access approaches is presented. This part of the dissertation identifies features of random access and scheduling access schemes and evaluates their performances under different networking conditions. Chapter 4 describes the novel hybrid access approach that combines random channel access with heuristic-based scheduling to avoid possible collisions in the special-purpose DISNs. The performance of the proposed protocol is evaluated via analysis and simulation-based study.

Chapter 5 presents a distributed grid-based scheduling access scheme, which mitigates high data loss in special-purpose DISNs. An analytical proof of conflict-free data delivery is demonstrated. Simulation-based evaluations are used to validate its performance in a variety of network topologies. An execution of a comparative study that assesses performances of the proposed technique and other advanced channel access protocols is presented. Chapter 6 describes the concept of adaptable channel access in data intensive sensor networks. The objective is to develop a uniform channel access framework that can handle different sensor application's requirements. We propose an analytical model to estimate network behavior with adaptable channel access and use simulation-based study to evaluate network performance. Finally, the contributions and future research directions are discussed in Chapter 7.

1.1 BACKGROUND

Nowadays sensor networks are being deployed for a wide range of applications, such as structure monitoring, habitat sensing, target tracking, etc. Meanwhile, existing Wireless Sensor Networks perform poorly when the applications have high bandwidth needs for data transmission and stringent delay constraints. Such requirements are common for *Data Intensive Applications* (DIAs). An example of a DIA that utilizes a WSN infrastructure is one related to the task of Structural Health Monitoring [18] [19] (concerned with monitoring the integrity of civil and military structures). Wireless sensors observe excitations around a surveillance structure, perform data gathering, and periodically report sensed data to a *Base Station* (BS) where the sensed data is processed. Another example of a DIA is the near-continuous monitoring (every

two seconds) of heat exchangers in a nuclear power plant. Such applications may generate considerable network load in a short period of time.

In addition to the specific characteristic of intensive data communication, data intensive sensor networks also inherit fundamental features of wireless sensor networks as described below.

Scalability: The number of deployed nodes in WSN can be multiple orders of magnitude more than the number of nodes in Wireless Local Area Networks (WLAN). Thus, maintaining a scalable and distributed access scheme is important for sensor networks.

Energy: The battery used in sensors mostly stores less energy because of low costs, size and hardware limit. Besides, the physical environment may not allow humans to easily replenish the batteries of sensors. Consequently, the energy constraint is critical.

Data Centric: Sensors' operations are based on received queries, which specify requests of interesting data. For instance, a query can be applied to all sensors to report the recorded rain fall greater than 50 centimeters. Thus, the delivered data correspond to an event instead of a sensor. Other wireless system, likes WLAN, is different in that the network is node-centric where a specific node may attempt to access some web servers that host useful information. Thus, the importance of a node in WLANs is higher than in WSNs. In other words, a WSN is commonly dedicated to a particular mission or multiple missions where all sensors try to accomplish the task as a team.

Application Explicit: WSN can support different applications in dynamic environments. These applications present various networking features (e.g., traffic pattern, mobility, node density …, etc). It is unlikely that a universal solution is available to address the requirements of all applications. Some research proposed that the sensor communication protocols be application-

specific [9]. In the same vein, the research in this dissertation explicitly focuses on data intensive sensor applications.

Simplicity: The cost of a sensor is expected to be low [77] [78] and so the sensor's software needs to be simple, the hardware should be compact and the energy in the battery is a scarce resource. These limitations force the protocol stack of a sensor to be simple and precise, compared with that of a general purpose wireless computing device.

A *Data Intensive Sensor Network* (DISN) consists of all of the above stated features. The following section will illustrate the constraints of current DISNs that motivate the research work of this dissertation.

1.2 CONSTRAINTS OF DATA INTENSIVE SENSOR NETWORKS

There are considerable challenges in efficient utilization of DISNs. Figure 1-1 (a) summarizes the key characteristics of DISNs. This figure *qualitatively* presents the performance of DISNs with the current IEEE 802.15.4 standard. As the data load increases, we observe considerable performance degradation of the key performance parameters of WSNs. The packet success ratio drops due to frequent collisions and retransmissions. The data glut results in increased time delay and overall energy consumption. After a certain load threshold, the performance characteristics of the WSN become unacceptable. A previous study [19] reported that the successful packet delivery ratio in an 802.15.4 network can drop from 95% to 55% as the load increases from 1 packet/sec to 10 packets/sec (see Figure 1-1 (b)). Note that it is common for sensors in an SHM system to generate 6-8 packets/sec of vibration data. The residence time for a packet in a medium-scale multi-hop WSN could be tens of seconds, making

the latency unacceptable for critical monitoring tasks. Further, considerable limitations on sensor node resources like battery power imply that excessive transmissions in response to sensor queries can lead to premature network death.

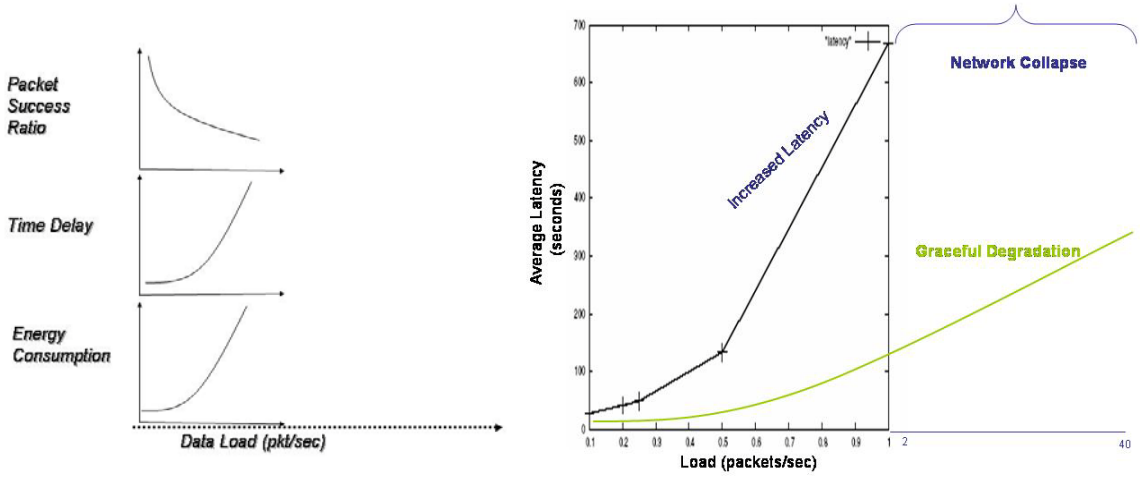

(a) (b)

Figure 1-1 (a) Significant Performance Degradation in DISNs (b) Effects of Collision and Retransmission [19]

We approach this from a data centric view of WSNs. Since applications of sensor networks always require coordination of the whole sensor network to complete a mission, network utility and resources (e.g., energy and bandwidth) of the whole network degrade if considerable information delivered towards the BS is incorrect and results in system failure. Degradation in terms of losing data in WSNs is more severe than in other wireless networks like WLANs or cellular phone systems. Maintaining reliable data delivery in DISNs thus is the primary concern of this research.

Another concern in addition to the unreliable data delivery is the overall energy consumption of all sensors. The energy is also a constraint in sensors networking because of limited battery resource. To cope with the energy constraint issue, we first recognize the main

sources of power consumption and discover where inefficient uses of power are. The sources of power consumption, with regard to network operations can be classified into two types: communication related and computation related [30]. The power consumption in communications involves power usage from the transmitter and receiver in operating nodes. On the other hand, the power consumption of computing functions is related to protocol processing in processors, memory, hard disk, and auxiliary hardwares. In Stemm and Feeney's study, it is shown that a majority of power is consumed by the communications related functions [31] [32]. So reducing energy consumption in communication functions becomes an inevitable path to reach the goal of energy efficiency. Our research also considers this idea in its design by pushing communication overheads to in-network processing.

There are four major types of energy wastes in communication functions. The first one is collisions, and it occurs when two transmitted packets arrive at the same destination at the same or overlapping times. In such cases, the packets are corrupted and discarded. Re-transmissions of discarded packets increase energy consumption as well as latency. Overhearing is the second source of energy waste. Here, a node receives packets that are destined to other nodes. The third source of energy waste is overhead. Transmitting or receiving control packets consumes energy unnecessarily. The final source of energy waste is idle listening. It refers to situations where a receiver is listening to the medium but receives no traffic. In the CSMA scheme, nodes have to listen to the channel to receive possible traffic for virtual carrier sensing. If a network is inactive for a long period, the power consumption in idle listening will be dominant, and this energy is wasted. The results from [31] and [33] have shown that a significant portion of energy consumption is due to idle listening in ad hoc networks. For the case of DIAs in sensor networks,

energy waste from the collision and the retransmission is the primary concern [19] [62] [63]. We focus on this issue in the dissertation.

1.3 EXISTING LITERATURE AND RESEARCH OPPORTUNITY

The issue of performance degradation in DISNs can be addressed at different layers of the protocol stack. Our specific focus is the channel access function in the *Medium Access Control* (MAC) layer where fine-grained control can reduce collided transmissions and energy waste [29].

The channel access schemes of wireless sensor networks can be divided into two categories: Random access and Scheduling access. *Carrier Sense Multiple Access / Collision Avoidance* (CSMA/CA) is a popular random access contention-based MAC scheme, which has been adopted in accepted wireless standards, such as IEEE 802.11 and IEEE 802.15.4. With CSMA/CA, the channel access is distributed. However, the performance of CSMA/CA degrades as the load increases [19] [34]. One reason behind this phenomenon is the hidden terminal problem where a node is unable to sense the transmission of another node in the same collision domain. To address the hidden terminal problem, control request to send/clear to send (RTS/CTS) handshakes are employed in IEEE 802.11. However, the RTS/CTS handshakes can improve system performance only when large data frames are used. In most data gathering tasks in sensor networks, the data frames generated by sensors are small. Thus, the RTS/CTS control frames may further worsen the performance by increasing channel contention. Moreover, this option is not available in IEEE 802.15.4. Recently, scheduling-based mechanisms [62] [63] [80] have been proposed to alleviate the poor performance of CSMA/CA at intensive data loads.

These approaches, however, lack robustness to changes in the network (e.g., interference or topology changes) or have drawbacks such as increased overhead and problems in scalability in creating schedules. Hybrid approaches enabling graceful degradation are preferable [82], but they share similar issues as scheduling-based approaches.

1.4 RESEARCH GOALS

Taking into consideration the challenges detailed in the previous sections, this dissertation has proposed efficient and scalable channel access techniques to maintain graceful performance degradation in DISNs as the data load increases. In particular, we propose lightweight distributed data delivery algorithms that utilize probabilistic transmission and scheduling based on heuristic strategies in order to meet the high performance requirements of DIAs. Our **research goal** aims at keeping sufficient packet delivery reliability while maintaining reasonably low energy consumption by avoiding excessive collisions and overhead. Our motivation for this stems from the work in scheduled access using *Data Transmission Algebra* (DTA) [62] [63] [84]. At one end of the spectrum, we have CSMA/CA. The performance with CSMA/CA is poor because of collisions during periods of high data loads. This is caused by several sensor nodes transmitting at the same time, despite the backoff mechanisms embedded in CSMA/CA. At the other end of the spectrum, we can ensure that no two transmissions in the network occur at the same time (we refer to this as serial transmission). While this approach saves on the energy waste due to collisions, it increases latency since *concurrency opportunities* (where multiple transmissions that do not interfere are possible at the same time) are not exploited. DTA is a centralized approach for creating *optimal* schedules that exploit concurrency

opportunities. In this work we propose distributed or decentralized protocols that exploit potential concurrency opportunities.

1.5 ESSENCE OF PROPOSED STUDY

This dissertation is an organized study of channel access management based on the probabilistic access and the heuristic scheduling. Opening with an exploratory analysis of random access vs. scheduling access, constraints and benefits of CSMA/CA and DTA for data intensive sensor networks are illustrated and used to setup motivations for the idea of hybrid channel access. Next, a hybrid transmission scheme based on probabilistic access and a distributed scheduling algorithm using neighbor information is proposed. The main purpose here is to deliver dependable data with minimum overhead in a scalable and distributed way. Through the exploratory analysis and the hybrid transmission proposal, we further understand existing challenges in DISNs and the current work so we proceed to propose a grid-based access scheduling protocol. The new design will inherit the framework of the initial hybrid transmission protocol with additional features based on Latin Squares Characteristics[2] to alleviate local collisions and a virtual grid structure to enhance scalability and to reduce collisions furthermore. Lastly, we introduce the concept of an adaptable channel access framework. It combines the Latin Squares Characteristics and the grid idea with the probabilistic access to tune a channel access mechanism meeting different sensor application's requirements. This new concept is

[2] A Latin Square may be thought of as a two-dimensional analogue of a permutation. Specifically, *a Latin Square of order n* is an $n \times n$ array in which n distinct symbols are arranged so that each symbol occurs once in each row and column. [75]

preliminarily investigated in this dissertation and, subsequently, we identify potential research topics in the future.

1.6 RESEARCH CONTRIBUTIONS

Our goal is to develop distributed mechanisms to exploit concurrency opportunities. In addition, the proposed schemes are scalable and the overhead of generating schedules is not very significant. We consider four methods towards understanding research challenges and then achieving this goal.

1) Channel access techniques are generally classified into two approaches: random access and scheduling access. It is essential to learn benefits and weaknesses of both the approaches in order to help us design a more feasible channel access scheme in DISNs. We thus perform a case study to analyze random access (such as CSMA/CA) and scheduling access (such as DTA) schemes. This work is described in Chapter 3.

2) We investigate the concept of hybrid channel access and propose the following two schemes. The *Cyclic Probabilistic Transmission* protocol (CPT) performs data transmissions based on predefined probabilities of transmission in time slots. The CPT protocol maintains a *Transmission Probability Matrix* (TPM) in each sensor node. Each element of the matrix holds a probability of a data transmission between a pair of sensors within a given time slot. The TPM specifies one network transmission cycle. In this case, every sensor is only aware of its own transmission probability in fixed time slots. Consequently, each sensor's channel access method is distributed and simple. The second approach, called *Neighbor Aware Probabilistic Transmission* protocol (NAPT), combines the probabilistic transmission used in CPT with a

“heuristic-based” scheduling that makes use of (limited) topological information (mainly the density of sensor neighbors). In densely populated areas where collisions are highly probable, information about neighbors is used to reduce the chances of collisions (e.g., by delivering data sequentially or in a serial manner). Chances of collisions are determined using local information obtained from neighboring sensors. Overall, the network performance of CPT and NAPT is better than that of CSMA/CA in DISNs. However, both CPT and NAPT still suffer from certain data loss because of probable colliding transmissions from neighboring sensors. This work is described in Chapter 4.

3) We propose the *Grid-based Latin Square Scheduling Access* protocol (GLASS) next. It is a distributed access scheme that alleviates transmission collisions by applying a virtual grid in a network and adopting Latin Square Characteristics to time slot assignments. The design of a virtual grid network spatially divides the sensors within collision range to avoid potential collisions while maintaining maximum spatial reuse. The *Latin Squares* function is used to facilitate the assignment of time slots for transmission among sensors within a grid cell, thus reducing the number of colliding transmissions further. This design demonstrates acceptable transmission efficiency in DISNs. Moreover, it efficiently handles sensor mobility with low overhead. This work is described in Chapter 5.

4) Section 1.1 explains the application explicit feature in WSNs, and such feature may lead sensor communication protocols to be application-specific. Nevertheless, building a uniform channel access mechanism, which is adaptable to different sensor application’s requirements, can be beneficial from an economical and flexibility standpoint. Simultaneously, this mechanism should use simple tuning efforts to achieve adjustable channel access functionality. We adopt the ideas of a grid network, Latin Squares, and probabilistic access to tune the channel access

scheme. The Latin Square algorithm is used to locally tune transmission probabilities of sensors in the time domain. The tuning process for the transmission probabilities results in different tradeoffs between data collisions and concurrency opportunities, or in other words, different tradeoffs between transmission efficiency, energy efficiency, and latency. The whole access process is light-weight, distributed, and scalable. This work is described in Chapter 6.

We consider analytical and simulation methods to validate all the proposed work and demonstrate the benefits and feasibility of our techniques. We compare our approaches to IEEE 802.15.4's CSMA/CA and a recently-developed distributed time-division approach called DRAND [80] in terms of transmission efficiency, energy efficiency, scalability, latency, and overhead cost. The star tree and random mesh topologies are chosen to represent networks with high traffic load in this study since the DIAs, like close supervision of nuclear power plants and structural health monitoring, both adopt the above topologies in their deployments. In lieu of a quasi-periodic traffic model, we use a Constant Bit Rate model (CBR), to generate intensive data communication in WSNs. CBR traffic from sensor nodes resulting in large numbers of concurrent data transmissions from different sensors within a short period of time. Although we often observe intensive and bursty traffic pattern in operation in a realistic sensor network, our defined traffic model (CBR) is fit to evaluate feasibility of the considered channel access protocols in a DISN due to the reproduction of an intensive traffic scenario. In future work, we can consider the apt approach to mimic bursty intensive traffic. Note that the transmission efficiency, which is the focus of the work in this dissertation, can be expected to be independent of the actual traffic patterns. In addition, all the considered schemes evaluate the side effects created by changes in a network topology. The expected utility of the proposed protocols should increase under higher data loads (Figure 1-2). We aim at maintaining a sufficient packet delivery

reliability while having a reasonably low energy cost by avoiding excessive collisions and overhead. The utility shown in Figure 1-2 is again a qualitative expression of the expected performance of the protocols.

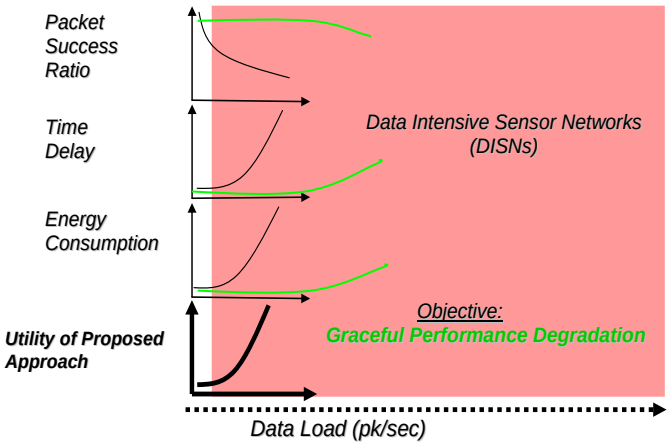

Figure 1-2 Utility of the Proposed Approach

2.0 LITERATURE REVIEW

This chapter reviews the literature that is closely related to this dissertation. Different medium access mechanisms of wireless ad hoc networks and wireless sensor networks are considered here. Meanwhile, the reviewed works aim at reducing energy consumption in network communications and alleviating the energy waste. The reviewed papers in the literature provide positive network performance, but they may result in increased delay, need complex synchronization, require extra overhead, or result in low utilization of bandwidth. Potential tradeoffs thus co-exist in these researches.

Channel access research can be classified according to their time synchronization, access schemes or network infrastructure. Time synchronization refers to the time coordination of all nodes in a network, while the access schemes refer to the various access approaches. Figure 2-1 shows a taxonomy of channel access research with respect to WSNs. In the taxonomy, unique networking characteristics (e.g., deterministic and randomness) correspond to running different access schemes (e.g., random access and scheduling access). The network utility therefore is different. The case study in Chapter 3 will provide a comparison of the performance of random access and scheduling access while the work in Chapters 4, 5, and 6 will validate the performance of our proposed techniques in DISNs. The remainder of this chapter will cover proposals of different categories in synchronous networks.

2.1 SYNCHRONOUS NETWORK COMMUNICATION

Synchronous communication (sometimes loosely synchronous) is adopted in many communication systems like cellular systems (IS-95 and GSM), the Internet or wireless LANs. It is widely accepted because time synchronization allows for reservations made by a node are known to the node's neighbors and results in better access efficiency. However, maintaining a synchronous network requires contributions from computing and communication resources. Thus, there is a price for the purpose of network synchronization. The beacon method [10] [11] and the Global Positioning System [36] are two possible alternatives for maintaining the network synchronization.

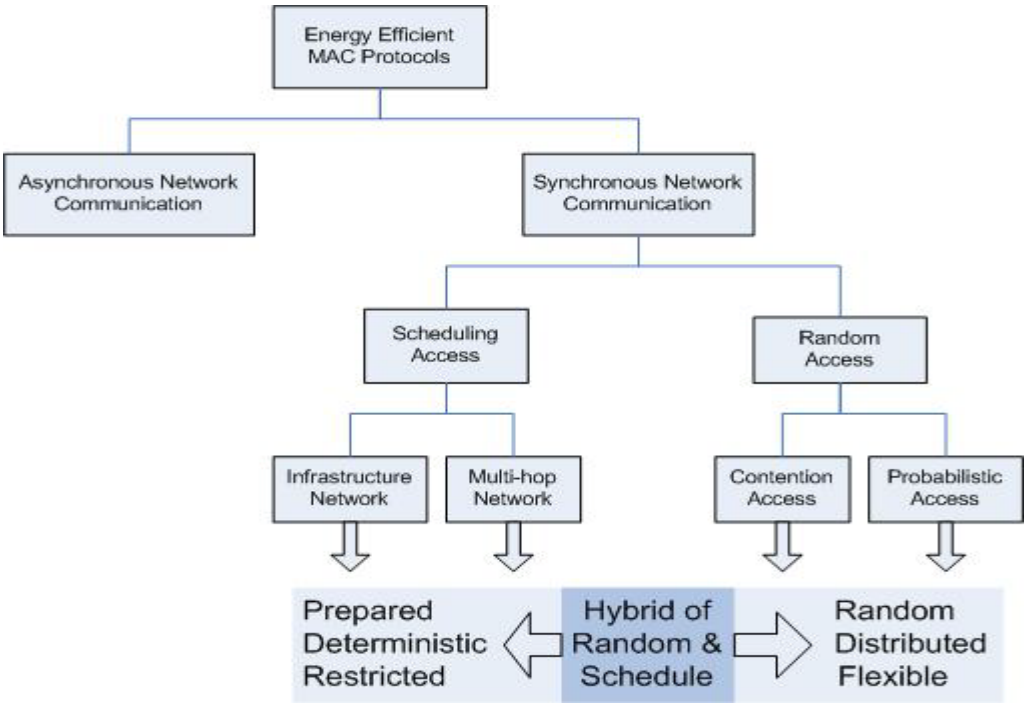

Figure 2-1 Taxonomy of MAC Protocols

2.1.1 Random Access

According to [35], channel access in synchronous sensor networks can be classified into scheduling-based and random-based access categories. The random access schemes manage traffic flows with the characteristics of less correlation. The scheduling access schemes on the other hand coordinate traffic flows with deliberate goals.

We furthermore classify previous work in random access based on the access methods: Contention-based and Probability-based. In contention-based access schemes, nodes have to contend or wait for their right to access the channel. In probability-based access schemes, nodes are programmed with designed access probabilities for channel access. However, both methods maintain access control with randomness. Bursty traffic pattern is commonly preferable with random access schemes, but it may be inefficient for delay-sensitive applications [35]. In addition, the random access mechanism provides many advantages like scalability, easy implementation, and distributed operation.

2.1.1.1 Contention Access

The wireless link fundamentally renders transmissions unreliable. One issue, which is common for all MAC layer protocols over a shared medium, is packet collisions. If we assume that all sensor nodes use the same frequency band for transmission, two transmissions that overlap will get corrupted (collide) if the sensor nodes involved in transmission or reception are in the same *collision domain*. This is independent of the MAC protocol selected.

Figure 2-2 explains the concept of collision domain. In general, any two communicating nodes *ni* and *nj* specify a *collision domain* CD(*ni,nj*). We define collision domain as the union of the transmission ranges for *ni* and *nj*. Consider two nodes *n1* and *n2* that wish to communicate.

In Figure 2-2, nodes *n1*, *n2*, *n3*, and *n4* are in the same collision domain. This implies that when *n1* and *n2* are communicating, *n3* and *n4* cannot participate in any communications. The reason for this is as follows. Even though node *n5* is outside the collision domain, if it sends a packet to *n3* at the same time that *n1* is sending a packet to *n2*, these two transmissions will collide at *n3*. The information in both packets is lost. Similarly, *n4* and *n6* cannot communicate when *n1* and *n2* are communicating.

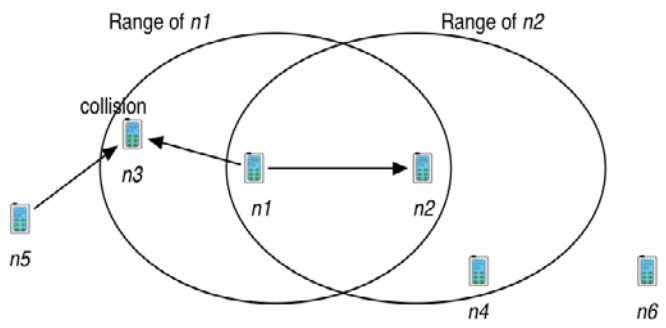

Figure 2-2 Collision domain of two communicating nodes

We can use Figure 2-2 to illustrate how collisions are handled in a typical wireless network such as IEEE 802.11 or IEEE 802.15.4 using *CSMA/CA*. In general, before starting a transmission, nodes must sense the channel for a predetermined amount of time (waiting time). Only if the channel is free for this entire period are the nodes allowed to transmit. If the channel is busy, the nodes wait for a predetermined amount of time after the channel becomes free. In addition, nodes back-off their transmissions for a random time period to avoid the possibility that two or more nodes (which had been waiting for the channel to become free) transmit at the same time after the waiting period. For this entire period, the node must sense the channel and this consumes energy. Each packet also needs to be acknowledged by the receiver since wireless channels are unreliable in general. The acknowledgements are prioritized by setting smaller waiting times for comparatively older transmissions than to the new transmissions. Because

wireless nodes physically sense radio channels, the whole sensing mechanism is called physical carrier sensing mechanism.

If only basic carrier-sensing is employed, it can lead to the *hidden terminal* problem [64]. Consider Figure 2-2 again. Node *n4* is outside the range of *n1*. When *n1* is transmitting a packet to *n2*, *n4* cannot sense the energy on the air and may start a transmission, either to *n2* or *n6*. This transmission will collide with the transmission from *n1* at node *n2*. The node *n1* is hidden from *n4* and vice versa. To overcome this problem, the IEEE 802.11 standard uses an optional Request-to-Send/Clear-to-Send (RTS/CTS) mechanism. The procedure with RTS-CTS is to have the sender and receiver exchange control packets, (i.e., request to send (RTS) packet, clear to send (CTS), and ACK) to notify both parties and their neighbors about incoming transmissions. The control packets include the information of the destination address and the expected duration of the whole data transmission, so every mobile that hears these packets will learn the latest network conditions through updating NAV – network allocation vector fields, and consequently avoid possible collisions. Since this mechanism achieves carrier sensing by virtually checking the NAV field, it is also called as a virtual carrier sense mechanism. This ensures that node *n4* does not transmit while *n2* is receiving a packet.

Both the carrier sensing mechanisms (i.e., physical and virtual) play an important role in medium access, and their influence in power consumption are also important since the more efficiently channel access is managed, the less energy will be consumed in each node. Using this idea, proposals in [38] and [39] modify the carrier sensing mechanisms in the 802.11 protocol to reduce excess energy consumption. Besides, CSMA/CA has the other advantages of simplicity, ease of implementation and efficiency for most data transmissions. But these characteristics may hurt the performance in terms of energy efficiency, QoS support, delay and throughput.

Moreover, communication in sensor networks using 802.11 is energy intensive (in relative terms) compared to the energy available in sensors.

In case of sensor networks where battery life is already a major constraint, packet collisions can lead to a premature death of the network. Recently, the contention-based IEEE 802.15.4 standard has been proposed for low-to-medium data rate, low-power wireless networking [11]. Because of its low power characteristics, the IEEE 802.15.4 standard appears to be suitable for low–power, low-data rate sensor networks. The data rates with 802.15.4 are 20, 40 or 250 kbps in the 868, 915 or 2400 MHz bands respectively. The transmit power with 802.15.4 is also expected to be very low (1 – 2 mW or 0 – 3.6 dBm). The Zigbee industry standard is developing network and application layer protocols to operate over the IEEE 802.15.4 standard.

Table 2-1 Comparison of accepted MAC layer technologies

Technology	Data Rate	Frequency Bands	Transmit Power	Collision Avoidance Features	Drawbacks
802.11	1- 54 Mbps	2.4 and 5 GHz	250 mW	RTS/CTS and waiting times	Complex PHY and MAC layers Energy hungry
802.15.4	20, 40 and 250 kbps	868/915 MHz, 2.4 GHz	1-2 mW	Waiting times only + contention free periods	Low data rates and inefficient collision handling can lead to excessive delay

Table 2-1 summarizes comparative characteristics of certain contention access technologies. 802.11 wireless networks consume too much energy to provide high data rates over long range. The data rates of 802.15.4 are quite low and can increase the latency of data delivery, which can be a big disadvantage for critical monitoring applications. The lack of RTS/CTS

mechanism in 802.15.4 may still result in the hidden terminal problem, which can lead to excessive collisions.

In [40], the *Power Aware Multi-Access protocol with Signaling* (PAMAS) has been proposed to transmit control packets, i.e., RTS and CTS, in a separate signaling channel and data packets in a traffic channel. A node with pending traffic sends an RTS over a signaling channel to a destined node and waits for a CTS reply from the destined node. If the CTS is successfully received, the sending node initiates data transmissions over the traffic channel, and the destined node broadcasts busy tones over the signaling channel to announce that the traffic channel is occupied. Thus, the neighboring nodes can avoid possible collisions in the traffic channel. On the other hand, if a failed CTS reply occurs, it implies that the channel is too poor to deliver traffic or the destined node is not available so that the sending node executes a random back-off procedure to avoid future contention in channel access. With these rules of packet transmissions in two different channels, the PAMAS's power management procedure helps overhearing neighbors to stay in a sleepy state. There are two cases that a node stays in a sleep state according to received busy tones and control packets. The first case is that a node has no packets to send and it hears a neighbor start transmitting packets that are not destined to it, while in the second case, a node that has packets to send finds the traffic channel to be busy. Accordingly, the power saving is achieved in these cases because neighboring nodes hear the busy tones and move to a sleep state. Besides, they also know when and for how long to stay in a sleep state.

In their simulations, the authors compare the energy savings between PAMAS without power conservation and PAMAS with power conservation. A sparse network simulation results in 20%-30% power saving at light loads while 10% power saving is observed at high loads. In a dense network simulation, the power saving at light loads is 60%-70% while at high loads this

drops to 30%-40%. The results show that a dense network will cause more energy waste; so the PAMAS saves more power in the dense network. It is because more nodes can power off during transmissions in dense networks. Moreover, the reason for the higher power saving at low loads is that, at low loads, there is less contention for the channel resulting in fewer control message transmissions. At high loads, almost all the nodes have packets to send and thus contention for the channel is high. This results in fewer actual packet transmissions and lower power saving. Through the additional signaling channel, synchronization is easier to implement among nodes and considerable amounts of power are saved.

However, the design and the simulations of the PAMAS protocol include some issues. It trades off scarce radio bandwidth and hardware capacity to the power saving. PAMAS uses extra radio bandwidth and implements additional components in each node to transmit control packets. If a node has limited capacity in communication and computing power, i.e., sensors, the second radio device in each node will be a vast weight in term of the power consumption unless it uses a low power radio technology. Besides, the energy consumption model in the simulations is over simplified. It ignores energy consumption in idle state and assumes the ratio of energy consumption between receiving and transmitting is 0.5. These assumptions are seriously in contrast with the majority of research [16] [25]. Another issue that needs to be mentioned is that the additional signaling channel does not guarantee a collision-free network. In the MAC layer, collisions in traffic channel are avoided due to the busy tones in the signaling channel, but mobiles still have to contend to send control packets in the signaling channel. Thus, it is still possible to face collisions in the signaling channel, especially in high loads and fast mobility conditions.

Jung et al. [42] proposed a mechanism that improves wakeup/sleep schedules for power management in the 802.11 protocol. It is called the *Dynamic Power Saving Mechanism* (DPSM). In the 802.11 protocol an *Ad Hoc Traffic Indication Map* (ATIM) frame is sent by a source node to announce its pending traffic in an ATIM window where the window size is fixed. After receiving one ATIM frame in the ATIM window, the nodes have to stay awake during the whole beacon interval no matter what size of traffic is sent. Therefore, unnecessary power consumption exists if traffic load is low. The DPSM includes two key features to overcome the power waste problem described above: dynamic adjustment of ATIM window and longer reduced power state. In the DPSM scheme, a sending node only transmits one successful ATIM frame to the destined node, which is similar to the ATIM procedure of the 802.11 protocol. Each packet delivered by a sending node to a destined node includes the number of packets pending for the destined node. This information tells the destined node when all pending packets in the current beacon interval are supposed to arrive. If the pending packets are too many to fit in one beacon interval, the remaining undelivered packets are sent in the subsequent beacon interval without the sending node having to send another ATIM frame to the destined node. Both sides enter a sleep state after all pending packets are processed, so the power efficiency in the DPSM will be superior to the 802.11 protocol. Besides, each node autonomously selects an ATIM window size based on the monitored network circumstance. The ATIM window size is dynamically adjusted to a finite set of ATIM window sizes. Four rules are applied to adjust the ATIM window size.

- If the number of pending packets could not be announced in the current ATIM window, it means the current window size is too small to transmit an ATIM frame to all destined nodes that have pending packets. One level of an ATIM window increment is added to the sending node.

- Each node piggybacks its ATIM window size on all transmitted packets. If a node overhears a neighbor's ATIM window size is two levels greater than its own, the node increases its ATIM window size by one level. This ensures the difference of the ATIM window sizes among nodes is not so large that high possibility of missing ATIM frames exists.
- If a node, who is in active state, receives an ATIM frame after its ATIM window is closed, the node is allowed to increase its ATIM window size by one level.
- When a node receives a marked packet, the node will increase its ATIM window size to the next higher level. A marked packet indicates failure to deliver the corresponding ATIM frame in a small number of attempts.

If a large ATIM window size is required (this indicates high traffic loads) the reduced power mode will be cancelled since ATIM frames and traffic occupy all time slots in a frame. Therefore, the energy saving is substantially eliminated due to high traffic loads.

The effect of the dynamic window size alleviates the mismatch problem. The mismatch problem is caused by different lengths between the ATIM window and the data window. The longer the ATIM window, not only more contentions are built in the data window, but energy is wasted for those who do not get a chance to transfer data in the current beacon interval. This is because the nodes, which don't deliver their packets successfully, still need to stay in active mode throughout the beacon interval. With the dynamic adjustment of ATIM windows, the mismatch problem is addressed. On the other hand, the DPSM also includes disadvantages, i.e., latency and low bandwidth utilization. The latency issue is created by the marked packet rule and the small window size at receiving nodes. Because it takes certain amounts of time to initiate a marked packet or to increase a small window size to a reasonable size, a delay is inevitable. The

degree of the delay will depend on how we define network properties. The low bandwidth utilization is the second disadvantage and caused by a large ATIM window in the DPSM. Because larger the ATIM window size, more bandwidth is used for control packets transmission, the bandwidth for actual data transmissions is indirectly reduced that makes the bandwidth utilization low.

Schurgers et al. [43] proposed a contention-based protocol called *Sparse Topology and Energy Management* (STEM) to save energy. STEM implements a two-radio architecture likes PAMAS that allows the data channel to sleep until communication is required. Channel monitoring alleviates collisions and retransmission. However, a busy tone has to wakeup the entire neighborhood of a node, since the intended receiver's identity is not included on the monitoring channel. Thus, neighbors waste extra energy. Vaidya et al. [44] tried to address such issues not addressed in STEM by introducing a rate estimation (RE) scheme on top of it. They wake up the node, which have previously been involved in communication, via RE using an optimal wakeup interval. In this way they minimize overall energy consumption. Both STEM and RE schemes assume a two-radio architecture. They ignore the complexity of adopting the second radio in a resource-constrained sensor node that may result in difficult transceiver design and additional energy consumption by the second radio.

Comparing the reviewed contention mechanisms, we notice that each mechanism has focus on certain areas of power waste, instead of the whole energy problem, or considered the power saving issues in a restricted network topology. For example, the PAMAS only targets the overhearing waste while the DPSM focuses on reducing the idle listening, but other kinds of power waste still exist in their designs. Since each mechanism tries to solve different

combinations of power wastes, it will be unreasonable to compare their power saving performance.

Table 2-2 summarizes the mechanisms, environments, advantages and disadvantages of contention access researches in a synchronous network. In the contention-based researches, the proposed mechanisms eliminate the overhearing and idle listen by monitoring packets or signals, i.e., busy tones, RTS, CTS, or Data. On the one hand, energy is saved due to the assistances of specific information. On the other hand, the latency issue exists because of the design for power saving. Therefore, finding a balance between the contention-based reduced power mode and the latency is an interesting topic for the future research.

Table 2-2 Contention Based Channel Access Mechanisms

Contention Access literature	Singh et al., 1998 (**PAMAS**)	Jung et al., 2002 (**DPSM**)	Schurgers et al., 2002; Vaidya et al., 2005 (**STEM**)
Power Saving Mechanism	PAMAS protocol designs an additional signaling channel for control packets besides the traffic channel for data packets.	DPSM dynamically adjusts the ATIM window size to achieve longer reduced power state.	Two-radio architecture: data channel and monitoring channel. Selectively wakeup receivers.
Operation Environment	Fully Connected Topology. Ad hoc networks.	Fully Connected Topology. Ad hoc networks.	Multi-hop Sensor Network
Advantages	Neighbors avoid overhearing by busy tones. Support the existing IEEE 802.11 protocol. Additional signaling channel helps synchronization.	Limit the idle listen by extending the sleep state. Support the existing IEEE 802.11 protocol. Fix the mismatch problem. Maintain synchronization.	Reduce collision, retransmission and overhearing problems.
Disadvantages	Extra bandwidth resources are for signaling channel. Extra components in each node to operate the second signaling channel.	Latency from the marked packets rules and the small window size at a receiving node. Low bandwidth utilization.	Extra bandwidth resources are for signaling channel. Extra components in each node to operate the second signaling channel.

2.1.1.2 Probabilistic Access

Probabilistic technique is the other access option in the random access category [45] [46] [47] [48]. Using the probabilistic access approach less control messages (overhead) is needed to access the channel. The channel bandwidth utilization therefore could be improved. The capability of self-organization is another reason to select the probabilistic access [35]. It enables nodes to perform channel access in an automatic and distributed way.

Zhang et al. [47] apply an optimization technique to tune the access probability for each sensor. The optimization goal is to minimize the data gathering duration on condition that each link in the data gathering tree can provide guaranteed QoS. This task is formulated as an optimization problem that uses a distributed heuristic algorithm to solve it in tree networks. This study aims at reducing the response time of packets by maintaining hop-by-hop transmission reliability but it is difficult to satisfy the requirements of DISN because the system throughput is not considered. Besides, the optimization relies on neighbor data and topological information (tree network). Change of the topology (e.g., added nodes or deleted nodes) or inaccuracy of the neighbor data could affect effectiveness of pre-defined access probabilities. It requires re-calculation of the optimization algorithm to address this issue. However, authors do not discuss such concerns in their paper.

Karnik et al. [48] proposed a framework that aims at achieving the self-organization within a WSN. In their proposal sensors first form an optimally connected network in Phase I and then proceed to find their optimal access rates in Phase II. In both phases the optimization goal is to maximize average communication throughput of sensors. In the Phase I authors proposed the *Maximum Average-weighted Spanning Subgraph* (MAWSS) algorithm to control the optimal network topology that takes into account the communication throughput. The

derivation of the throughput is based on Equations (2-1 and 2-2) which consider factors of the free space path loss model, the neighbors' interference and the access probabilities. Equation (2-1) denotes the probability of successful transmission from sensor *i* to *j* under a (access probability of a sensor). The last term in (2-1) is $P(H_{ij} >= ß)$ where H_{ij} denotes the *Signal to Interference Ratio* (SIR) of a transmission from *i* to *j*. d_{kj} is the distance between *k* and *j*, d_0 is the near-field crossover distance, N_0 is thermal noise power, and Y_k is 1 if *k* transmits, 0 otherwise. Equation (2-2) determines the average throughput of sensor *i* with a given topology *G'*. $n_i(G')$ represents the number of neighbors of sensor *i* in the topology *G'*. Using these two basic equations in their centralized and distributed MAWSS algorithms, the optimal topology can be determined based on the maximum network throughput in this phase.

$$P_{ij}(\alpha) = \alpha_i (1-\alpha_j) P\left(\frac{(\frac{d_{ij}}{d_0})^{-\eta}}{\sum_{k \neq i,j} (\frac{d_{kj}}{d_0})^{-\eta} Y_k + N_0} \geq \beta\right) \tag{2-1}$$

$$M_i(G', \alpha) = \frac{1}{n_i(G')} \sum_{j \in Ni(G')} P_{ij}(\alpha) \tag{2-2}$$

With the chosen optimal network topology from the Phase I, authors next observed that the throughput performance is maximized with different • values. Thus, it is essential to actually operate the network at a throughput-maximizing value of • in the Phase II. The authors proposed the *MAXMIN throughput attempt probabilities* (MMTAP) algorithm to tune the value of • with the assumption that the value of • shall be the minimum throughput of all nodes because network throughput could be limited by the lowest throughput sensor in the network.

Comparing these two probabilistic access schemes, two major differences are noted. First, Karnik's work considers local performance for each single node, while Zhang et al. take into account the end-to-end delay performance. Second, Zhang's work does not need to maintain

topology control and does not insist that all the sensors use the same access probability, compared with Karnik's optimization technique. Since the objective of optimization in both schemes is different, we can not perform a fair comparison but it is clear that Karnik's algorithm is more intricate due to extra considerations in the network topology and the radio channel model, i.e., Zhang's optimization algorithm calculates the collision-free transmission probability without consideration of SIR.

Our hybrid approach is also a partial probabilistic access scheme but we do not consider complex optimization techniques like Karnik's methods to enhance network utility. Our idea is to utilize neighboring information and special numerical features to improve network performance. More details of this idea will be presented in Chapters 4 and 6. Table 2-3 summarizes the mechanisms, environments, advantages and disadvantages of probabilistic access researches in a synchronous network.

Table 2-3 Probabilistic Based Channel Access Mechanisms

Probabilistic Access literature	Zhang et al., 2006	Karnik et al., 2004
Power Saving Mechanism	Tune access probability of sensors to minimize the data gathering latency on condition that each link maintains a level of QoS.	Tune access probability of a sensor to achieve optimal throughput for each node. Topology control is also included to assist the throughput performance.
Operation Environment	Multi-hop sensor network.	Multi-hop sensor network.
Advantages	Low computational complexity. Provide guaranteed link quality.	Self-organisation capability. Provide fairness among sensors. Optimal throughput per sensor.
Disadvantages	Potential rising latency due to probabilistic feature. Low bandwith utilization in dense networks. Need to test the scalability.	Miss cooperative data delivery in sensor networks. Complex algorithm.

2.1.2 Scheduling Access

Scheduling access is the other popular approach for channel access in WSN. It is widely accepted due to its success in transmission reliability and energy efficiency. Scheduling access is mostly adopted into a Time Division Multiple Access (TDMA)-like mechanism and it is especially proficient in managing the channel access of continuous and periodic traffic applications [35].

In this review, we classify the work on scheduling access according to the network infrastructure: Infrastructure Network/Single-hop Network and Multi-hop Network. In general, the scheduling algorithm in infrastructure networks is simpler due to the nature of available infrastructure, fully connected network, easy synchronization and absence of multi-hop delivery.

2.1.2.1 Infrastructure Networks (Single-hop Networks)

In scheduling access schemes, a node may decide its wakeup/sleep schedule either via hearing broadcast control packets or via receiving a schedule directly from a central controller. Sivalingam et al. [49] proposed an *Energy Conserving-Medium Access Control* (EC-MAC) protocol with the issue of energy efficiency as a primary design goal. The EC-MAC protocol is designed to operate in an infrastructure network where a central controller plays an important role in setting up transmission schedule. The same idea can be applied to an Ad hoc network where a random node is chosen as the controller. The central controller is responsible for reservation and scheduling strategies. The transmission of EC-MAC is organized by the controller into frames, and the time slots of the frame serve various purposes. For example, the synchronization task is handled in the *frame synchronization message* (FSM), the connection request is processed in a request/update phase, the transmission schedule is broadcast by the

controller in a scheduled message, and data transmissions are performed in a subsequent data phase for both ways. In consequence, collisions are reduced and retransmission attempts are avoided. In addition, the receiving party does not need to listen to idle channels so more power is saved. In their performance analysis, the energy consumption comparison of EC-MAC to other protocols including the 802.11 protocol has been provided. The comparison demonstrates that EC-MAC outperforms others schemes because of its collision-free and zero idle listen nature. On average, the receiver usage time of the EC-MAC is three factors less than the 802.11 protocol, and the metric measuring the energy spent per useful bit also shows similar results.

Although a schedule is reserved among nodes in different stages, a collision is still highly possible in the *new user phase* because mobility can worsen the process of node registration. Thus, a random back-off process is implemented in the node registration. Besides, an optimization in transmissions will be achieved if a node is scheduled to transmit and receive in contiguous slot allocations. The downsides of this design are the bottleneck issue, the requirement of a synchronous network and the fixed frame length. The fixed frame length ensures smooth synchronization operation so the sleep mode mobile knows the time to wakeup. However, it creates barriers for transmitting bursty traffic. The bottleneck issue is caused since all scheduling processes rely on a controller. If the controller fails, the whole system will be down. Therefore, the EC-MAC should include a fault tolerant plan to avoid the bottleneck problem.

Liu et al. [41] also proposed a scheduling type of a power saving mechanism. In [41], a contention-free schedule is derived from overheard ATIM frames, sent by neighbors, under the assumption of a fully connected network. Each node must receive all transmitted ATIM frames within the network to ensure the complete schedule. In this scheme, the ATIM frame includes

information about the number of packets to be transmitted by each node, so every node can calculate the transmission schedule. Unlike the 802.11's power management procedure that requests the mobile to stay in an active state for the whole period of a beacon interval if the ATIM and acknowledge packets are exchanged, the contention-free schedule can allow the nodes finishing their transmissions early in the data window and then switching to low-power mode in the middle of the data window. This advantage allows the nodes with short transmissions, which is especially common in a high-speed network (e.g., transmission rate of 54 Mbps in IEEE 802.11a), to stay longer in low-power modes. To extend the power-saving capacity in this scheme, the nodes with fewer packets transmit earlier than the nodes with more packets. This makes more stations enter the low-power mode and stay in the low-power mode longer. With the contention-free schedule, the contention process for ATIM is still required but is eliminated in data transmissions that are normally much larger than an ATIM window size. Thus, power is saved due to lesser numbers of collisions, less retransmission and less monitoring. In the performance analysis, the authors estimate an average energy saving of around 60%, based on the number of slots a station has to stay in sleep mode on average. However, the paper does not illustrate the benchmark of the energy evaluation so there is no sufficient data to support the result. Besides, a switch between a low-power state and a high-power state takes some time and amount of energy [42], so a lower bound for the length of the beacon interval is specified to avoid frequent changes and to reserve power. The energy saving percentage may be altered if the threshold for switching to sleep state in the middle of beacon interval is different.

This scheme also adopts the idea of variable length of beacon interval to meet the mismatch problem. The variable length of the beacon interval alleviates the mismatch and

improves the system efficiency by adjusting the beacon interval to increase the probability of transferring all traffic, but it makes the task of sharing a synchronous clock within the network more difficult, and may introduce long latency due to extra long beacon intervals. According to the simulation results of [41], we compare the metric – the number of packets transferred between a current 802.11 protocol and an enhanced 802.11 protocol. In the current 802.11 case, the number of packets transferred is limited by the size of ATIM window. Larger the ATIM window, the more is the number packets that are transferred. However, an upper bound in the number of packets transferred is imposed by the size of the beacon interval. In the enhanced 802.11 case, the number of packets transferred increases linearly if the ATIM window size is large enough, while the system throughput remains at a steady level. It is because contention-free data transmission and variable beacon interval lengths reduce the collision probability and allow more traffic to arrive at destined nodes. Next, we compare the schemes of the scheduling access in the infrastructure network.

Comparing the EC-MAC [49] with the enhanced 802.11 protocol [41], we found that the EC-MAC generates schedules in a centralized way while the enhanced 802.11 protocol allows every node to generate its schedule from the information it receives, which is more distributed. With the centralized orientation in the EC-MAC, the EC-MAC has to face the bottleneck problem that is not present in the enhanced 802.11 protocol. Besides, both schemes enjoy the benefit of reducing the idle listen and collisions; so the energy conservation is achieved. Since these two schemes do not share the same benchmark in their simulation studies, it is not fair to compare their power saving performance. However, it is clear that the EC-MAC is not suitable for ad hoc wireless networks due to its centralized characteristic.

Table 2-4 Scheduling Based Channel Access Mechanisms (Infrastructure Network)

Scheduling Access literature	Sivalingam et al., 2000 (**EC-MAC**)	Liu et al., 2003 (**Enhanced 802.11**)
Power Saving Mechanism	Transmissions are scheduled in frames by a controller. Synchronization, registration, scheduling and transferring data functions are assigned in different slot allocations of the frame.	Transmission schedule is generated based on the ATIM frames in each node. Node switches to lower power state once no more packet pending in BI.
Operation Environment	Infrastructure mode or Ad-hoc mode with randomly selected controller in a fully Connected topology.	Ad-Hoc network in a fully Connected topology.
Advantages	Collision and retransmission are reduced by scheduling. Constant neighbors' monitoring (idle listen) is avoided.	Stay in a sleep state longer to limit collision and idle listen. Support the existing IEEE 802.11 protocol. Address the short transmission time caused by high speed data rate and the mismatch problem.
Disadvantages	Central control doesn't integral well in ad hoc network, and also causes the bottleneck problem. Need to maintain clock synchronization. Inefficient for bursty traffic.	Variable length of BI fixes the mismatch problem but makes the synchronization maintenance complex. Need to maintain clock synchronization. Latency issue may exist due to the long length of BI.

Table 2-4 summarizes the mechanisms, environments, advantages and disadvantages of scheduling research in a synchronous infrastructure network. In the table, the scheduling-based research papers use a pre-defined schedule (EC-MAC) or a collected schedule (enhanced 802.11) to prevent collisions, the retransmissions, and the idle listen but pay a common price in the mandatory synchronization requirement. Other prices, such as the bottleneck issue, latency, or limitation of bursty traffic, are dependent on the mechanism.

2.1.2.2 Multi-Hop Networks

Ye et al. [38] proposed another mechanism called *Sensors-MAC* (S-MAC) that is similar to PAMAS and both designs try to achieve the overhear avoidance. The primary difference between these two designs is the use of a signaling channel. Unlike the PAMAS, the S-MAC only uses in-channel signaling. To avoid the overhearing, this protocol lets interfering nodes go

to a sleep state after they hear any RTS or CTS. Definition of interfering nodes is the neighbors of sender and receiver who are one-hop apart. The nodes that go to the sleep state wakeup according to the NAV setting that are collected from RTS and CTS. Since data packets are commonly longer than control packets, the design prevents the interfering nodes from listening to unrelated data packets, and consequently saves power from overhearing data packets. According to the simulations, 802.11 MAC uses more than twice the energy used by the overhearing avoidance of S-MAC.

Moreover, the S-MAC also adopts a static scheduling-based scheme of periodic listen and sleep to reduce the time spent on idle listening when the traffic load is light, and the message passing scheme that fragments long messages into many small fragments, and transmits them in a burst. Only a copy of RTS and CTS are exchanged for the long message, instead of a set of RTS-CTS for every small fragment. Therefore, the excess overhead concern due to multiple fragments is eliminated. The main motivation behind the message passing is to avoid transmitting a long message as a single packet that will create a high cost of re-transmitting the long packet if only a few bits have been corrupted in the first transmission. An issue with the scheme of periodic listen and sleep is the latency problem. If a cycle of the periodic listen is long, the average delay for data transmissions will definitely be long too. Besides, the delay is accumulated on each hop so that the latency problem is going to be worse in a multi-hop WLAN. Thus, this scheme will not work well in a highly mobile ad hoc network. In addition, the message passing provides an advantage of limiting long messages, but it may cause a fairness issue. In the 802.11 protocol, if a sender fails to get an ACK for any fragment, it must give up the transmission and re-contend for the medium so that other nodes have a chance to transmit. This approach can cause a long delay but provide per-node fairness. If the same problem occurs, the

message passing will extend the transmission time and re-transmit the current fragment. It has less contention and a smaller delay but per-node fairness is lost. The importance of the per-node fairness depends on the application run on the network. For instance, in sensor networks the per-node fairness is not very important since the network is data-centric, and may have long periods of inactive state and suddenly become active for a short time. Thus, the most important thing in the sensors network is to complete the task in application level, and considers the per-node fairness as a minor requirement. However, a wireless ad hoc network based on the 802.11 protocol is concerned with the significance of per-node fairness differently. It assumes each node has an equal share of traffic loads that need medium access, so a fair distribution of bandwidth among nodes is critical. Last concern with S-MAC is there is no on-demand interaction with the receiver in case there is a need to communicate between sender and receiver (it uses a static sleep interval).

Lightweight MAC (LMAC), which was proposed by van Hoesel et al. [50], was implemented as a distributed time slot scheduling algorithm for collision-free communications. Time is divided into slots and sensor nodes broadcast information about time-slots they believe that they control. Neighboring sensor nodes will avoid picking such slots and pick others to control. During its time slot, a sensor node will transmit a message with two parts: control and data. The control part includes sufficient information for neighbors to derive a time slot schedule of local sensors so transmissions among neighboring sensors will not collide. Sensors must listen to the control parts of their neighbors. Time slots can be reused at distances where interference is small (three hops for instance). With such an algorithm, the goal of collision avoidance is achieved at the price of extra control overhead and listen time. Chatterjea et al. introduced *Adaptive, Information Centric and Lightweight MAC* (AI-LMAC) [51] that uses captured local

information about neighbors' traffic patterns to modify channel access assignments accordingly. The protocol is an extension of the LMAC and adapts to the requirements of sensor applications. Authors believe that sensor network is application-specific. Thus, designing protocols that are specifically designed for a particular application is necessary for network efficiency. In AI-LMAC, a *Data Distribution Table* (DDT) is built into every sensor that helps make deductions about characters and distributions of incoming traffic. The table is built over time by observing the passed data, which flows from the leaf sensors to the root. With the information provided in the DDT, a sensor allows to own multiple time slots depending on the amount of data that is expected to flow through it. For LMAC this feature is not existed and every sensor only owns a time slot per frame. Eventually, AI-LMAC enables a sensor network with less collision with the ability to adapt to particular traffic patterns. While AI-LMAC is adaptive and information-centric, it still shares the LMAC's extra control overhead and faces possible performance deficiency from unexpected bursty traffic. Both LMAC and AI-LMAC were designed not with the goal of supporting high data loads, but with the objective of reducing the switching time/cost from sleep mode to transmit mode.

Another distributed TDMA scheduling procedure was proposed by Ammar et al. [52]. Its design goal is to permit a mobile to move and then reallocate itself a time slot without involving the entire network. The method of a time slot assignment is to utilize exchanges of control messages among neighbors to achieve collision-free communications on a data channel. The control message is delivered through a separate control channel. Use of the control channel implies that control message will not collide with data frames, yet they may collide with other control messages and produce incorrect time slot schedules. Moreover, current sensor devices are limited by hardware functions and resources due to the requirement of low cost. Thus, adopting

an extra radio component into sensors is not recommended. Ali et al. [53] proposed distributed and adaptive TDMA algorithms for multi-hop mobile networks. This protocol focuses on solving two problems. First, how to adjust the time slot assignments if an added link is detected. Second, how to efficiently schedule time slots when two mobiles are no longer within range of each other. To answer these problems, the first thing needs to know is the availability of a link. It is answered by received transmissions from other nodes. In the other words, the use of an initial flag field in the header of each transmission enables sensors to detect new connections to neighbors. If a sensor detects a new link or a deleted link, it will transmit a control packet with necessary information for its local neighborhood. Then a new time slot schedule will be derived by neighbors and potential collisions are reduced. One concern with this design is that dynamic topology changes may lead to frequent exchanges of control packets that could consume bandwidth and energy resources.

Rhee et al. [80] [82] propose a *Distributed Randomized TDMA Scheduling* algorithm (DRAND) that is used within a MAC protocol called *Zebra-MAC* (Z-MAC) to improve performance in sensor networks by combining the strength of scheduled access during high loads and random access during low loads. The distributed implementation of DRAND enables a sensor to select a time-slot, which is distinct from time-slots of its two-hop neighboring sensors. This feature reduces data packet collisions. The DRAND algorithm includes two major phases: Neighbor Discovery-Hello and DRAND Slot Assignment. In the neighbor discovery phase, sensors broadcast Hello messages periodically to announce their existence. Next, sensors exchange control messages like Request, Grant, Release or Reject to determine the time slots of sensors. With this scheme, the message complexity is $O(n)$ where n is the maximum size of a two-hop neighborhood in a wireless network. While DRAND provides reliable data

transmissions, some constraints are noted. First, this algorithm is suitable for a wireless network where most nodes do not move. If the topology changes dynamically, the algorithm should be run frequently to ensure delivery reliability. The frequent executions of the algorithm will likely consume more resources in sensor networks. Next, the algorithm ensures data delivery by assigning collision-free time slots to sensor nodes. However, transmissions can still collide in the DRAND slot assignment phase because of randomized transmissions and the channel contentions. Finally, the interference irregularity can occur even among nodes that cannot communicate with each others at all [81]. When two nodes cannot communicate directly, their interference relations can only be deduced through multi-hop communications. There are also cases where even multi-hop communication (two-hop distance) between two interfering nodes is not possible.

Zadorozhny et al. [62] [63] propose an algebraic optimization framework based on *Data Transmission Algebra* (DTA) that performs collision-aware query scheduling in WSNs. This work is designed to alleviate excessive packet collisions and retransmissions in DISNs. The DTA approach makes use of a set of operations that take transmissions between sensors as input and produce a schedule of transmissions as output by a DTA optimizer. Any one-hop transmission from sensor node *ni* to node *nj is* called an *elementary transmission* (denoted *ni~nj*). Each transmission *ni~nj* is associated with a *Collision Domain* CD(*ni*, *nj*) as defined earlier. A transmission schedule is either an elementary transmission or a composition of elementary transmissions using one of the operations of the DTA. The basic DTA includes three operations that combine two transmission schedules, A and B:

***o*(A,B)**. This is a strict order operation, that is, A must be executed before B.

***a*(A,B)**. This is an overlap operation, that is, A and B can be executed concurrently.

***c*(A,B)**. This is a non-strict order operation, that is, either A executes before B, or vice-versa.

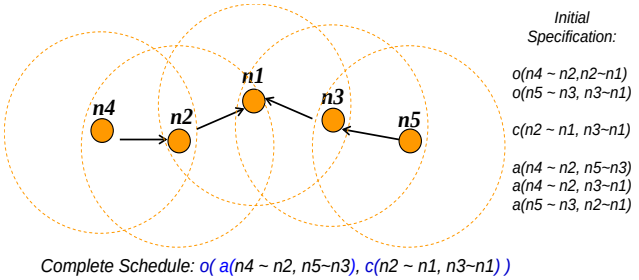

Figure 2-3 Example of DTA specifications

For example, consider the query tree in Figure 2-3 that shows the *initial DTA specification* reflecting basic constraints of the query tree. For instance, operation *o(n4~n2, n2~n1)* specifies that transmission *n2~n1* occurs after *n4~n2* is completed because of the query tree topology. Operation *c(n2~n1, n3~n1)* specifies that there is an order between transmissions *n2~n1* and *n3~n1* since they share the same destination. However, this order is not strict. Operation *a(n4~n2, n5~n3)* specifies that *n4~n2* can be executed concurrently with *n5~n3*, since neither *n3* nor *n5* belongs to CD(*n4*,*n2*), and neither *n4* nor *n2* are in CD(*n5*,*n3*). Figure 2-3 also shows an example of a complete schedule that includes all elementary transmissions of the query tree. The generated transmission schedule is collision-free due to the knowledge of the collision domains of elementary transmissions. We will perform the comparative study of the DTA framework vs. the 802.15.4 CSMA-CA to prove DTA's benefits and concerns in Chapter 4.

In [65], authors have formally proved the correctness of the DTA inference. However, basic DTA scheduling may be expensive due to its combinatorial nature. The number of alternative schedules grows at least exponentially with the number of sensor nodes and elementary transmissions participating in a query. In order to decrease this complexity the optimizer implements randomized algorithms [66] [67] [68].

While the above scheduling schemes are able to reduce time and/or energy waste from possible transmission collisions, they simultaneously introduce one or more of the following problems. Many feature considerable control message overhead (e.g., LMAC, AI-LMAC, DTA and DRAND) for building data delivery schedules. A sensor network is an error-prone and dynamic environment so it may often be difficult to use deterministic schedules (e.g., DTA). For instance, packet retransmission for dropped packets (due to channel conditions) may lead to high delays, especially in a large multi-hop network [47] [62]. In addition, generating and delivering an optimal schedule for data transmissions is complex in a large-scale sensor network [47]. These concerns bring up questions about the scalability of the scheduling approach.

Table 2-5 summarizes the mechanisms, environments, advantages and disadvantages of scheduling-based access research in a synchronous multi-hop network.

Table 2-5 Scheduling Based Channel Access Mechanism (Multi-hop Network)

Scheduling Access literature	van Hoesel et al., 2004 (**LMAC**)	Chatterjea et al., 2004 (**AI-LMAC**)	Ammar et al., 1991	Ali et al., 2002	Heidemann et al., 2002 (**S-MAC**)	Zadorozhny et al., 2005 (**DTA**)
Power Saving Mechanism	Sensors generate local schedules by received control messages. Each sensor is assigned with 1 time slot per frame.	Sensors generate local schedules by received control messages and past traffic patterns. Each sensor is assigned with 1 or multiple time slots per frame.	Authors proposed the dual channels mechanism: control and data channels. Using the control channel, sensors generate local schedules by received control messages.	Sensors discover neighbor's condition by flags and then use control messages to setup a new schedule among local neighbors.	Neighbors avoid overhearing by received RTS and CTS so interfering nodes are prevented from overhearing unrelated data packets. Periodic wakeup/sleep schedule are used to improve power efficiency. Message passing.	Network uses DTA framework to generate collision-aware transmission schedules for all sensors.
Operation Environment	Multi-hop sensor network.	Multi-hop sensor network.	Mobile packet radio network.	Multi-hop mobile network.	Multi-hop sensor network.	Multi-hop sensor network.
Advantages	Collision and retransmission are reduced by scheduling.	Collision and retransmission are reduced by scheduling. Data delivery is adaptive.	Collision and retransmission are reduced by scheduling. Mobility is supported.	Collision and retransmission are reduced by scheduling. Mobility is supported.	Avoid overhearing. Limit idle listen. Long wakeup durations help synchronizations.	Collision and retransmission are reduced by prepared schedules.
Disadvantages	Constant neighbors' monitoring for control messages. Extensive control overhead.	Constant neighbors' monitoring for control messages. Extensive control overhead. Bursty traffic may cause operational difficulty.	Constant control channel monitoring for control messages. Extensive control overhead. Extra resource consumption for the 2nd radio channel.	Constant neighbors' monitoring for control messages. Extensive control overhead by the dynamic topology change.	Lack of per-node fairness. Latency from the periodical sleep.	High complexity for schedule generation of a large network. Thus, scalability is concerned here.

2.2 EVALUATION OF REVIEWED WORK WITH DATA INTENSIVE APPLICATIONS

So far, we have illustrated various medium access mechanisms and their distinctive features. Their benefits and concerns were also discussed. According to these reviews, we will next analyze the reviewed protocols for use in special-purpose DISNs. By qualitatively examining the protocols with respect to their characteristics of energy, data delivery and network topology of DISNs, the applicability of reviewed protocols will be presented below.

First, we consider the feasibility of contention access protocols in DISNs. A reason for concern is the high channel contention contributed to by the intensive traffic scenario in DISNs. Besides, the contention access protocols originally were not designed for intensive traffic loads. They were normally used to handle random and bursty traffic. Therefore, it is unfair to apply contention access protocols in DISNs. Some schemes like PAMAS and STEM require a second radio component to assist channel access but this design is not suitable for current sensors because the sensors are limited by hardware and battery capacity.

Second, we consider probabilistic protocols for evaluation. They depend on over-complicated optimization techniques to determine access probabilities of sensors in static WSNs. With Zhang's protocol, the throughput performance may be difficult to match with the requirements of DISNs. The optimization techniques aim at minimizing packet latency with stable link quality, instead of system throughput. Consequently the bandwidth utilization may be low if the access probability is low. Here the optimization function makes trade-offs between the delivery reliability and the aggressiveness of transmissions. In Karnik's protocol, the authors aim at maximizing the communication throughput with considerable overhead price from the complex optimization process.

Third, single-hop scheduling access protocols like EC-MAC and Enhanced 802.11 are not a feasible solution for DISNs because they are not directly applicable to a multi-hop scenario.

Finally, the multiple-hop scheduling access protocols (e.g., DTA and DRAND) were presented with the expectation of higher network utility in DISNs. Such expectation arises from the alleviation of collisions and increasing throughput via well-organized transmission schedules. Further, reliable data delivery and energy saving is achieved. Control messages commonly are generated during the process of schedule preparation. This is the one major concern for such scheduling approaches because they contain no application data and still consume energy. Besides, creation of a transmission schedule is not trivial in a large network. A distributed scheduling method like the DRAND protocol thus is preferred.

2.3 CONCLUDING REMARKS

Many schemes have been proposed for access control of wireless ad hoc networks and sensor networks but to date none has proposed a comprehensive MAC scheme with minor overhead for the data intensive applications of sensor networks, or provided relevant evaluations for such a challenge. From the review of previous literature, we find that the scheduling approach seems to be a suitable solution to address the DIAs, or the probabilistic approach could also provide a fair result. Therefore, in next chapter we will demonstrate via a comparative performance evaluation of a scheduling access proposal vs. a random access proposal. In this evaluation, we do not only focus on the network performance but also intend to verify the scalability since it is a basic requirement of general sensor networks. Next, we target to research the probabilistic related work that range between the random access and the scheduling access.

We propose a novel idea using the concepts of the probabilistic access and heuristic scheduling to manage medium access in DISNs and expect to mitigate the significant performance degradation problem. The descriptions of the new proposals and their evaluation results will be shown in Chapters 4, 5, and 6.

3.0 EXPLORATORY ANALYSIS: RANDOM ACCESS VS. SCHEDULING ACCESS

The problem of significant performance degradation in the special-purpose DISNs is a critical issue with the current main-stream standards like the 802.11 and the 802.15.4 [19]. Thus, a demand exists for addressing this problem for DIAs. Through our review of past literatures, we have determined that two approaches are currently utilized to address medium access in sensor networks. They are the scheduling and the random access methods for synchronous networks. In order to demonstrate the potential benefits of both schemes, in this chapter, we present a case study that evaluates *Data Transmission Algebra* (DTA) that performs collision-aware query scheduling in WSNs [62] [63] and IEEE 802.15.4 *Contention Access Period* (CAP) mode using the CSMA/CA method for sensor networks [11]. The descriptions of DTA and 802.15.4 CSMA/CA are already provided in Chapter 2. Only the performance evaluation of DTA vs. 802.15.4 CSMS/CA protocol will be covered in this chapter. Through this evaluation, we learn the features and benefits of both mechanisms while the potential risk which accompanies these also will be discussed [84]. After completing the case study, partial results of DTA are used to motivate the proposed protocols described in Chapters 4 and 5.

3.1 SIMULATION SETUP

For this study, we developed a simulation test-bed based on the ns-2 simulator [73] with the CMU wireless extension [69]. We used 250 Kbps as the channel data rate and assumed that the sensor transmission range is 15 meters. The MAC layer follows the IEEE 802.15.4 standard [11] incorporated into ns-2 by Zheng and Lee [34]. Figure 3-1 shows the flow chart of how the DTA schedules are implemented over the same MAC layer.

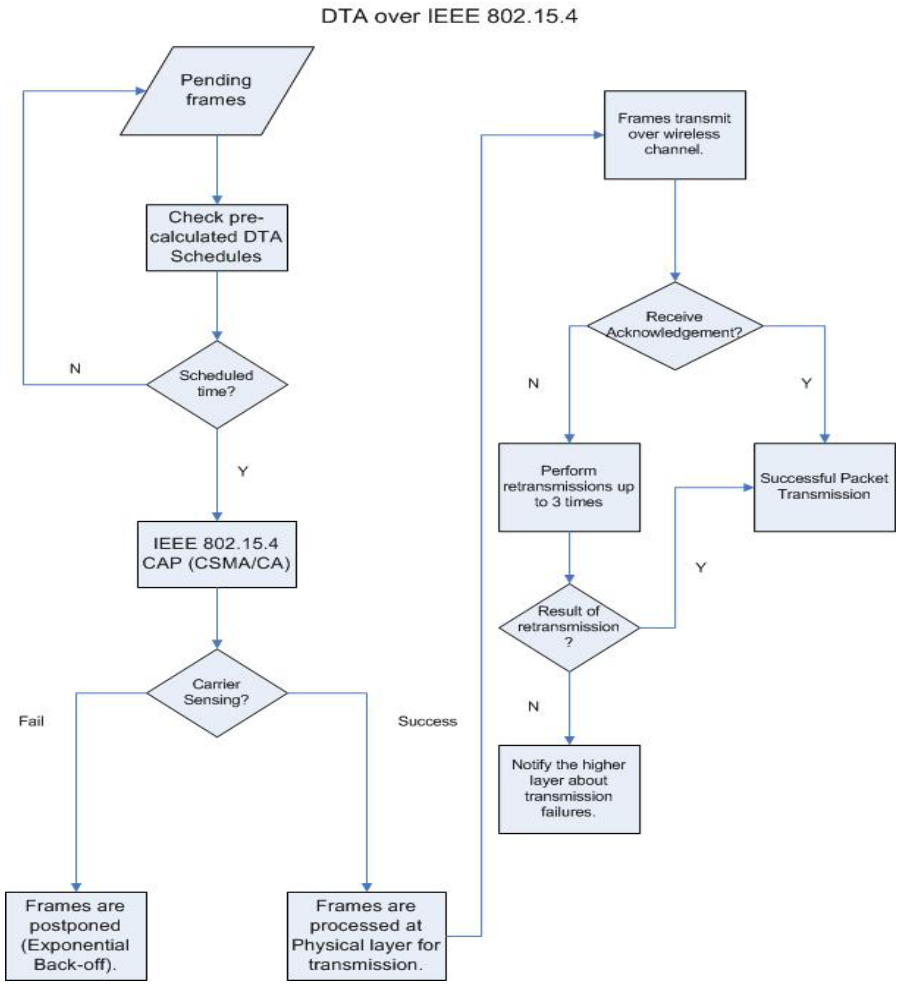

Figure 3-1 Flow Chart of Simulation of DTA over IEEE 802.15.4

Ideally, with the use of DTA, a controller could create specific time slots for transmission that can eliminate carrier sensing and waiting times that are part of the 802.15.4 MAC protocol. However, for fair comparison, we still use the CSMA MAC layer with DTA scheduling to include the waiting times and backoffs if they occur. The proposed technique utilizes the existing wireless standard without introducing extra control overhead or disruption of network protocol hierarchy.

The payload of simulated packets was set to 100 bytes to mimic the small size of packets in sensor applications. Traffic generation from the application of source nodes was simultaneously executed according to a CBR (*Constant Bit Rate*) model. We configure the leaf nodes (the nodes near the bottom of tree topologies) with pending traffic in simulations. These nodes deliver their data to the sink in a multi-hop fashion. For example, in the case of 1 packet/sec data generation rate, leaf node *n1* transmits 1 packet to its next hop neighbor *n2*, and *n2* transmits 2 packets which includes its own sensing data and data from the previous leaf node *n1* to the next hop and so on. We performed the simulations with various network loads with data generation rates of 1, 3, 6, 9, 14, 16, 20, 24 and 27 packets/second. We test the network with offered loads up to 27 packets/second to ensure that the data intensive condition is verified in experiments (e.g., SHM applications could result in the traffic load of 6 packets/second). For the radio propagation model, a two-ray path loss model was chosen, and fading was not considered in the simulations. The reported simulation results are averaged over 10 runs. Each simulation run was for 200 seconds of simulation time.

We report on *packet success ratio*, *overall packet delay*, and *average delay of successful packets* for both DTA and IEEE 802.15.4 CAP schemes. We use CSMA/CA as the abbreviation of IEEE 802.15.4 CAP mode in the rest of Chapter 3. We define these parameters as follows.

Packet Success Ratio: The packet success ratio represents the ratio of the transmitted packets that reach the sink node successfully to the total number of generated packets from the application layer. A higher packet success ratio implies a more reliable network. In other words, the network is less susceptible to dropped packets caused by packet interference or collisions if the packet success ratio is high. In addition, we infer the availability of the network by the packet success ratio. If the packet success ratio of a network is lower than 70%, this network is marked as unreliable because the correctness of received sensed data at the BS may be insufficient. This threshold is adjustable according to the requirements of sensor network applications.

Overall Packet Delay: Overall packet delay corresponds to the resident time in the network of all packets received by the sink node, after they leave the source nodes. The one exception in which the network is considered to be erratic and results in infinite overall delay is when the packet success rate violates the previously mentioned threshold (less than 70%).

Average Delay: The average delay of successful packets represents the average time for a packet to successfully reach the sink node.

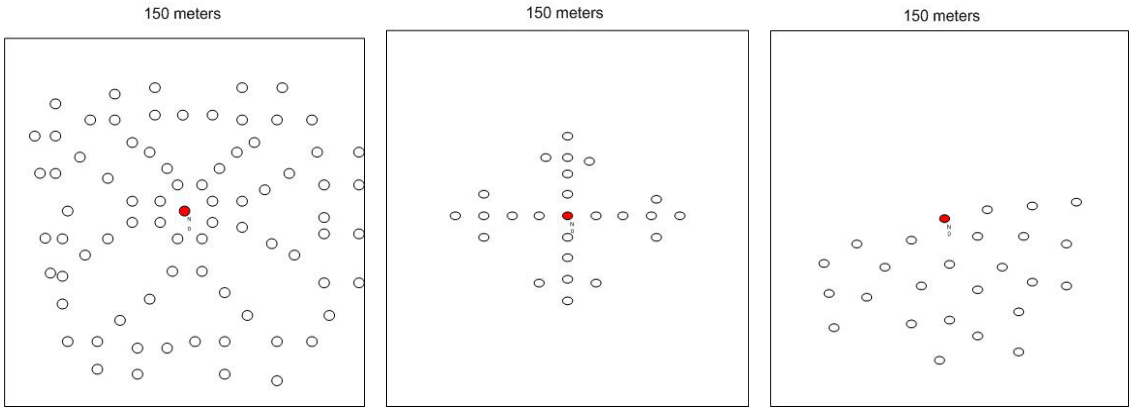

(a) (b) (c)

Figure 3-2 Network Topologies: (a) Dense topology (b) Sparse topology (c) Medium Dense topology

We experimented with three different network topologies: Dense topology, Sparse topology, and Medium Dense topology. The dense topology (Figure 3-2 (a)) consists of 80 nodes positioned within a 150×150 m^2 flat area while the sparse (Figure 3-2 (b)) and medium dense (Figure 3-2 (c)) topologies include about 25 nodes in the same area. Filled circles indicate sink nodes and unfilled circles are sensor nodes. The difference between the medium dense topology and the sparse topology is the density of network nodes. Thus, the chance for collisions in the medium dense topology is higher due to the high node density.

3.2 PERFORMANCE EVALUATION

A. Dense Network Topology

Figures 3-3 to 3-5 show the simulation results for the dense network of 80 nodes. In Figure 3-3(a), the data generation rate is defined as the number of packets transmitted by each sensor per second. This figure represents the packet success percentage as the data generation rate increases. It shows that with low data generation rates, the packet success ratio with DTA is around 95%. The ratio decreases to 40% as the data generation rate increases to 24 packets/second. This is because the total traffic generated in the network exceeds the channel capacity (250 Kbps). On the other hand, the packet success ratio with CSMA is as low as 20% because of the high rate of collisions from both the hidden terminal problem and the excessive traffic load in the dense network. The overall packet delay with DTA increases almost linearly (Figure 3-3(b)) with the increase in network traffic load. Here, the load is equal to the sum of the data transmitted by source nodes. This trend is significantly affected by the data generation rates and the number of DTA transmission schedules. In a dense network, DTA creates a long

sequence of schedule. Thus, the overall packet delay is also increased proportionally. For example, at 173 Kbits per second traffic loads the overall packet delay is about 46 seconds, and the delay becomes infinite at 1.3 Gbits per second traffic loads due to the low packet success ratio. The overall packet delay of the CSMA scheme is infinite even at lower data generation rates. Therefore, the DTA considerably outperforms CSMA in the dense network.

Figures 3-4(a) and (b) represent the average delay of successful packets. From Figure 3-4(b), we see that the performance of DTA and CSMA are almost identical at lower data generation rates (0.5 and 1 pkt/sec). As the rates increase and create more packet interference, the CSMA delay performance starts to degrade while the DTA's delay performance is still acceptable. This phenomenon can be explained by the fact that while DTA reduces collisions of packets via scheduling of collision-aware transmissions, CSMA results in collision of packets due to the hidden terminal problem. However, this difference disappears when both schemes operate at high data generation rates (Figure 3-4(a)). As the traffic in the network generated by each sensor exceeds the channel capacity (250 Kbps or approximately 20~27 packets/sec/source node), both DTA and CSMA schemes suffer from the loss of a large numbers of packets. Meanwhile, DTA's performance worsens due to long transmission sequences in the dense network. In other words, the longer delay caused by lengthy DTA transmission schedules is a concern of DTA scheduling in the dense networks with high traffic loads.

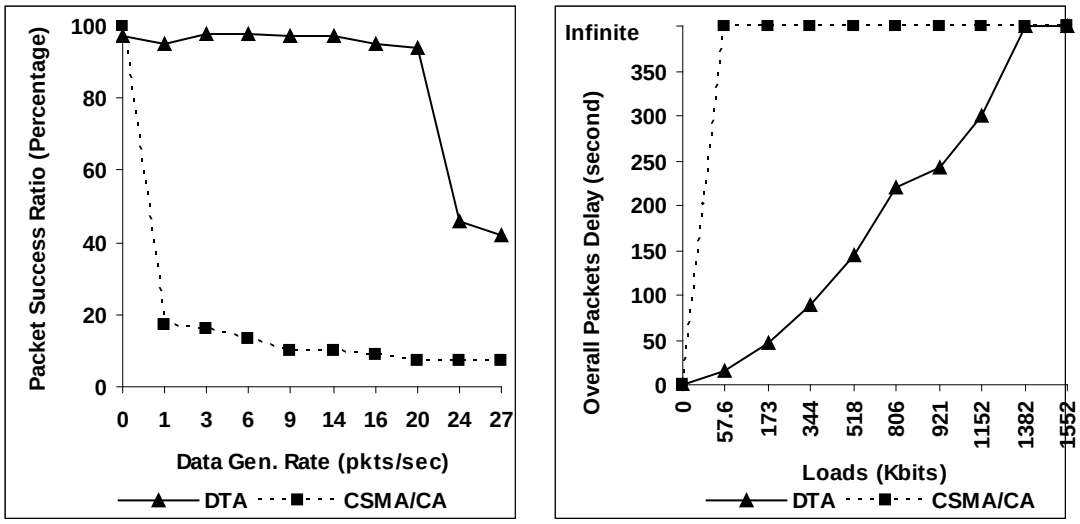

(a) (b)

Figure 3-3 (a) Packet Success Ratio (b) Overall Packet Delay in Dense Topology

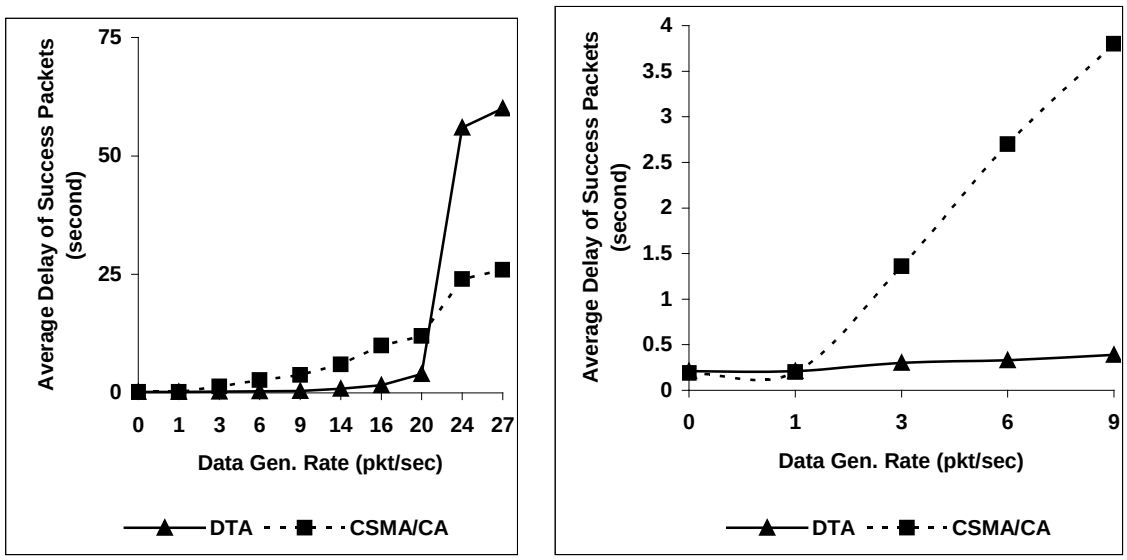

(a) (b)

Figure 3-4 (a) Average Successful Packet Delay (b) Zoom-in on Average Success Packet Delay in Dense Topology

In order to better explain the relationship between packet success ratio and packet delay, Figures 3-5(a) and (b) show the cumulative distributions of packet delay for DTA and CSMA (note the difference in scale of the Y axes). For example, in Figure 3-5(a) at 1 packets/sec

generation rate, approximately 85% of the packets are received by the sink node within 0.21 seconds: all packets are received 0.35 seconds. At the 27 pkt/sec generation rate, 40% of packets are received within 60 seconds. The other 60% are lost and their delay is infinite. The high delay and infinite latency are due to the excessive network load.

Figure 3-5(b) shows that CSMA has a much lower percentage of successfully received packets by the sink node. According to both cumulative distribution plots, increases in the network load will result in packet delay increases and packet success ratio decreases. As we observe, DTA considerably outperforms CSMA in terms of both packet delay and success ratio.

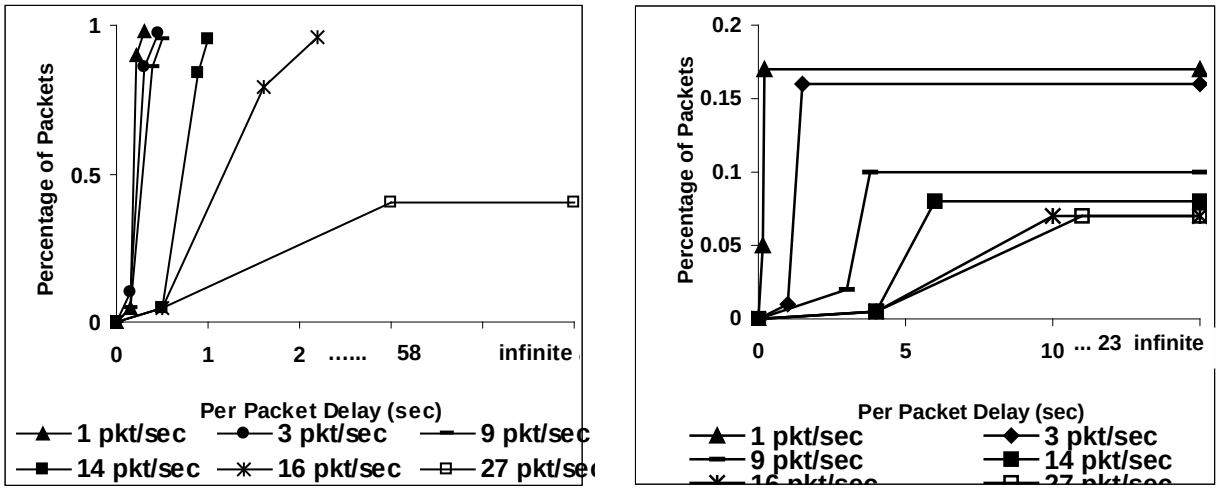

(a) (b)

Figure 3-5 (a) CDF Plot of DTA (b) CDF Plot of CSMA/CA in Dense Topology

B. Sparse Network Topology

Figures 3-6 to 3-8 show the simulation results for the sparse network with 25 nodes. Figure 3-6(a) shows that with data generation rates (1 ~ 27 pkt/sec) for each source node, the packet success ratio of DTA is around 98%. On the other hand, CSMA performs much worse in terms of the packet success ratio. At low rates (0.5 and 1 packet/sec), CSMA can deliver around 70% of the data to the sink node since partial packet collisions are alleviated by the exponential

back-off procedure. When the traffic load increases, the back-off procedure becomes inefficient and, eventually, the network is overloaded with collided or lost packets; thus, the packet success ratio drops to 30%.

Figure 3-6(b) reports on the overall packet delay. There exists a strong relationship between the packet success ratio and the overall packet delay. The overall packet delay using DTA increases almost linearly. This trend once again depends on the data generation rate and the number of DTA transmission schedules. In the sparse network, the DTA does not create a long sequence of schedule. The overall packet delay decreases proportionally, as compared to the dense network. For example, at a data generation rate of 9 packets/sec, the overall packet delay of the dense network is about 140 seconds while the delay in the sparse network is only 9 seconds. The overall packet delay with CSMA can be infinite at higher data generation rates (high load) but the delay at lower data generation rates is fairly low. This implies that in the sparse network, CSMA performs well at lower data generation rates but DTA considerably outperforms CSMA at higher data generation rates.

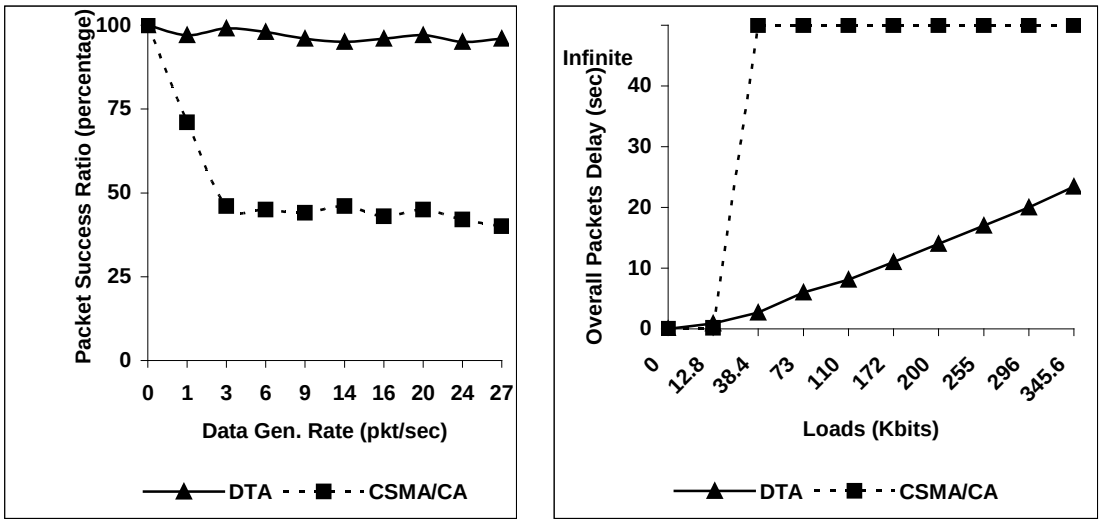

(a) (b)

Figure 3-6 (a) Packet Success Ratio (b) Overall Packets Delay in Sparse Topology

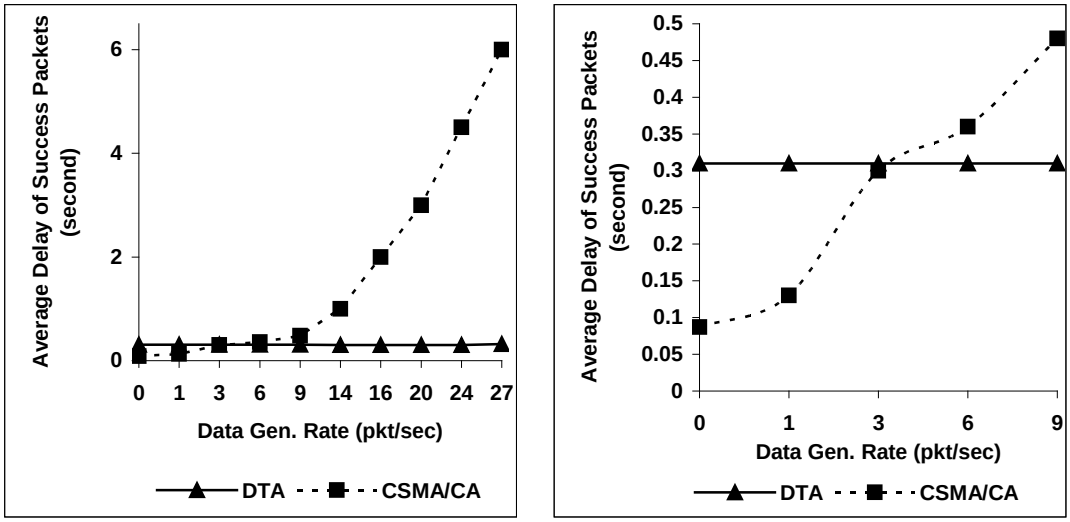

(a) (b)

Figure 3-7 (a) Average Success Packet Delay (b) Zoom-in on Average Success Packet Delay in Sparse Topology

The average delay of successful packets is presented in Figures 3-7(a) and (b). Figure 3-7(b) shows that the performance delay with CSMA is a little better than with DTA for lower loads (0.5 and 1 pkt/sec). This can be explained by the buffer time in DTA and the minimum contention time in CSMA. Note that the average delay of a successful packet in the sparse DTA network is still less than in the sparse CSMA network unlike in the dense network where the DTA schedule has a long sequence.

Figures 3-8(a) and (b) plot cumulative distributions of the packet delay. We observe that as the traffic load increases, the packet delay increases and the packet success percentage decreases. However, the DTA curves overlap for all loads. This shows that the performance of DTA remains mostly independent of the network traffic load unlike CSMA. It is obvious that DTA considerably outperforms CSMA-CA. It should be noted that the topology size does not degrade the DTA performance as severely as CSMA-CA.

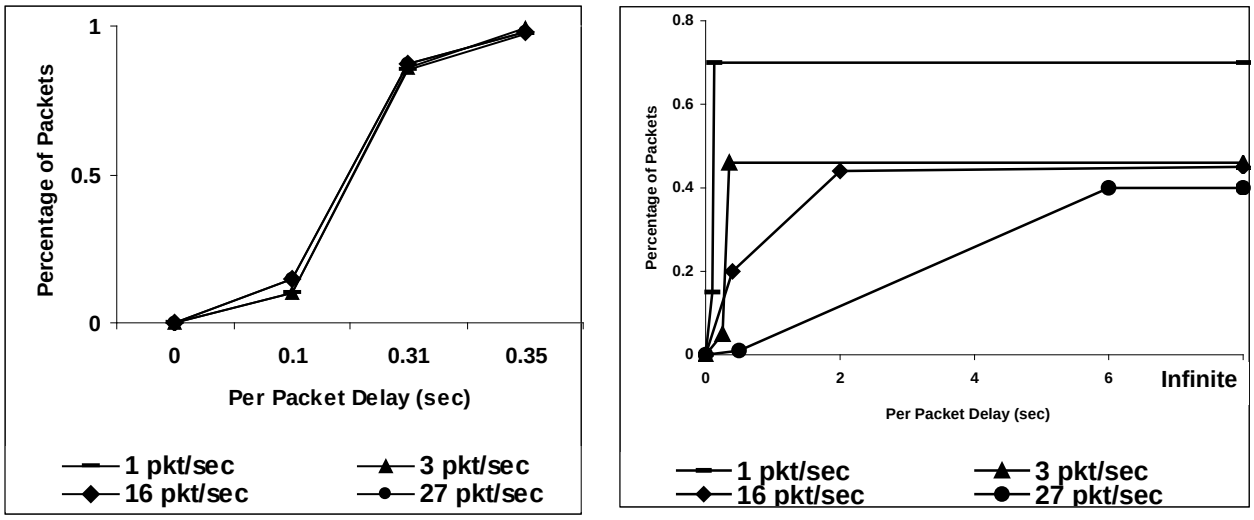

(a) (b)

Figure 3-8 (a) CDF Plot of DTA (b) CDF Plot of CSMA/CA for Sparse Topology

C. Impact of Topology: Medium Dense Network vs. Sparse Network

In this section, we investigate the effect of varying the network topology on the performance of DTA and CSMA schemes. In comparison to the sparse network, the medium dense network is characterized by a higher density of sensor nodes resulting in higher degree of mutual interference among the sensor nodes as well as higher collision rates. The sparse network represents a star-tree topology while the medium dense network is a random mesh topology. The results of the simulations illustrate trends in the network response with different types of topologies when DTA and CSMA schemes are employed. We select these two networks with identical numbers of nodes to setup a fair topological comparison study.

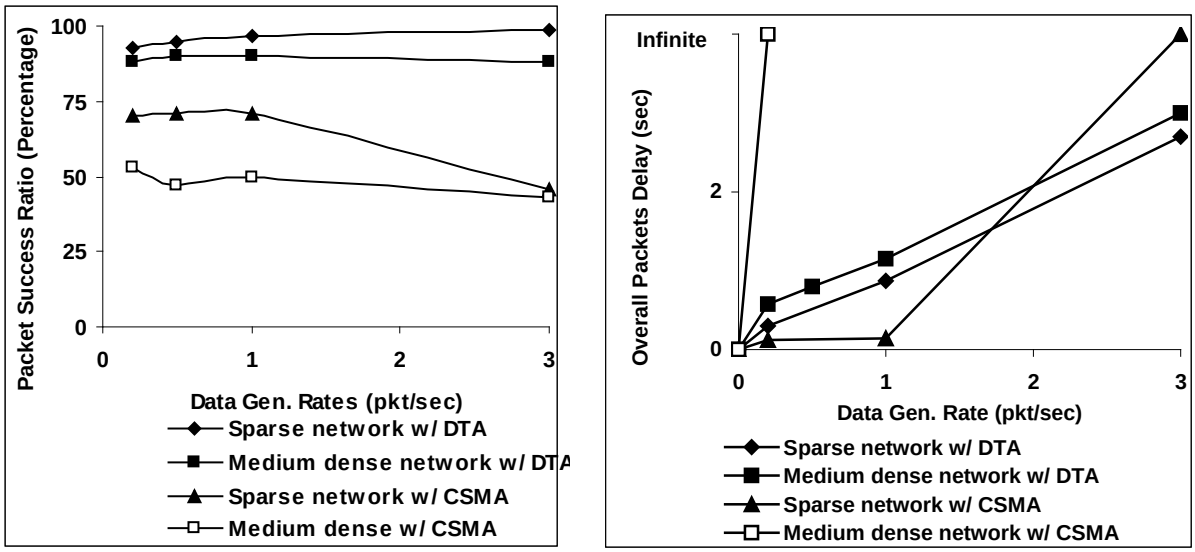

(a) (b)

Figure 3-9 (a) Packet Success Ratio Comparison (b) Overall Packets Delay Comparison for Medium Dense and Sparse Topologies

Figures 3-9 (a) and (b) show the performance of DTA and CSMA in the medium dense network (Figure 3-2 (c)) and the sparse medium star-tree topology (Figure 3-2 (b)). We plot the packet success ratio curve (Figure 3-9 (a)) and the overall packets delay curve (Figure 3-9 (b)) for each access scheme in both medium dense and sparse topologies. It is obvious that the DTA success ratios in both topologies are superior to that of CSMA. The overall packet delay with CSMA becomes infinite at much lower data generation rates with the medium dense network compared to the sparse network, but it is still worse than DTA at higher data generation rates. The overall packet delay with DTA in the medium dense topology is slightly larger than the delay in the sparse topology as the medium dense network decreases concurrency opportunities inherent to DTA scheduling.

To summarize, we observe that the network topology does not impact DTA performance dramatically, while CSMA is very sensitive to the actual network layout.

3.3 ANALYSIS AND CONCERNS

So far, we have executed the performance comparison of the algebraic cross-layer optimization scheme (DTA) and the existing 802.15.4 CSMA-CA scheme for data delivery in wireless sensor networks. We demonstrated that, in the cases of delivery reliability and latency, DTA considerably outperforms CSMA-CA. In particular, the percentage of transmitted packets reaching the sink node improves at least by 20% and the overall packet delay with DTA increases linearly with the increase in the network traffic load. DTA enables better utilization of sensor networks for a wide class of critical applications generating heavy network loads.

While the DTA approach provides a substantially positive influence on the performance in sensor networks, some concerns also come along. The following list enumerates disadvantages of the scheduling approach:

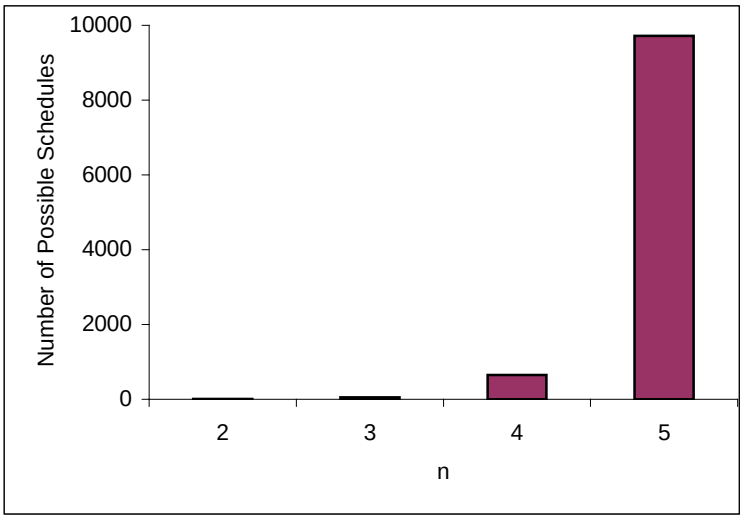

Figure 3-10 Number of Possible DTA Schedules vs. n (Elementary Transmissions)

Scalability: In Figure 3-4 (a), we discovered that the longer delay caused by lengthy DTA transmission schedules is a weakness of DTA scheduling in large networks. This problem

is worse in the situation where network load is intensive and packet retransmissions are required. It may lead to high delays and challenge the scalability of DTA. The scalability concern caused by considerable delays in a large DTA network has been demonstrated by the simulation study. We will next describe a complexity analysis of DTA schedule generation to show the difficulty of searching for a proper DTA schedule.

DTA scheduling may be expensive due to its combinatorial nature. The number of alternative schedules grows exponentially with the number of sensor nodes and the number of elementary transmissions participating in a query (see Figure 3-10). In general, for a query tree with *n (n>1)* elementary transmissions, the total number of all possible complete DTA schedules involving those transmissions will be equal to the number of permutations of *n* transmissions without repetitions multiplied by the number of total variations of the three DTA operations with repetitions of length *(n-1)*:

$$\textit{Number of Possible DTA schedules (n)} = n! \times 3^{(n-1)}$$

For example, with two elementary transmissions *t1* and *t2* we can generate $2! \times 3^{(2-1)} = 6$ schedules, namely: *o(t1,t2), o(t2,t1), c(t1,t2), c(t2,t1), a(t1,t2), a(t2,t1).* In order to cope with the expected scheduling complexity, the DTA-optimizer should utilize *approximate* scalable techniques, such as randomized algorithms [67]. Meanwhile, it is well-known that performance of the approximate optimization schemes degrades with increase in the task complexity.

In addition to the concern about generating optimal schedules for a large-scale networks [47], control overhead [50] [51] is another concern. To build a successful DTA schedule, the optimizer requires information from each node in the network. The overhead message of delivering global data to the DTA schedule optimizer is vital for correctness of the schedule and its message complexity is *O(N)* where *N* is the total number of sensors in the network. If the

network topology is changed (e.g., addition or deletion of nodes, node mobility, etc.), the DTA schedule needs to be re-generated and this introduces additional overhead cost. This concern makes questions about the feasibility of the scheduling approach, especially in dynamic and mobile networks. More details about this concern will be illustrated in Section 5.5.

Global Network Information: An optimal DTA schedule relies on lower layer information such as coverage of collision domains and/or estimated amount of scheduled data and energy requirements. Such information belongs to all sensors of a network, so it is mandatory to exchange these data between sensors and the BS before the DTA schedule can be generated by the BS. In other words, the DTA schedule generation requires global network information to for completion. Since a sensor network is a dynamic and error-prone environment, obtaining error-free global network information becomes more challenging, especially in a large network. Other TDMA scheduling approaches likes DRAND rely on local network information to setup distributed time slots schedules [80]. Thus, they may introduce less overhead to collect local information and to construct the time slot schedule, compared with DTA. Message complexity of DRAND is $O(n)$ where n is the size of the 2-hop local neighborhood. In other words, it is more scalable.

Determinism and Sensitivity to Incorrect Estimation of the Global Network Information: In addition to the need of global network information, accuracy of such information is also important for creation of DTA schedule. Because the DTA framework is designed to create an optimal schedule, the effective schedule generation is not possible with incorrect network information. Moreover, the generated schedule is deterministic until a new schedule is created. Therefore, before a new schedule is updated by the BS, the whole network will suffer from using the old and inefficient schedule (that was perhaps generated with incorrect

estimation of global network information) if the network is changed considerably. Let us suppose that the topology changes as shown in Figure 3-11. Then, the transmissions of *n4 – n2* and *n5 – n3* will interfere after the topology is updated. Thus, the topology change requires the update of the DTA schedule to address this issue. Frequent updates of DTA schedules are an option but the cost of extra control overhead from the frequent updates brings new concerns. Thus, a trade-off exists between effective DTA schedules and control overhead. We will evaluate the impact of this trade-off in Section 5.5.

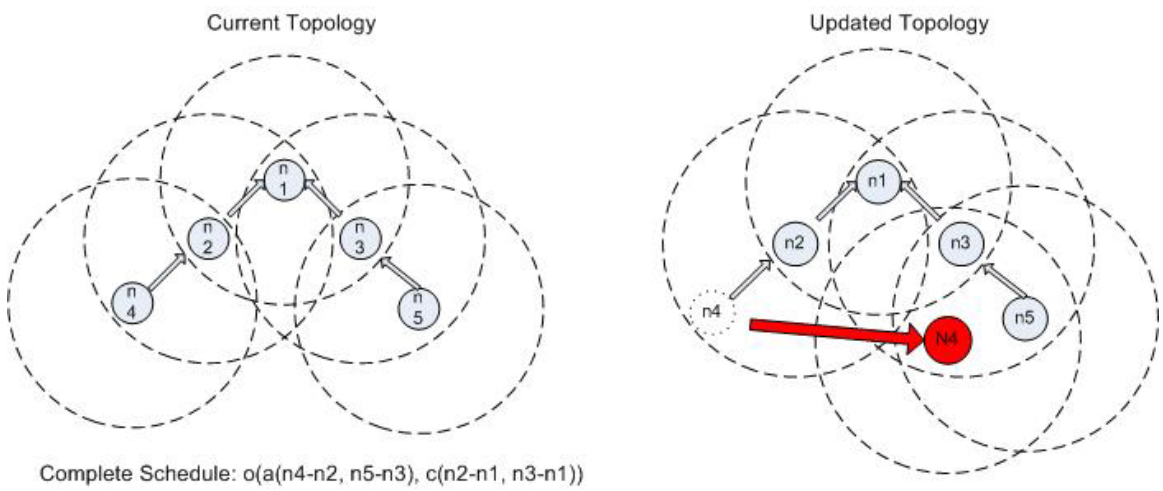

	TS 1	TS 2	TS 3
n2-n1			•
n3-n1		•	
n4-n2	•		
n5-n3	•		

	TS 1	TS 2	TS 3
n2-n1			•
n3-n1		•	
n4-n2	•		
n5-n3	•		

Figure 3-11 Demonstration of Changed Topology to Correctness of DTA schedule

4.0 DATA DELIVERY USING HYBRID CHANNEL ACCESS - PROBABILISTIC TRANSMISSION AND HEURISTIC SCHEDULING

After the exploratory analysis of DTA vs. IEEE 802.15.4 CSMA/CA in last chapter, we discussed the primary concerns with the query-scheduling concept – DTA and the contention access concept – CSMA/CA. Concerns with CSMA/CA were also explained in Chapters 1 and 2. With regards to the scheduling approach, while it is able to reduce time and energy waste by eliminating possible transmission collisions, it simultaneously introduces some problems as follows. 1. Techniques like LMAC, AI-MAC, DTA, and DRAND feature considerable control message overhead for building data delivery schedules. 2. A sensor network is an error-prone and dynamic environment; so it may often be difficult to maintain deterministic schedules. For instance, packet retransmission for dropped packets (due to channel conditions) may lead to high delays, especially in a large multi-hop network [47] [62] [84]. 3. Generation and delivery of an optimal schedule for data transmissions is challenging in a large-scale sensor network [47]. These concerns introduce questions about the scalability of the scheduling approach and drive the development of distributed and energy-efficient MAC protocols in wireless sensor networks that can still handle DIAs.

We propose robust protocols that combine random channel access with heuristic-based scheduling to avoid possible collisions in the special-purpose DISNs. First, we configure random probabilities for packet delivery in a protocol called *Cyclic Probabilistic Transmission protocol*

(CPT) [85]. Consequently, channel access of all sensors in networks becomes random and distributed. By tuning the random transmission probabilities, our protocol can reduce the performance degradation with increase in network load.

Next, observations from the scheduling protocols like DTA show that well-prepared transmission schedules in networks can enhance network performance considerably. We design a protocol called *Neighbor Aware Probabilistic Transmission protocol* (NAPT) to heuristically schedule transmissions in dense sensor areas with high chances of collisions. This way, potential collisions can be reduced and the network performance improves [85]. In other words, NAPT utilizes a hybrid approach that adopts the strength of scheduling access while maintaining scalable and highly distributed channel access using probabilistic strategies. Note that the NAPT protocol utilizes (limited) topological information to assist channel access. This idea was also adopted in other previous works like Sagduyu et al. [79]. Both of the protocols apply the geographical information of sensor locations to enhance scheduling in channel access but our proposal reduces dependence of overhead of control messages considerably and is applicable to the special-purpose DISNs.

Overall, CPT is a hybrid scheme with tight relationship with random channel access while NAPT is a hybrid scheme that is close to scheduling channel access. As a result, both protocols considerably outperform the existing CSMA/CA-based MAC protocols, like IEEE 802.15.4, while matching the scalability and improving reliability of deterministic scheduling approaches with fewer control messages. The performance of the 802.15.4 CAP mode is the baseline for performance comparisons. We also evaluate our proposed work with the distributed scheduling protocol – DRAND [80]. Figure 4-1 provides a qualitative summary of the different

MAC schemes in terms of the scalability of access method and expected utility (transmission efficiency/throughput without losing packets) in Data Intensive Sensor Networks.

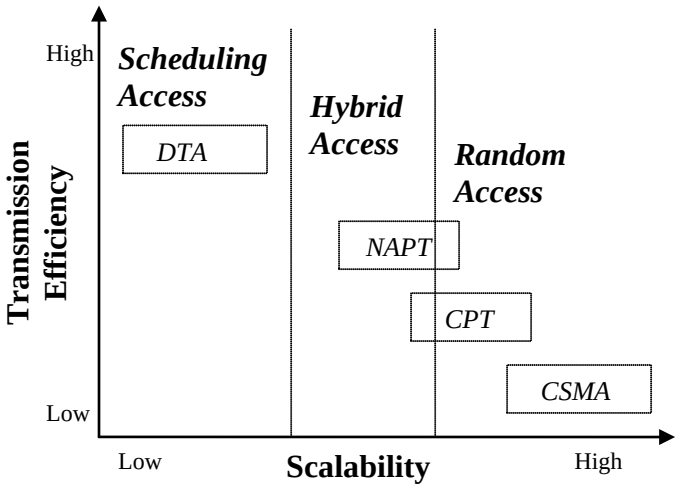

Figure 4-1 General Framework for MAC Schemes Classification

4.1 SYSTEM MODEL

Conceptually our approach combines the advantages of both scheduling and random channel access. Time is equally slotted for the whole network. A sensor can transmit a packet at the beginning of a time slot and complete the transmission within the same time slot with a pre-defined probability. In the rest of this chapter, we assume the following system model:

- Every sensor uses the same radio transceiver and is able to transmit or receive on a common carrier frequency. All sensors adopt a uniform transmit power that covers a limited footprint. All sensors are stationary with a unique identification and are equipped with omni-directional antennas.

- Time synchronization is managed by the central base station using the beacon method [11]. Time is slotted and sensors are synchronized on time slots. During the time slot, a sensor can be either in transmit mode, receive mode or idle mode.
- Sensors deliver data towards a base station. Such data delivery results in a tree-like pattern. We assume that the data delivery tree has been pre-determined based on algorithms for constructing a data gathering tree [70]. Each sensor delivers a certain number of packets to its next hop periodically. We adopted the periodic traffic model as more appropriate for Data Intensive Applications. This model also represents a challenging scenario due to the large amount of data transmissions within a short period of time.
- Collisions may occur when a sensor receives more than one transmission simultaneously from different parties. We use the capture effect in our simulations – where the packet is correctly decoded by the receiver if the signal to interference ratio (SIR) exceeds a specified threshold.

4.2 DESCRIPTION OF CPT PROTOCOL

The CPT protocol assumes that delivery of every data frame is based on independent probabilities. Thus, for two sensor nodes N_i and N_j the probability of transmission in a time slot that starts at t is $P(N_i, N_j, t)$**.** By default the probability of transmissions are generated independently from a uniform distribution, so that the channel is fairly shared by every sensor in the network. If a transmission is successful in a given slot, a sensor node that has something to send will try again in the next slot with the specified probability.

Consider a sensor network with a tree topology of *N* one-hop transmissions. First, the CPT protocol reserves *N* time slots for each transmission. The choice of *N* would allow the CPT protocol to allocate at least 1 time slot per one-hop transmission. This would enable a worst-case scenario with a serial data delivery scheme that forces different transmissions to occur in consecutive time slots thus avoiding collisions completely. While avoiding collisions, the serial scheme underutilizes potential concurrency opportunities (where two sensor nodes in different collision domains could transmit simultaneously) and may result in increased transmission latency.

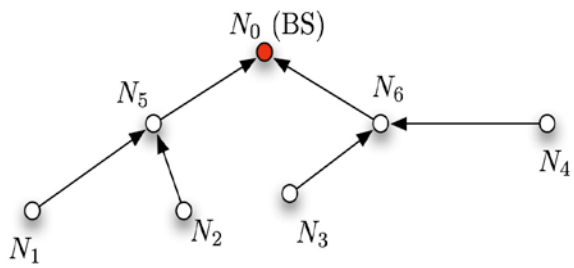

DTA	1	2	3	4	5	6
N_1 ~ N_5	1	0	1	0	1	0
N_2 ~ N_5	0	1	0	0	0	1
N_3 ~ N_6	1	0	0	0	1	0
N_4 ~ N_6	0	1	0	1	0	0
N_5 ~ BS	0	0	0	1	0	0
N_6 ~ BS	0	0	1	0	0	1

Probabilistic Transmission	1	2	3	4	5	6
N_1 ~ N_5	0.3	0.5	0.8	0.4	0.9	0.1
N_2 ~ N_5	0.6	0.3	0.9	0.3	0.1	0.7
N_3 ~ N_6	0.9	0.7	0.3	0.5	0.3	0.1
N_4 ~ N_6	0.3	0.3	0.1	0.8	0.7	0.9
N_5 ~ BS	0.5	0.5	0.2	0.7	0.9	0.1
N_6 ~ BS	0.1	0.2	0.5	0.6	0.4	0.9

Serial Transmission	1	2	3	4	5	6
N_1 ~ N_5	1	0	0	0	0	0
N_2 ~ N_5	0	1	0	0	0	0
N_3 ~ N_6	0	0	1	0	0	0
N_4 ~ N_6	0	0	0	1	0	0
N_5 ~ BS	0	0	0	0	1	0
N_6 ~ BS	0	0	0	0	0	1

Figure 4-2 Transmission Probability Matrix of DTA, Probabilistic Transmissions and Serial Transmissions

The CPT protocol maintains an $N \times N$ Transmission Probability Matrix (TPM), as illustrated in Figure 4-2, where each row corresponds to a transmission between two neighboring sensors while each column represents the time slot for the transmission. Each cell of the TPM holds a probability $P(N_i, N_j, t)$ of the data transmission $N_i \sim N_j$ to occur within a given time slot t. An individual sensor only needs to know its transmission probabilities in the N time slots and these probabilities repeat periodically. Figure 4-2 illustrates the concept of TPM. The table on the bottom right corresponds to serial (sequential) data delivery where each transmission is deterministically assigned to one time slot. This is reflected with each row having $P(N_i, N_j, t) = 1$ for one time slot and $P(N_i, N_j, t) = 0$ for the rest of them. The table on the bottom left assigns some non-zero probabilities for each transmission to occur at each time slot. The second matrix has a higher degree of concurrency of data delivery, but also has a higher probability of collisions. For instance, consider the example of transmissions from N_1 and N_2 to N_5 during time slot 1 in Figure 4-2. With probabilistic transmission (left hand side), the chance of concurrent transmissions is 0.18 while the chance of concurrency with serial transmission is 0. A potential optimal schedule with DTA is also shown (top) where the concurrency opportunity is 1 in each time slot (we assume that N_1 and N_2 are in the same collision domain and so on). By adjusting the probabilities in the TPM we can optimize the concurrency/collisions tradeoff in the CPT protocol. The consideration of tuning the concurrency/collisions tradeoff is beyond the scope of this chapter, although we return to it in Chapter 6 of the dissertation.

Each TPM specifies one network transmission cycle. By default, the length of a time slot is around 5.7 ms if the channel data rate is 250 Kbps (*Length of a time slot = (Data packet size + Ack packet size)/channel data rate + Propagation Delay*). Suppose that there are 30 one-hop transmissions in the network. Then the duration of a network transmission cycle will be 171 ms

(30×5.7). In other words, a base station may receive a complete sample of sensed data from all sensors within 171 ms provided no frame is lost due to errors. This condition may not hold if collisions occur in the system. Therefore, while a TPM represents a complete data delivery cycle for a whole network, it does not guarantee a complete sample of sensed data. It should be noted that the number of time slots can differ from the number of transmissions in a TPM. Different configurations of TPMs can reflect different requirements of sensor applications. For the ease of presentation, we choose the $N \times N$ format to present the protocols of this paper. The TPM table is executed repeatedly for continuous data sensing and delivery in the network.

By default CPT configures a time slot equal to the duration of processing and transmitting a packet with 130 bytes and an acknowledgement. This is the maximum packet size allowed – so the configured time slot will cover the time needed for delivering any smaller packet. In addition, we try to keep the time slot as short as possible. Our intention is to limit unnecessary idle listening that occurs after completion of a frame delivery in a time slot and to maintain savings on packet delay. An alternative policy would be to set up a time slot so that each sensor would try to send all data pending in its buffer. For example, the transmission (N_1~N_5) would try to send all pending data stored in the queuing buffer of the sensor N_1, with a probability P within the first timeslot. If all pending data cannot be delivered to the desired sensors, the remaining data will be sent in the next time slots with corresponding probabilities. In theory, this policy would not affect the average system throughput with the CPT even though the number of probabilistic decisions on data delivery is reduced by efficiently utilizing entire duration of a time slot. The system throughput is statistically unaltered because of random probabilities in the CPT. The side effect of such a policy is the increase in complications in terms of how to frame data for transmission (i.e., data segmentation), compared with the default option.

Another approach would be defining the duration of a time slot dynamically. Since we expect higher traffic demands on a sensor with multiple transmission links, the size of a time slot for such a “high traffic sensor” could be set to be of larger value than that for a “low traffic sensor”. For instance, the sensors surrounding a BS typically have more packets to send to the BS, compared with leaf sensors. As a result, CPT may configure leaf sensors with time slots equal to X seconds while busier sensors may be configured with the time slot equal to $4X$ seconds. We have not explored these options in this dissertation, but they are part of potential future work.

Figure 4-3 shows the first execution cycle of the CPT algorithm. The next cycles will re-use the TPM generated during the first cycle. The variable *tx* represents a frame transmission while the variable *ts* indicates a time slot. We denote the set of time slots of a *tx* as TS_{tx}. First, a row of TPM that represents a sensor’s transmission probability in all time slots is generated in lines 1 and 2. The created probability *tx.ts.prob* here is the previously discussed $P(N_i, N_j, t)$. Next, we apply the *Probabilistic Process* (PP) that is described in line 3 to determine the transmission decision of the *tx*. Through these steps, sensors can generate their own probabilities and determine transmissions independently in a scalable and distributed fashion.

```
CPT (tx)
{
        /* Initialize. * /
        /* TPM Generation for tx. * /
1       for (ts ∈ TS_tx ∪ {tx})
2           tx.ts.prob = Uniform(0,1);
        /* Decision of Transmission at ts.* /
3       if (tx.ts.prob ≥ rand(0,1))
4           tx wins the transmission at ts;
5           ts++;
}       /* End of CPT. * /
```

Figure 4-3 CPT Cycle Specification

Figure 4-4 shows the flow chart for a frame transmission with the CPT protocol. If there is pending data that has arrived at a sensor's transmission queue at t, the sensor will decide to transmit the frame with the probability $P(N_i, N_j, t)$. The higher the value of probability is, the higher probability of a frame to be transmitted by a sensor in that slot. Every frame delivery must pass the Probabilistic Process to earn its transmission opportunity. If a frame does not pass the Probabilistic Process, it will be discarded and the transmission attempt will be repeated within the next delivery period.

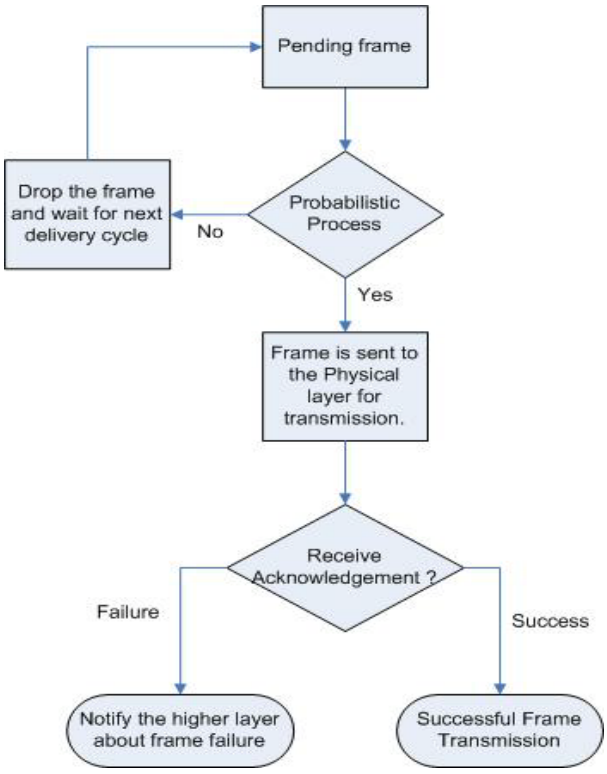

Figure 4-4 Flow Chart of a CPT Frame

4.3 DESCRIPTION OF NAPT PROTOCOL

The performance of the CPT protocol degrades in dense sensor networks due to high probability of packet collisions as shown later. To address this problem we propose the NAPT protocol where each sensor maintains information about the neighbors' hop counts to the BS in order to determine (in a distributed way) if it is in a densely populated area. Such information is gathered in the deployment phase when a data delivery tree is constructed with, for example, the algorithms described in [70]. These algorithms typically employ flooding to exchange data and to establish a path toward a BS or sink. While performing the flooding, sensors calculate their hop counts to the BS. Because wireless communication is omni-directional, sensors will overhear neighbors' transmissions that are within two hops. After the hop count is determined by all sensors, the BS broadcasts the subscription for data of interest to the network. Those sensors that receive the subscription relay the subscription as well as information about sensors' hop counts to their neighbors.

Every sensor makes an attempt to build a neighbor table that includes neighbors' ID with the same hop count and plus or minus 1 and 2 hop counts. If the neighbor table is large for a sensor, the sensor belongs to a densely populated area and there is a high chance of transmissions encountering collisions. Otherwise, transmissions of the sensor seldom collide with other transmissions. Neighbors with the same hop count (1HC case) belong to one layer of the data delivery tree and so it is highly probable that they will initiate data transmissions simultaneously due to continuous and periodic traffic patterns (assumed here for DIAs). If sensors with the same hop counts start transmissions together, it is foreseeable that collisions will occur. In addition, the neighbors with plus or minus 1 and 2 hop count (2HC case) can cause collisions as they

belong to the same collision domain. Performance comparisons taking into account neighbors with the same hop count and plus or minus 1 and 2 hop count are evaluated in our simulations.

After creating the neighbors tables, the NAPT protocol specifies (in a distributed fashion) the order of transmissions in dense areas. To do this, each sensor with a neighbor table compares its ID with neighbors' ID to determine a transmission sequence for collision avoidance. A sensor's ID is a unique numerical value so the comparison calculation can be done easily by sensors. Each sensor will deterministically schedule its transmissions based on the following rule: the sensor with a lower ID number will deliver traffic earlier; and the sensor with a higher ID number will transmit later. Consider an example where a sensor with two neighbors of the same hop count is located in an area where collisions are highly likely. Let us assume that the IDs of the sensors are 3, 5 and 11 correspondingly. Sensor 3 will deliver the data immediately whenever the periodic event occurs while sensor 5 will delay its transmission for one time slot and sensor 11 will delay its transmission for two time slots. With the transmissions from sensor 5 and sensor 11 being delayed, the potential for collisions will be alleviated. This policy is applied recursively to the whole network.

A sensor with an empty neighbor table performs random channel access following the basic CPT protocol. In principle, the sensors with empty neighbor tables can also transmit deterministically. However, deterministic transmission relies on limited local information and may be subject to the hidden terminal problem.

Figure 4-5 shows the first execution cycle of the NAPT algorithm and includes three main sections: (1) creating Neighbor Tables, (2) checking availability of Neighbor Tables, and (3) data delivery. The variable *tx* denotes a frame transmission; the variable *ts* is a time slot. The set of neighbors of *tx* is defined as NA_{tx} while CA_{tx1} is the set of *tx* neighbors with the same hop

count and CA_{tx2} is the set of *tx* neighbors with the same hop count and plus or minus 1 and 2 hop count (assuming *tx*'s neighbor table is available). The term *NT* is an abbreviation for "neighbor table" and *hc* denotes hop count. First, the algorithm attempts to create a neighbor table for each *tx* (lines 1~10). Then it verifies the availability of *tx*'s neighbor table and if the *NT* is not available, the CPT algorithm is applied to *tx* (line 11). Finally, lines 13~19 select a transmission sequence in the neighbor table.

Figure 4-6 shows the flow chart of the NAPT frame. The highlight of the chart is the adoption of local information, which translates to alleviation of potential collisions. Meanwhile, it maintains distributed and scalable medium access control.

```
NAPT (tx)
{
        /* Initialize. */
        /* Build a neighbor table, Given
           hop count data of each sensor. */
1         for (na ∈ NA_tx ∪ {tx})
2             na.hc = hop counts of NA_tx ;
3             if (na.hc == tx.hc)
4                 na ∈ CAtx1 ;
5                 tx.NT is true ;
6             if (na.hc == tx.hc & na.hc == tx.hc ± 1, 2)
7                 na ∈ CAtx2 ;
8                 tx.NT is true ;
9             else
10                tx.NT is not true ;
        /* Check the availability of
           Neighbor Table.* /
11        if ( tx.NT is not true )
12            CPT (tx);
        /* Solve leadership in CA..* /
13        else
14            for (m ∈ CA_tx )
15                m.id = Id of CA_tx;
16            if (∀m ∈ CA_tx, tx.id ≤ m.id )
17                tx wins the transmission at ts;
18                CA_tx = tx ∉ CA_tx;
19                ts++;
}       /* End of NAPT. * /
```

Figure 4-5 NAPT Cycle Specification

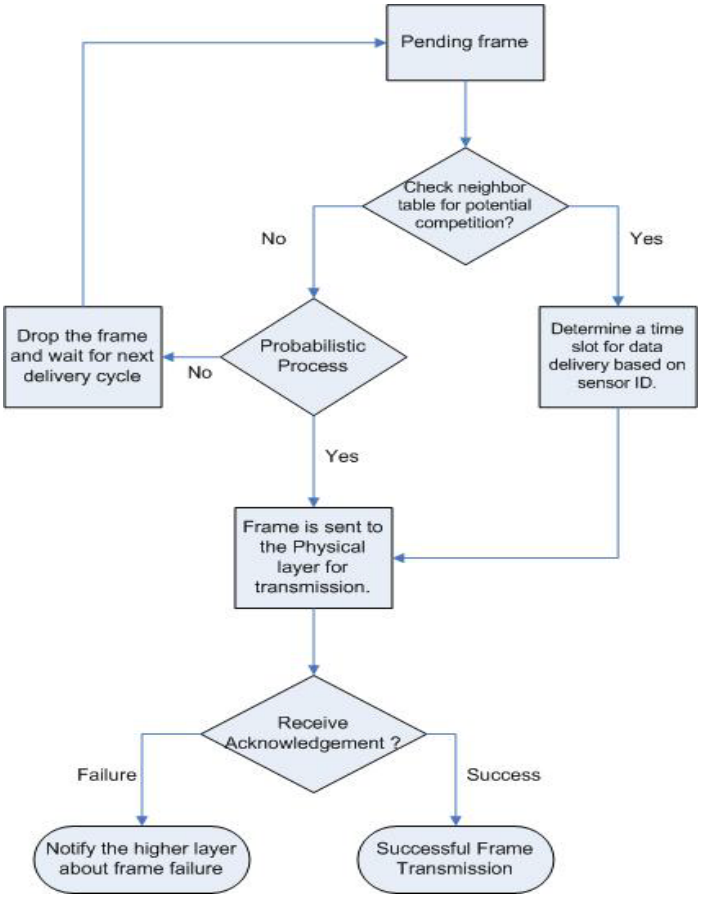

Figure 4-6 Flow Chart of NAPT Frame

To illustrate the NAPT protocol, consider the network topology in Figure 4-7 (a). In the first step, each node constructs its *neighbor table*. Such neighbor tables are generated for the cases of one hop count (1HC) and two hop counts (2HC) as shown in Figure 4-7 (b). Then, the transmission schedule of a sensor is built according to the neighbor table (see Figure 4-7 (c) and (d)). Transmission probabilities represent a cycle of repetitive patterns in the TPM as explained next. Consider the transmission N_0 ~*BS* and its 1HC neighbor table. Both N_0 and N_2 are within one hop of the BS so the transmission probability (the 1st row of the TPM in Figure 4-7(c)) of N_0 ~*BS* is set to 1 in the first time slot and to 0 in the second time slot, while probabilities of N_2~*BS*

(the 3rd row of the TPM in Figure 4-7 (c)) are in the reverse order. This pattern can be repeated in the following timeslots of TPM. The same policy applies to $N_3 \sim N_2$ and $N_4 \sim N_2$. Note that a CPT-like protocol is applied to $N_1 \sim N_4$ in the TPM of NAPT_1HC, since the neighbor table of N_1 is empty (Figure 4-7(b)).

We apply the same procedures to the case of 2HC. However, there is a major difference in the neighbor information. Consider the transmission $N_0 \sim BS$ and its 2HC neighbor table (Figure 4-7(d)). Again, both N_0 and N_2 are within one hop of the BS, so the probability of $N_0 \sim BS$ is 1 in the first time slot, and 0 in the second time slot. Consider now probabilities of the transmission $N_2 \sim BS$. The neighbor table of N_2 indicates that N_0 and N_2 are within one hop of BS, N_3 and N_4 would need two hops to reach BS, while N_1 needs three hops to reach BS. Hence, transmission probabilities of $N_2 \sim BS$ are 0, 0, 1, 0, 0 in time slots 1 to 5 respectively. A similar approach will apply to nodes N_1, N_3 and N_4. In the case of 2HC, it is also possible that a repetitive pattern is not long enough to cover all time slots in a TPM. In this case, such a pattern should be repeated until each time slot of the TPM is assigned to a transmission probability. We adopted this technique in the experimental evaluation of the proposed protocols. Another approach would be to fill the remaining TPM cells with ones resulting in the increase of conflicting transmissions due to different lengths of repetitive patterns for different transmission groups. Alternatively, we can put zero in the empty cells of TPM, reducing the number of potential collisions because of fewer transmission attempts. Finally, we can apply the CPT protocol to set up transmission probabilities of the empty cells. Further consideration of this topic is outside this dissertation. Note that other scheduling-based approaches, such as DTA and DRAND, would carefully schedule all transmissions to improve concurrency while alleviating collisions. NAPT is designed as a light-weight protocol reducing the scheduling overhead,

perhaps at the cost of transmission reliability. We provide an experimental evaluation of the NAPT overhead compared to DRAND's overhead in Section 4.5.

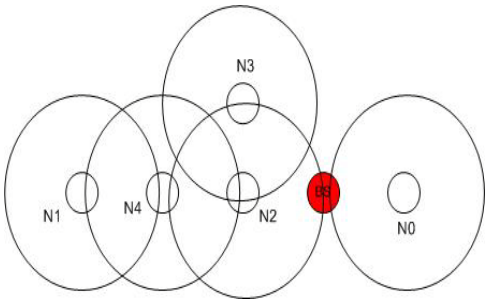

(a)

Neighbor Table of the N_id using 1HC	N_0	N_1		N_2			N_3		N_4		
Hop Count Number	1	3		1			2		2		
Neighbors' ID	2	None		0			4		3		
Neighbor Table of the N_id using 2HC	N_0	N_1		N_2			N_3		N_4		
Hop Count Number	1	1	2	1	2	3	1	2	1	2	3
Neighbors' ID	2	2	4	0	3 4	1	2	4	2	3	1

(b)

TPM of NAPT_1HC	TS 1	TS 2	TS 3	TS 4	TS 5
N_0 ~ BS	1	0	1	0	1
N_1 ~ N_4	CPT	CPT	CPT	CPT	CPT
N_2 ~ BS	0	1	0	1	0
N_3 ~ N_2	1	0	1	0	1
N_4 ~ N_2	0	1	0	1	0

(c)

TPM of NAPT_2HC	TS 1	TS 2	TS 3	TS 4	TS 5
N_0 ~ BS	1	0	1	0	1
N_1 ~ N_4	1	0	0	1	0
N_2 ~ BS	0	0	1	0	0
N_3 ~ N_2	0	1	0	0	1
N_4 ~ N_2	0	0	0	1	0

(d)

Figure 4-7 (a) Simple Network Topology; (b) Neighbor Tables of the NAPT (1HC table is shaded and 2HC table is transparent); (c) Transmission Probability Matrix of NAPT_1HC; (d) Transmission Probability Matrix of NAPT_2HC

Note that the NAPT_2HC scheme provides more reliable data delivery than NAPT_1HC. For instance, in the TPM of NAPT_1HC TPM (Figure 4-7 (c)), transmissions from N_2~BS and N_4~N_2 will collide in the second time slot. Meanwhile, no collisions occur with the NAPT_2HC

scheme. However, NAPT_1HC has a lower scheduling overhead. We provide more detailed comparisons of NAPT_1HC and NAPT_2HC in Sections 4.4 and 4.5.

4.4 ANALYSIS OF CPT AND NAPT

In this section, we provide a simple analytical framework to characterize performance of the CPT and NAPT protocols. Transmission power levels, multiple path interference and noise are not considered in this analysis. The network is represented as a directed graph $G = (N, L)$, where $N = (N_0, N_1, \ldots, N_n)$ is the set of sensors, and L is the set of wireless links. Link, (N_x, N_{x+1}), denotes the transmission from N_x to N_{x+1}.

Definition 1: Let $P(N_x, N_{x+1}, t)$, an element of a TPM, be the probability that sensor N_x decides to transmit a frame to sensor N_{x+1} in the time slot t. Then $(1 - P(N_x, N_{x+1}, t))$ is the probability that sensor N_x does not transmit a frame to sensor N_{x+1}. Please note that $P(N_x, N_{x+1}, t)$ is neither a random process nor a joint probability function. At time slot t, $P(L(N_x, N_{x+1}), t)$ is defined as the probability that time slot t is collision-free for Link (N_x, N_{x+1}).

$$P(L(N_x, N_{x+1}), t) = [P(N_x, N_{x+1}, t)(1 - P(N_{x+1}, N_j, t)) \prod_{i \in N_1(x+1) \setminus \{Nx\}} (1 - P(N_i, N_{x+1}, t))] \times g, \quad j \in N \qquad \textbf{(4-1)}$$

Here we model the $P(L(N_x, N_{x+1}), t)$ similar to a geometric variable. When we multiply $P(N_x, N_{x+1}, t)$ by $(1 - P(N_i, N_{x+1}, t))$s we assume that the probabilities $P(N_x, N_{x+1}, t)$ are independent. Moreover, this equation assumes that the probabilities do not change in the columns of a TPM and is correct for the first column. For subsequent columns, the actual probabilities in the columns of a TPM are dependent on the probabilities in the previous columns. This is because, the probability that a transmission occurs depends on the availability

of a packet, which in turn depends on whether a previous transmission was attempted and was successful. Link (N_x, N_{x+1}) is collision-free if and only if sensor N_x is transmitting while sensor N_{x+1} and its one hop neighbors except N_x are not transmitting in time slot t. Here, we refer one hop neighbors of N_{x+1} except N_x to i and any destination of N_{x+1} to j in Equation (4-1). In addition, Equation (4-1) uses the parameter g to reflect packet losses due to collisions between beacon and data packets and limitations of channel capacity. If g is set to 1, the equation excludes such effects caused by variations in time synchronization and physical channel limitations. Thus, the result will be an upper bound on the probability of successful transmissions, which only considers interference between data frames. The value of g in the Equation (4-1) ranges from 0 to 1.

In order to capture multi-hop transmissions, we use a variable *Hb* to represent the number of intermediate nodes that the packet has to pass to reach the BS. When a source node sends a packet to its next hop toward the BS, the probability of this transmission at the corresponding time slot t_1 is $P[\text{success} \mid N_{source}, N_{source+1}, t_1] = P(L(N_{source}, N_{source+1}), t_1)$. Suppose that the transmission was successfully forwarded. The node $N_{source+1}$ next intends to send the same packet to its next hop $N_{source+2}$. This time, the probability of a successful transmission at the corresponding time slot t_2 is $P[\text{success} \mid N_{source+1}, N_{source+2}, t_2] = P(L(N_{source+1}, N_{source+2}), t_2)$. Again, if the transmission was completed, this packet has *Hb-2* hops to forward and so on. This means that we can represent the multi-hop packet transmissions as a *Discrete Time Markov Chain* (DTMC) in which each state is the number of remaining hops toward the BS. Figure 4-8 depicts the DTMC model for multi-hop packet transmission. In this model, state *Hb* represents a source node with pending traffic toward BS while the state 0 is the absorbing state, i.e., the

packet has passed through *Hb* intermediate nodes and has arrived at the BS. The state in 0 is the steady state of the DTMC with arrival probability equal to 1.

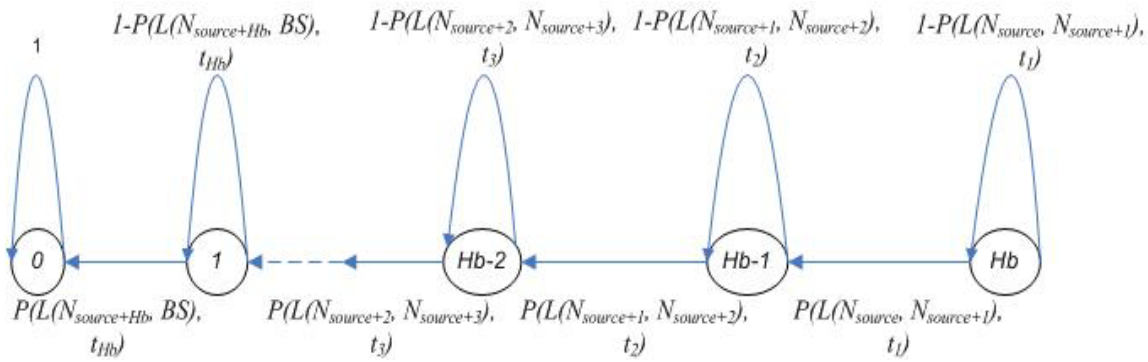

Figure 4-8 Discrete Time Markov Chain Model

Using the DTMC model we can calculate the expected time (i.e., number of time slots) required to deliver a data packet to the absorbing state from a state between *1* and *Hb*. Thus, we can determine the average response time for a packet from any source node to BS. The response time increases linearly with the number of intermediate nodes for the transmitted packet. We therefore assume that the response time is equal to the sum of the expected time of one-hop transmissions that occur on the packet's routing path to BS. Suppose a packet is in state *Hb*. The average number of utilized time slots for the transition to the state *Hb-1* follows the geometric-like distribution $P(L(N_{source}, N_{source+1}), t_1)$. So, the expected transition time from state *Hb* to state *Hb-1* is $\frac{1}{P(L(N_{source}, N_{source+1}), t_1)}$.

The *Response Time* (RT) of a packet from node N_{source} to BS is equal to the expected number of used time slots to reach the steady state 0 beginning from state *Hb*. So it can be computed as follows:

$$RT_{source} = \begin{cases} \sum_{j=0}^{Hb} \left(\frac{1}{P(L(N_{source+j}, N_{source+1+j}), t_j)} \right) & if\ \forall P(L(N_{source+j}, N_{source+1+j}), t_j) : 1 \geq P(L(N_{source+j}, N_{source+1+j}), t_j) > 0 \\ \infty & otherwise \end{cases} \quad \textbf{(4-2)}$$

For the deterministic TPM, we note that the value of RT_{source} is approximately equal to the number of recurring transmission cycles multiplied by the number of time slots within the cycle, because a node's transmission is repeated periodically with a fixed interval based on the length of recurring transmission cycle. However, RT_{source} with the probabilistic TPM depends on a probable transmission in *every* time slot so it results in a shorter response time of a packet (in the unit of time slots) if that the transmission is not interfered with transmissions by neighboring nodes.

Furthermore, we are interested in finding the *Supported Traffic Generation Rate* (STGR) per node. This quantity corresponds to a lower bound on the sustainable traffic capacity of a node in the network. Nodes in proximity of the BS usually represent a bottleneck of the network traffic. This bottleneck is more notable in the tree network topology with a single sink (BS). Therefore, we need to estimate the required amount of time slots for the bottleneck nodes to handle the generated traffic from source nodes. The *STGR's* threshold is limited by the number of multi-hop transmissions or the number of most congested nodes around the BS. So we can characterize the limiting value of the *STGR* using Equation (4-3):

$$STGR < \frac{NTSS}{Max.\left(RT_{z*}k_z, RT_i \right)} \qquad RT \Leftrightarrow \neg(RT = \infty), i \in N, z \in G_{bottleneck} \quad \textbf{(4-3)}$$

Here, *NTSS* indicates a number of available time slots per second, $G_{bottleneck}$ is the group of bottleneck nodes and k_z presents the number of sub-nodes destined to node *z*, a bottleneck node. The larger the value of *STGR*, the more traffic is supported by the network. Transmission performance however may be degraded due to the data overflow in congested nodes if the *STGR*

threshold is violated. In addition, unreliable transmissions due to interference or collisions degrade network utility. The above estimation of the *STGR* is applicable to evaluate the TPMs of the NAPT protocol. In general, the above equations can give us an insight to the sustainability of the traffic in the proposed protocols. More refined analysis would require taking into account additional effects, such as multi-flow interference and noise. However, the proposed equations can be used to demonstrate the key characteristics of the proposed protocols.

Regarding the *STGR* in CPT, since transmissions of a sensor node rely on uniform probabilities (0, 1), the average number of attempts for a successful transmission for each sensor is two. *STGR* for CPT is then limited as follows:

$$STGR_{CPT} < \frac{NTSS}{Max.\left(2 * k_z, 2 * HopCount_{\max}\right)}, \qquad i \in N, z \in G_{bottleneck} \qquad \textbf{(4-4)}$$

where $HopCount_{\max}$ is the maximum number of hop counts to the BS from any given node in the network.

Using Equation (4-1) we can estimate the average *Packet Reliability* (PR) in the network of *n* nodes as follows:

$$PR = \frac{1}{n}\sum_{l \in N} P(L(N_i,\ N_{i+1}),\ t) \qquad \textbf{(4-5)}$$

We will use the above equations to calculate the *STGR* and *PR* of the CPT and NAPT protocols for the topology presented in Figure 4-7 (a). The CPT probability $P(N_x, N_{x+1}, t)$ is from a uniform distribution between 0 and 1. The *g* parameter is set to 1. The *NTSS* parameter is defined as171 time slots per second (1 second/time slot duration (5.7ms) 171 ts). Figure 4-9 shows the results comparing *PR* for NAPT and CPT. We observe NAPT considerably outperforms CPT as anticipated. The use of heuristic scheduling in densely populated areas indeed makes a positive impact on the NAPT schemes. We further distinguish between the two

scheduling options of the NAPT: 1HC that only considers neighbors with the same hop count and 2HC that considers neighbors with the same hop count +/- 1 and 2 hop counts. The 2HC case has a higher packet transmission reliability compared to 1HC due to the additional neighbor information utilized, while the 2HC's *STGR* result is slightly lower. This is because the extra local information utilized by 2HC increases the length of the recurring transmission cycles in the 2HC case. CPT provides a higher supported traffic (*STGR*) by each node, but with lower transmission reliability. This is an expected behavior. Because a CPT transmission is based on the randomly probabilistic scheduling, packet delivery is prone to uncertainty but the response time of data transmission is shorter due to the lack of recurring transmission cycle that exists in the case of NAPT. Overall, the analytical results shown in Figure 4-9 highlight the result that NAPT provides a more reliable and more conservative transmission scheme, comparing to CPT. Consequently, the energy efficiency of NAPT is better than that of CPT. We will demonstrate these points in an experimental study using simulations next (See Figures 4-11 and 4-13).

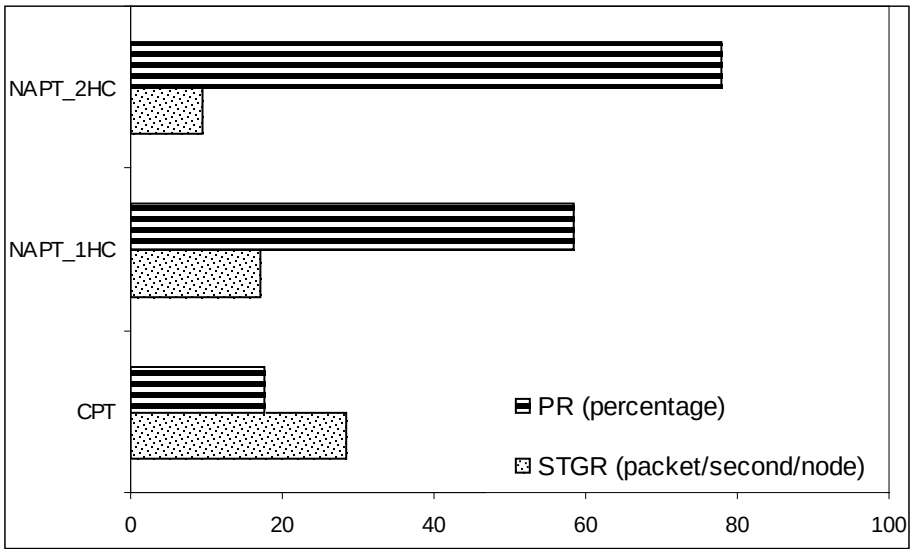

Figure 4-9 Analytical Comparison of CPT and NAPT

4.5 EXPERIMENTAL RESULTS

We perform two sets of simulations. First, we compare the proposed work with the contention-based approach – IEEE 802.15.4 CSMA/CA – that is the baseline for comparisons. Next, a distributed scheduling protocol – DRAND - is added to the comparison.

4.5.1 Simulation Configuration

We implemented the CPT and NAPT protocols by modifying the 802.15.4 MAC and physical layer codes in ns-2 [73] with the CMU wireless extension [69]. We set the channel data rate at 250 Kbps with the sensor transmission range at 15 meters. Sensors were placed according to the network topologies shown in Figure 4-10. There is only one BS (filled circle) and all sensors (unfilled circles) intend to report sensed data to the BS. The payload of each packet was set to 70 bytes. Traffic generation from the application of source nodes was simultaneously executed according to a CBR model. We configure every node with pending traffic in simulations. These nodes deliver their data to the sink in a multi-hop fashion. We performed the simulations with various network loads with data generation rates of 0.5, 1, 2, 4, 8, 16 packets/second/node. This is up to two times the packet generation rate in SHM systems. We do not look at higher data generation rates as in Chapter 3 because the capacity of links cannot support such data generation rates as explained in Chapter 3. A two-ray path loss model for radio propagation was chosen, and fading was not considered in the simulations. We applied the energy cost model from [74] that empirically measures energy consumption in different steady states, e.g., idle, transmit and receive modes. To compute the average power consumed in sensor networks, T_{idle}, T_{Rx} and T_{Tx} must be multiplied by the steady state power in the corresponding

mode (P_{idle}, P_{Rx} and P_{Tx}) where T indicates time spent in different modes. A subsequent equation shows the average power calculations (P_{avr}). According to the measurements in [74], the transmit power is 31 mW, receive power is 35 mW and idle power is 0.71 mW in simulations. Transient energy when switching from one mode to another is not considered here since transient delay is insignificant. The reported simulation results are averaged over 10 runs with 95% confidence intervals. Each simulation run was for 250 seconds of simulation time.

$$P_{avr} = T_{idle} \times P_{idle} + T_{Rx} \times P_{Rx} + T_{Tx} \times P_{Tx}$$

We report on the delivery reliability, throughput at the BS and energy consumption per successful packet received by the BS for the CPT, NAPT, 802.15.4 CSMA/CA, and DRAND protocols. In the rest of the chapter, CSMA is used as an abbreviation for IEEE 802.15.4 CSMA/CA. In order to estimate delivery reliability, we collect statistics on three metrics:

Tx: Number of packets that all sensors actually transmit to the BS within a second.

Rx: Number of packets that the BS successfully receives from sensors within a second. It also reflects the throughput at the BS.

Packet Utility: The Packet Utility is the ratio of received packets (*Rx*) to transmitted packets (*Tx*) and is always less than one. The higher the value of Packet Utility, the more reliable the network is. It also characterizes other network parameters like energy consumption per successful packet.

The throughput at the BS defines how many packets actually are received by the BS after all sensors report their data. The *Energy Consumption of a Successfully received Packet* (ECSP) at the BS is a measure of the energy efficiency of the protocol since it considers the energy cost from the viewpoint of the whole network instead of from an individual sensor. This metric is defined as the total power consumed in the network per second divided by the number of packets received at the BS (Rx).

4.5.2 Analysis of Results

We studied three topologies in our simulations: Sparse, Dense and Random Networks. The sparse network (see Figure 4-10 (a)) consists of 25 nodes positioned within a 150 ×150 m^2 flat area while the dense network (see Figure 4-10 (b)) covers 80 nodes in the same area. Finally, a random topology is chosen (see Figure 4-10 (c)) with 20 sensors randomly positioned in a 60 × 60 m^2 flat area where the average 2-hop neighborhood size is 12 sensors. A sink station is placed in the center of area. This topology reflects a densely populated network with challenges such as the hidden terminal problem.

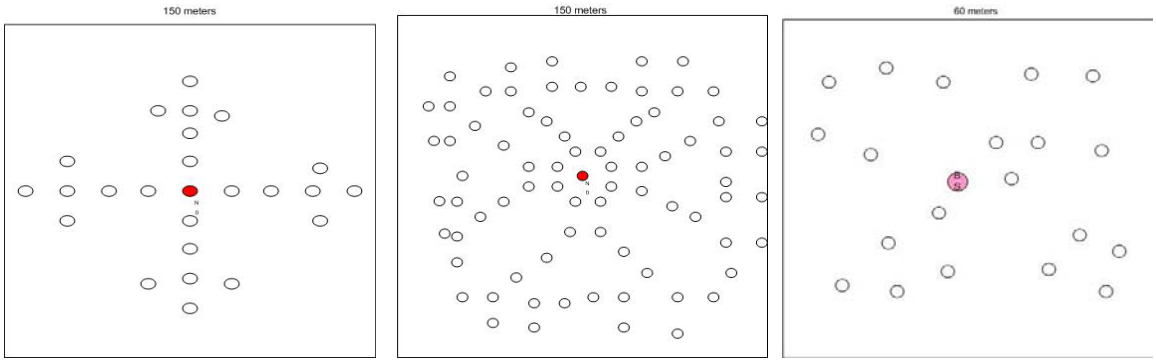

(a) (b) (c)

Figure 4-10 Network Topologies Used in Experiments: (a) Sparse Network, (b) Dense Network (c) Random Network

A. Sparse Network Topology

Figure 4-11 shows the simulation results for a sparse network with 25 nodes. DRAND performs the best overall as it uses time-division based scheduling. Consider Figure 4-11 (a). Here, the data generation rate is defined as the number of packets *intended* to be transmitted by each sensor per second. CSMA transmits more packets compared to other protocols because many sensors may pick random numbers that result in simultaneous transmissions and

retransmissions. But the number of received packets at the BS with CSMA is small as shown in Figure 4-11 (b). The major reasons for this phenomenon are the high rate of collisions due to the hidden terminal problem, the excessive traffic loads, and the considerable amount of retransmitted data.

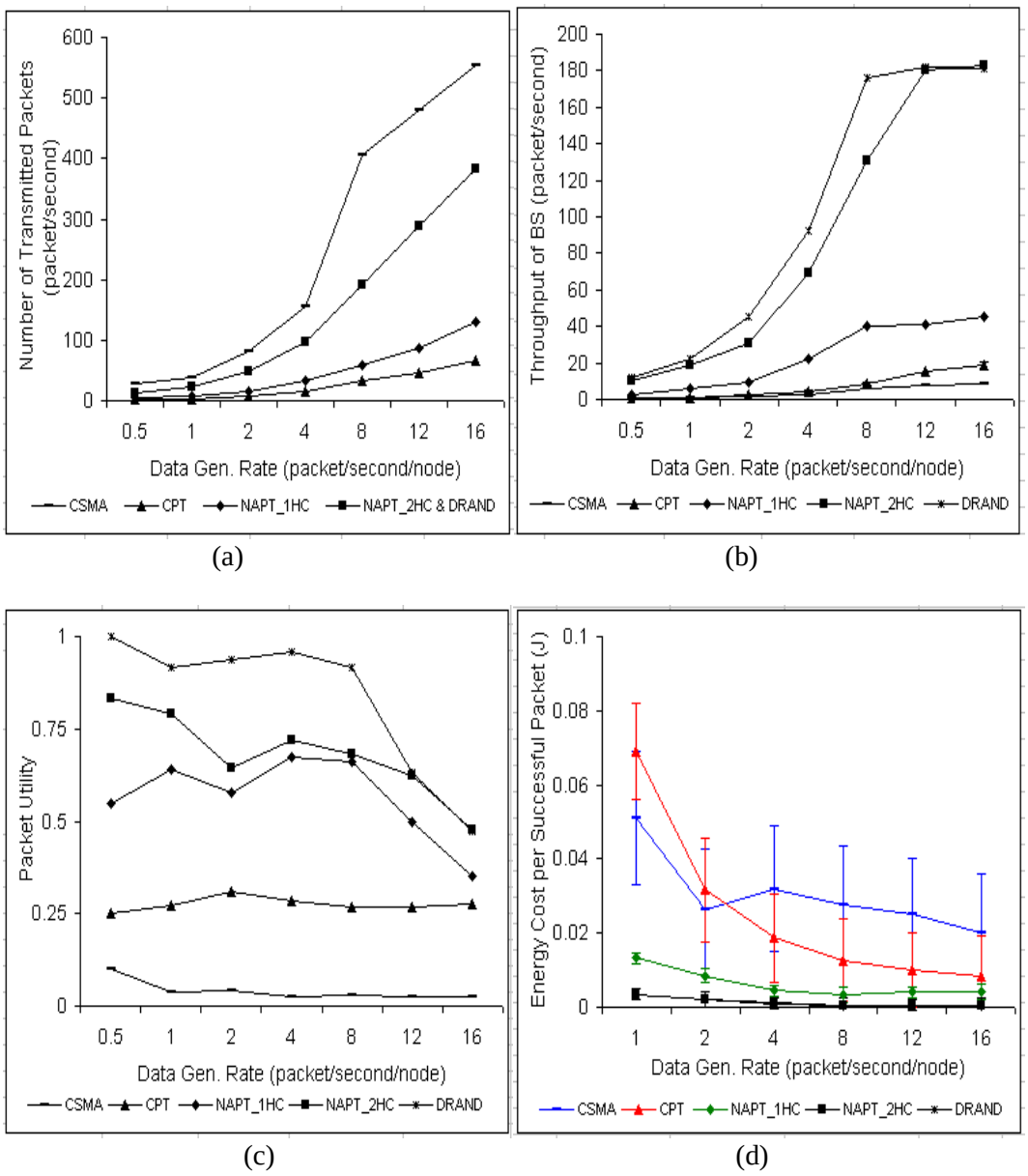

Figure 4-11 Performance in Sparse Network Topology (a) Number of transmitted packets (b) Throughput of BS (c) Packet utility (d) Energy consumption per successful packet

Figure 4-11 (b) shows that the throughput at the BS is strongly dependent on the protocols with the increase in data generation rate reflecting higher traffic loads. The throughput with CSMA is better if compared to that with CPT at lower data generation rates. As the data generation rate increases, CPT and NAPT clearly outperform CSMA.

The throughput performance of CPT increases linearly as traffic load increases because the channel access follows the random probability with a uniform distribution. Thus, every sensor in the CPT network can receive a fair opportunity to deliver data. NAPT is even better than the CPT due to the awareness of local information. However, the throughput at the BS degrades or remains at the same level after the data generation rate passes a certain threshold. This “bottleneck” phenomenon can be explained by the fact that if the traffic load becomes intensive, i.e., it surpasses the supported data rate in simulations, the performance in terms of throughput is restricted. Besides, sensors in NAPT are programmed to individually generate a transmission schedule. In this case, transmissions from different sensors can possibly overlap in the time domain. In order to address this issue, we need to gather more local information or use some heuristics in the NAPT process to avoid such collisions (see Chapter 5). Note that using information about plus or minus 2 hop counts improves the performance of NAPT significantly, bringing it close to that of DRAND, which is based on time-division scheduling.

From the simulation results we observe considerable improvement of throughput at the BS with our protocols. At a data generation rate of 16 packets/second/node, NAPT using limited neighbor information (NAPT-1HC) has an average throughput that is 45 packets/second while the throughputs with CPT and CSMA are 18 packets/second and 9 packets/second correspondingly. CPT and NAPT-1HC are around 2 and 5 times better than CSMA at this high

data generation rate, making them more suitable for DIAs. They have no additional complexity compared to CSMA.

Figure 4-11 (c) shows the behavior of packet utility. We observe that NAPT's average packet utility is around 70%, while that of CPT is roughly 30% and that of CSMA is less than 10% at different data generation rates. As we discussed earlier, the packet utility with NAPT decreases significantly around a data generation rate of 8-16 packets/second/node due to the bottleneck phenomenon. The packet utility of CPT remains constant around 30% due to collisions from the randomness of access that does not change significantly with load. Besides, the packet utility of CPT does not fluctuate significantly because of the uniform transmission probabilities. It is worthwhile to mention that the packet utility not only expresses the delivery reliability of a network, but also characterizes energy and latency performance as discussed next.

Figure 4-11 (d) represents the energy study of the proposed protocols. We use the average energy consumption for a successfully received packet (ECSP) at the BS as the comparison metric. We observe that NAPT performs well in conserving energy since its packet utility is high. NAPT-2HC is very close to DRAND in terms of ECSP and presents small data variations due to the scheduled nature of channel access. The energy cost is relatively high for the CPT with lower traffic loads. As the data generation rate increases, the throughput of CPT increases and the energy efficiency is also improved, which causes the CSMA curve to cross the CPT curve. The energy performance of CSMA is always worse than that of NAPT, and is worse than that of CPT under higher traffic loads. This is contributed to by the considerable amounts of unsuccessful transmissions and retransmissions using contention access in DISNs. Overall, the energy costs with CSMA and CPT show inefficiency with high deviations, thus shortening the life-time of a WSN.

B. Dense Network Topology

Figure 4-12 shows the simulation results for a dense star-like network with 80 nodes. This network features high channel contention due to the higher node density. Results are mostly similar to that with the sparse network with some slight differences. Figure 4-12 (b) plots the performance of throughput. NAPT outperforms CPT and CSMA in most cases. However, NAPT-1HC saturates beyond a data generation rate of 4 packets/second and is in fact slightly worse than CPT at 16 packets/sec. The throughput of the CPT in the dense topology also shows a linear trend which is similar to the CPT results in the sparse topology. The throughput of CSMA in the dense topology is better than the CPT throughput under lower traffic loads while this behavior is reversed under higher traffic loads. DRAND performs the best overall as expected.

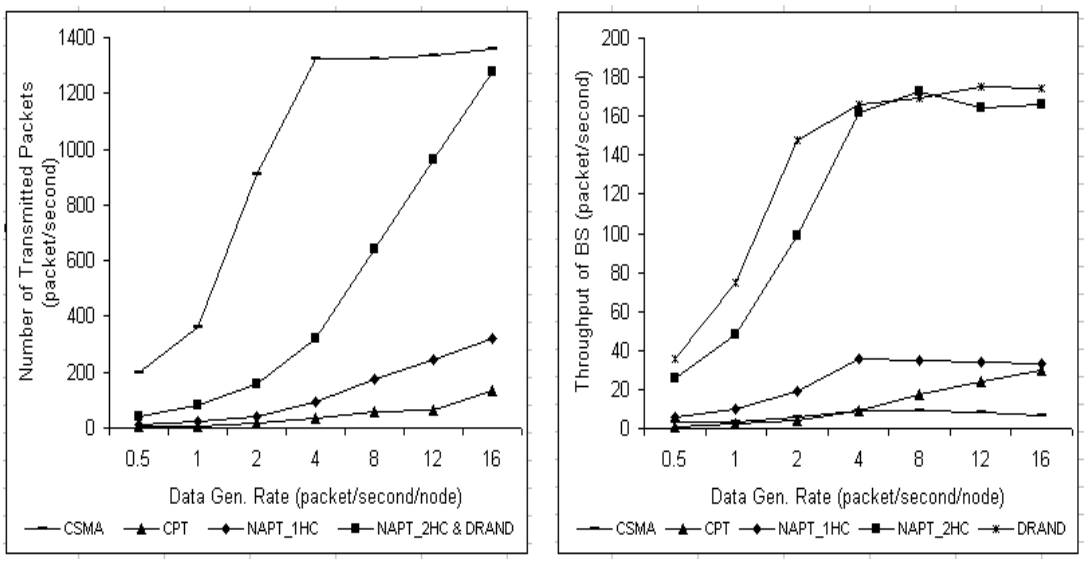

(a) (b)

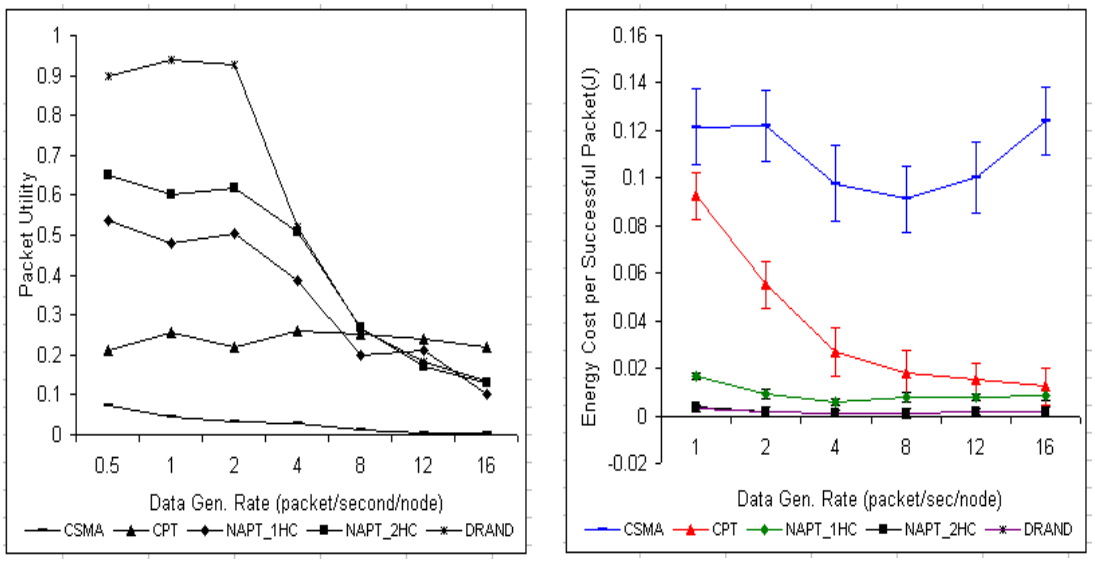

(c) (d)

Figure 4-12 Performance in Dense Network Topology (a) Number of transmitted packets (b) Throughput of BS (c) Packet utility (d) Energy consumption per successful packet

Figure 4-12 (c) reports on the packet utility metric for the dense network topology. The results for dense topology are similar to the results for the sparse network with two exceptions. First, the packet utility of NAPT (1HC and 2HC) under low traffic loads is about 15% less than the corresponding utility in the sparse topology. Besides, the packet utility degrades faster as the data generation rate increases (bottleneck phenomenon). Second, the packet utility of CPT is constantly around 20%, which is about 10% less than the result for the sparse topology. According to these observations, we can estimate that the *node density* of a network has noticeable impact on network throughput when applying our proposed work.

Figure 4-12 (d) reports on the results of an energy study of the dense topology. Again, we use the average energy consumption for a successfully received packet (ECSP) in BS as a tool of comparison. The simulation result for the energy study in the dense topology is similar to the results in Figure 4-11 (d). The NAPT-2HC and DRAND performance in energy cost is the smallest while the CSMA is the highest overall. The CPT protocol shows a higher energy cost

under lower data generation rates and it improves as the data rates increase. A major difference in the energy consumption results of the dense topology is that the average energy consumption for a successful CSMA packet delivery is about 3 times larger than the corresponding result for the sparse network. In general, the energy consumption of the proposed protocols is not affected considerably by the network size and node density.

C. Random Network Topology

The results observed for the random network topology are similar to the results for the sparse and dense networks. They are summarized in Figures 4-13 (a)-(d). Despite varying transmission distances due to the random node placement, the performances of the proposed protocols were not considerably different when compared to the results from the sparse and dense networks. This indicates that our protocols are robust and not sensitive to different types of network topologies (e.g., star or mesh topologies).

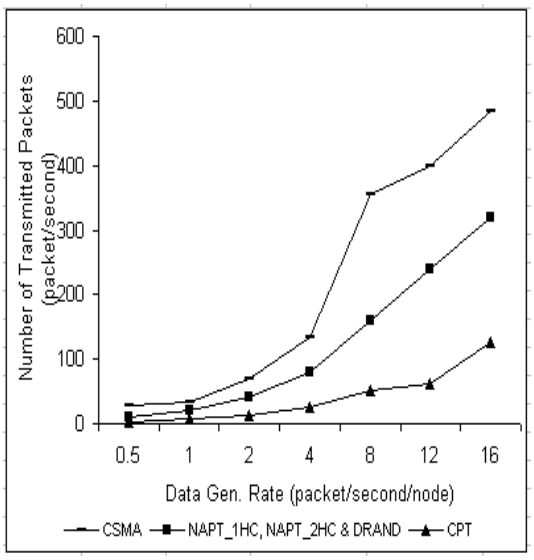

(a)

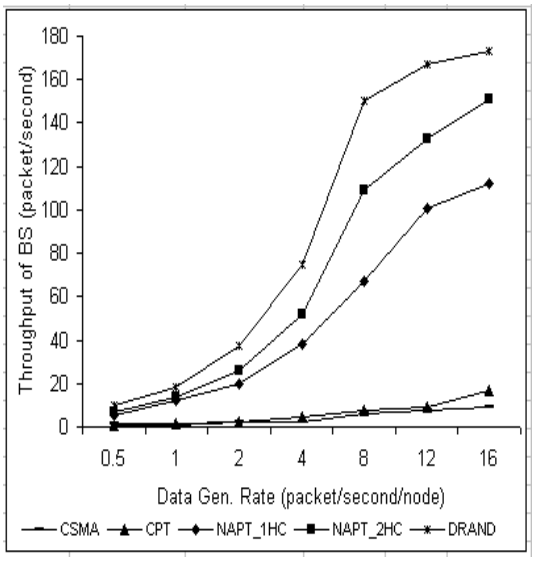

(b)

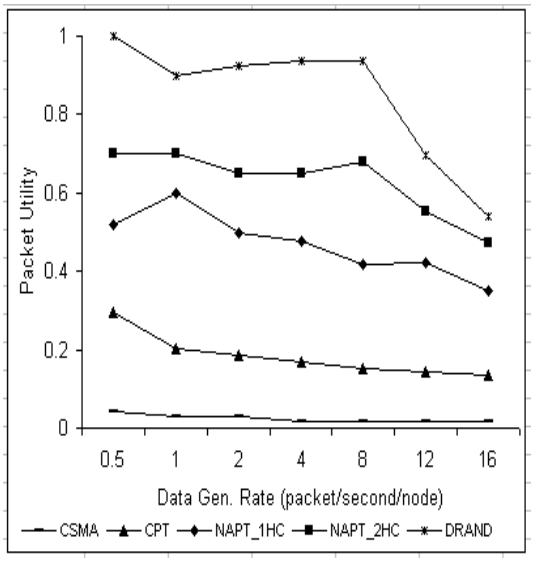

(c)

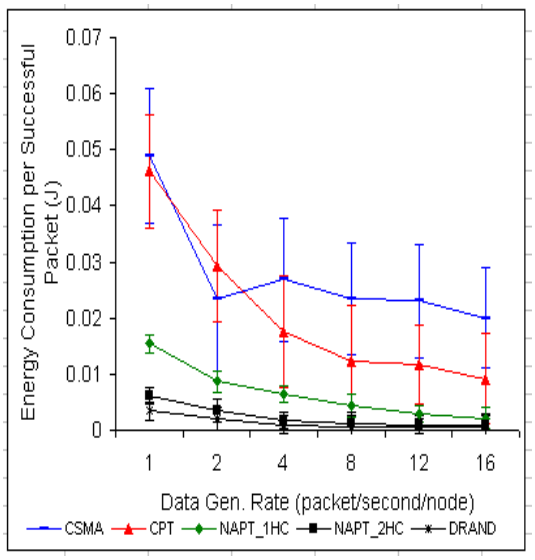

(d)

Figure 4-13 Performance in Random Network Topology (a) Number of transmitted packets (b) Throughput of BS (c) Packet utility (d) Energy consumption per successful packet

Below, we compare performance characteristics of the different topologies as summarized in Figures 4-11, 4-12 and 4-13. First, we consider the number of transmitted packets. We observe that the CPT protocol always generates the smallest number of packets due to its probabilistic nature. The number of transmitted packets increases linearly with the increase in data generation rate. The NAPT_1HC protocol transmits more packets than CPT, since it implements a more sophisticated hybrid access scheme. Under the random topology, NAPT_1HC executes transmissions deterministically due to high node density. Therefore, the difference in the number of transmitted packets between the CPT and NAPT_1HC is higher for the random topology. Since the NAPT_2HC protocol utilizes more extensive neighbor information to arrange channel access, its transmissions are more deterministic and the number of transmitted packets is the same as in DRAND for all three topologies. Overall, NAPT_2HC transmits more, or the same number of packets compared to NAPT_1HC and CPT. CSMA, utilizing retransmissions to handle unacknowledged delivery, generates a considerably larger

number of packets. Note that this number is lower at higher data generation rates because of the busier channel and frequent back-offs.

Next we consider throughput performance in each of the three topologies. We observe that the CPT throughput is relatively low, but it still outperforms CSMA at higher data rates. The reason for lower CPT throughput is the smaller number of transmitted packets due to random probabilistic access. This especially applies to dense and random networks where the throughput is constrained by severe interferences from neighbors. The NAPT_1HC protocol performs better than CPT, but its throughput is lower compared to NAPT_2HC and DRAND, since NAPT_2HC and DRAND utilize more refined neighbor information to schedule medium access. In random topology, throughput of NAPT_1HC increases because of the deterministic schedule, compared with the sparse topology. Throughput of NAPT_2HC and DRAND slightly reduces in the random topology since sensors have less time slots reuse due to more neighbors. Note that their throughput remains constant at higher data rates. This is caused by the limited support of channel capacity in the simulation configurations. Note that the upper bound for the throughput is affected by the scale of a network. With larger numbers of nodes in denser networks, the throughput graph gets bounded earlier.

Now we consider packet utility metrics reflecting transmission reliability of the protocols. We observe that the packet utility of CPT is higher than the packet utility of CSMA for the following reasons: (1) the contention back-off policy of CSMA is not effective in handling intensive data traffic; (2) hidden terminal problem and the retransmission functionality considerably increase the number of transmitted packets. There is approximately 5% of difference in the packet utility for CPT due to the node density, as far as random and sparse topologies are concerned. Overall, NAPT is more reliable than CPT, especially in the case of

NAPT_2HC. This is due to the more refined local neighbor information. The packet utility of NAPT in the dense or random topology is about 5%~10% less than the one in the sparse network. In DRAND, neighbor information is also exchanged among local sensors so it achieves the highest packet utility with some overhead costs.

Finally, we evaluate the energy efficiency of the protocols. The CPT protocol is associated with high energy consumption at lower data generation rates due to the low throughput. As the data rate increases, the energy efficiency of CPT improves and it eventually outperforms CSMA. As expected, the performance of NAPT is better than the performance of CPT. With improved packet utility in the proposed protocols, NAPT_2HC reduces the ECSP cost and approaches the performance of DRAND in all three topologies. CSMA is the least energy efficient due to its low packet utility.

D. Overhead Comparison

Some access control mechanisms may exchange control packets to establish channel access including DTA, DRAND and NAPT. Such control packets hold no application data and consume energy, so we regard these packets as overhead. Figure 4-14 presents the overhead comparison of the scheduling protocols. We do not discuss the CSMA and CPT protocols here because they do not involve overhead control messages in their operations. Figure 4-14 (a) shows the average control message count in Neighbor Discovery phase (ND) and Time Slot Schedule and Dissemination phase (TSSD). The number of NAPT control messages is 0 in the TSSD phase and is always 2 in the ND phase (assuming the broadcast transmission is ideally adopted in ND for NAPT and DRAND). NAPT is therefore superior to DRAND in this regard. In other words, NAPT eliminates the reliance on exchanging messages for transmission scheduling. It pushes the communication cost to in-network processing, which is preferable in

energy constrained sensor networks [29]. Additionally, we are interested in learning the effect of network density on the overhead of scheduling access schemes. We performed the experiments with multi-hop network topologies varying the average number of two hop neighborhoods from 0.5 to 11 nodes. This neighborhood size of the network is changed by varying the numbers of nodes from 20 to 160 within a 150 x 150 m^2 flat area. Figure 4-14 (b) shows that the number of control messages of DRAND increases proportionally as the network density increases. Meanwhile, NAPT's overhead cost is not affected by the network size or density.

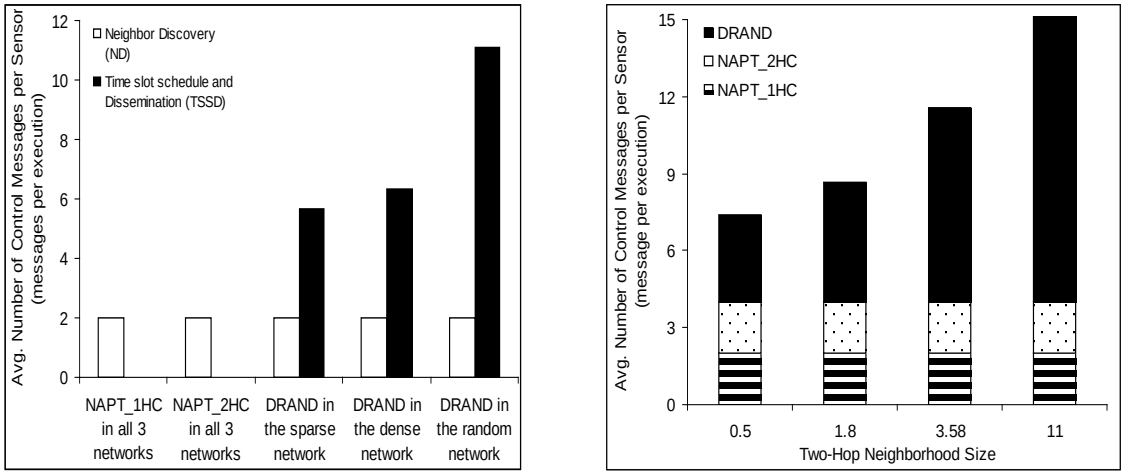

(a) (b)

Figure 4-14 Overhead for Control Messages (a) Overhead comparison with different topologies (b) Overhead comparison in different scales of network

4.6 APPLICABILITY OF THE PROPOSED PROTOCOLS

Our protocols implement a light-weight channel access that meets the performance requirements of special-purpose Data Intensive Sensor Networks: when compared to CSMA, they come very close to time-division based scheduling approaches. The CPT protocol is the

simplest and it implements a scalable and distributed random access scheme. It requires no knowledge of topology, yet it performs considerably better than CSMA. Under higher traffic load, the utility of CPT will decrease due to lack of intelligence for collision avoidance. Thus, tuning the TPM of the CPT protocol becomes an important issue. Currently, we are investigating the approach to heuristic-based tuning of the TPM that utilizes knowledge of discrete mathematics using Latin Squares [75] and a geographical aid. The goal is to minimize collision probabilities while increasing concurrent data delivery. This work is described in Chapter 6.

The NAPT protocol utilizes topology awareness to avoid collisions. It should be noted that complexity of creating local schedule in NAPT is $O(n)$, where n is the number of neighbors in the neighbor table. NAPT also requires updating the neighbor tables for reliable transmissions when the network topology changes (to reflect added nodes, deleted nodes or nodes going to sleep). Since the algorithm may need to run periodically to address the changed topology, a low complexity algorithm is always desired. Due to the low complexity of our scheme and relatively infrequent changes in the topology of the special-purpose application, the update overhead is negligible. The concerns with conflicting transmissions with the NAPT protocol were discussed in Section 4.5.2. This is due to by limited coordination among local sensors. So, the heuristic transmission schedule, generated by the NAPT protocol, is not conflict-free, unlike DRAND. We address this concern by proposing a grid-based access scheduling scheme, i.e., GLASS [86], that matches the DRAND protocol in transmission reliability while resulting in less overhead cost. Details of this new design are described in Chapter 5. Sleep mode is a common technique to save energy in wireless local area networks. Our protocols may enhance the energy saving performance if the sleep state is assigned to certain time slots of sensors that are absolutely free

of transmissions and receptions. Achieving this needs extra coordination between local sensors. In the next chapter, the proposed scheme, GLASS, is able to complete this objective.

4.7 CONCLUSION

We proposed novel, hybrid probabilistic/scheduled based transmission protocols to mitigate the impact of high traffic load in sensor networks with minimal control overhead. We devised an analytical model to characterize the performance of our hybrid access schemes and verify the analytical results using simulations. We also tested our protocols with various network topologies and with increasing traffic loads. The simulation results demonstrate acceptable utility of the CPT and NAPT protocols. In particular, our protocols outperform the IEEE 802.15.4 CSMA/CA protocol in terms of transmission reliability and energy efficiency. NAPT compares favorably with DRAND in terms of low overhead cost and features high utility. Our proposed hybrid technique is capable of meeting the stringent performance requirements of Data Intensive Applications.

5.0 DATA DELIVERY USING GRID-BASED ACCESS SCHEDULING

The ultimate goal of this dissertation is to design an efficient channel access mechanism for special-purpose data intensive sensor networks. In this chapter, we propose a decentralized and efficient technique called *Grid-based Latin Squares Scheduling Access* protocol (GLASS) that maintains graceful performance degradation in DISNs as the data load increases [86]. Meanwhile, the protocol is designed to be lightweight, overhead-efficient, highly-scalable, and robust in the presence of mobility. Our motivation for this stems from the previous work in hybrid access using NAPT and CPT. At the one end of the spectrum, we have the IEEE 802.15.4 CSMA/CA and CPT protocols, which are distributed and scalable. The performance with these schemes however is poor because of the collisions during periods of high data loads. This is caused by several sensor nodes transmitting at the same time, despite the backoff mechanisms embedded in CSMA/CA and the random probabilistic access embedded in CPT. At the other end of the spectrum, we can ensure no conflicting transmission in the network (we refer to the DRAND and DTA protocols here). While this approach saves on the energy waste due to collisions, it increases the energy waste due to excessive overhead messages. This concern further worsens as the network scale expands, which, it is likely in WSNs. At the middle of the spectrum, i.e., with the NAPT protocol, the overhead concern is alleviated but its performance does not match the performance of completely scheduled access (like DRAND or DTA). GLASS is a decentralized Time Division Multiple Access (TDMA) approach for creating *conflict-free*

(high network utility) time slot schedules for transmissions, analogous to the DRAND. Meanwhile, it aims to reduce the overhead consumption. Figure 5-1 provides a qualitative summary of MAC schemes in terms of the scalability of access method and expected utility (throughput without losing packets) in Data Intensive Sensor Networks.

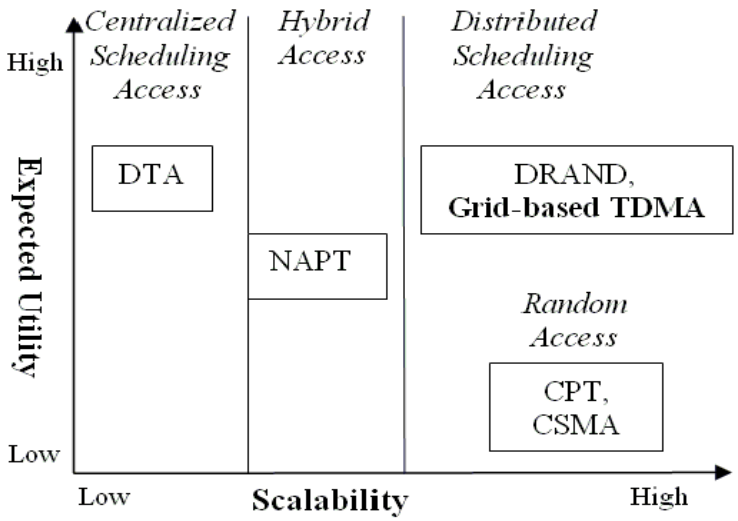

Figure 5-1 General Framework of MAC Schemes Classification

In GLASS, sensors use *location information* to improve channel access. First, sensors virtually divide the monitoring area into a grid. Then, each sensor associates itself with one virtual grid cell. This design allows neighboring sensors to maintain *spatial and temporal separation* between potentially colliding packets while keeping channel access distributed. In addition, the Latin Squares function [75] is used to facilitate the assignment of time slots for transmission among sensors within a grid cell, thus reducing the number of colliding transmissions. We demonstrate the feasibility of our technique using analysis and simulation. In particular, the simulation results show that the overhead cost with GLASS is about 70% less than that of DRAND and the performance of GLASS is robust to changes in topology while their transmission efficiencies are comparable. Note that GLASS assumes that each node in a WSN is

aware of its geographic location[3]. While location-based approaches have been adopted in routing mechanisms [88] [89], to the best of our knowledge they have not been utilized for optimizing channel access.

5.1 SYSTEM MODEL

We assume the following system model:

1. Initially, sensors are evenly deployed in a field. Each sensor is aware of geographical data (e.g., coverage and location) associated with the monitored area. The location information need not be fine grained.

2. Sensors *move* to proper rendezvous points and deliver collected data to next-hop neighbors. As before, we adopt a quasi-periodic traffic model as more appropriate for *Data Intensive Applications (DIAs)*. This model also presents a challenging scenario in terms of channel access due to the large numbers of concurrent data transmissions within a short period of time. Collisions occur when a sensor receives more than one transmission simultaneously from different parties.

3. Every sensor transmits or receives on a common carrier frequency. It transmits in assigned time slots and "idle-listens" or receives otherwise. A sensor can transmit a message at the beginning of a time slot and complete the transmission, including receiving an ACK message, within the same time slot (which is 7 ms given a 250 kbps data rate). All sensors

[3] We note that using global positioning system (GPS) is not always possible in WSNs because of energy and location precision constraints. WSNs commonly utilize ad hoc localization methods based on nodes, calculating their coordinates using special beacon nodes whose positions are known. Further consideration of this subject is beyond of the scope of this dissertation.

transmit at the same power that covers a limited footprint. Sensors are uniquely identified and equipped with omni-directional antennas.

4. Time synchronization is managed by a Base Station using beacons. Note that sensors may lose beacon messages and there may be clock drift between synchronizations. Hence, sensors are designed not to transmit during the first ms of every time slot. This provides a slack time for synchronization errors and prevents collisions at the boundary of time slots.

5.2 DESCRIPTION OF GLASS PROTOCOL

The GLASS protocol includes three phases: Grid Searching, Transmission Frame Assignment, and Time Slot Assignment. Sensors follow these steps to determine time slot schedules cooperatively. The protocol is completely decentralized. To account for relocation of nodes in a mobile WSN, the GLASS protocol periodically checks the accuracy of time slot assignment. The cost of time slot re-assignment is low (see experimental evaluation in Section 5.4) due to the low complexity and small overhead. Also, the performance of GLASS is robust to changes in topology.

1) Grid Searching

We devise a *Grid Searching* (GS) algorithm to assign sensors in a monitoring area to grid cells. We assume that the monitoring area virtually consists of grid cells where their shapes and sizes are uniform (see Figure 5-2). R is the length of one edge of any grid cell, and it is ranged between $2r$ and $2.1r$ where r is the sensor's transmission range.

$$2r < R <= 2.1r \tag{5-1}$$

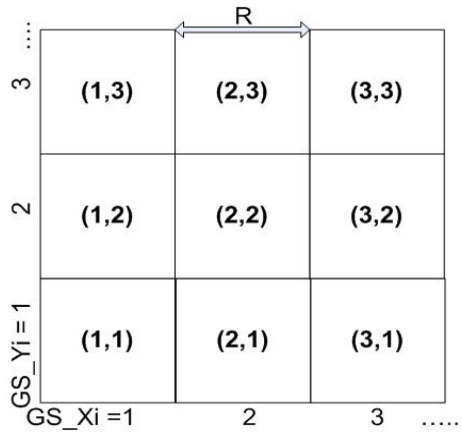

Figure 5-2 Virtual Grid Network

```
/* Given the 2 dimensional monitoring area = (X', Y')
          the location of sensor i = (xi, yi)
To find the grid  cell location of Sensor i:                    */
if xi ≤ X' and yi ≤  Y'
      Z= (xi ÷ R)
         if Z is an integer
           select a random number between 0 and 1
             if the number >0.5
               GS_Xi = Z
             else
               GS_Xi = Z+1
         else if Z is a number with decimal
               GS_Xi = ⌈Z⌉
else
       disable Sensor i /*Outside the monitoring area*/
Repeat the same steps above to solve GS_Yi
End
The Grid cell location of Sensor i = (GS_Xi, GS_Yi)
```

Figure 5-3 Pseudocode of Grid Cell Search

Such a configuration for *R* is critical for alleviation of collisions and overhead. In this chapter we set the *R* value as *2.1r*. We will explain this in Section 5.3. In addition, each grid cell is identified by a sole *Identification* (ID), associated with its location, i.e., a pair of coordinates (GS_Xi, GS_Yi). GS_Xi and GS_Yi represent the vertical and horizontal coordinates of a grid cell correspondingly. Every sensor applies the GS algorithm, presented in Figure 5-3, to

determine the ID of the grid cell using its location information. Here (xi, yi) is the location of Sensor i and (X', Y') defines the area covered by a WSN. Using spatial relationships between the sensor and the monitoring area, the sensor independently calculates the ID of the grid cell. If a sensor is located on a border between two grid cells, namely the value of *Z* (here *Z* corresponds to the *x* and *y* coordinates of a sensor in units of *R*, the length of a side of the grid cell – see Figure 5-3) is an integer, this sensor will randomly choose a grid cell's ID between these two grid cells.

2) Transmission Frame Assignment

After a sensor locates its grid cell, it proceeds with *Transmission Frame* (TF) assignment. We define a TF as a group of continuous time slots. The TF structure repeats to manage sensors' transmit, idle or receive states. The TF can be divided into multiple equal *Sub Transmission Frames* (STFs). In this chapter, we use a configuration with two STFs: A and B. Fig. 5-4 (a) describes the algorithm of assigning a STF for a sensor. The sensor uses the GS result from the first phase to independently assign itself an STF (either A or B). As a result, sensors in adjacent grid cells operate at different STFs, reducing the potential for collisions. We can also configure four STFs using the algorithm shown in Fig. 5-4 (b), which is similar to the algorithm in Fig. 5-4 (a).

```
Given the grid cell location of Sensor i = (GS_Xi, GS_Yi)
To find the Sub Transmission Frame of Sensor i:

if GS_Yi is odd and GS_Xi is odd
    STF of Sensor i = A
else if GS_Yi is odd and GS_Xi is even
    STF of Sensor i = B
else if GS_Yi is even and GS_Xi is odd
    STF of Sensor i = B
else if GS_Yi even and GS_Xi is even
    STF of Sensor i = A
```

(a)

```
Given the grid cell location of Sensor i = (GS_Xi, GS_Yi)
To find the Sub Transmission Frame of Sensor i:

if GS_Yi  is odd and GS_Xi is odd
    STF of Sensor i = B
else if GS_Yi  is odd and GS_Xi is even
    STF of Sensor i = A
else if GS_Yi  is even and GS_Xi is odd
    STF of Sensor i = C
else if GS_Yi  is even and GS_Xi is even
    STF of Sensor i = D
```

(b)

Figure 5-4 Pseudocode of Assigning the Sub Transmission Frame for Sensor i (a) Two STF scenario (b) Four STF scenario

Figure 5-5 presents examples of STF assignments. There is a network with 9 grid cells and 5 nodes with two different STF scenarios (see Figure 5-5 (a) and (b)). Each node uses the algorithm to find its STF as shown in Figure 5-5 (c). Thus, collisions of transmissions, for example, from Sensors 2 and 3 are avoided due to temporal separation. With the four STFs configuration (see Figure 5-5 (b)), this scheme extends sensors' transmissions over more STFs and intuitively guarantees collision-free inter-grid transmissions in the network. But it may result in worse bandwidth utilization and higher packet delay compared with the two STFs configuration because of the reduction in concurrent transmissions by sensors. Therefore, we pick the two STFs configuration for the rest of this chapter.

In the two STFs case, the length of TF is configured differently for different sensor distributions:

$$\text{Length of TF} = 2 * \text{STF} = 2 * \left(\left\lceil \frac{\text{Number of deployed sensors}}{\text{Number of grids in the network}} \right\rceil + \alpha \right) \quad (5\text{-}2)$$

The number of deployed sensors and number of grid cells are known in the pre-deployment stage. a is an adjustable variable between zero and (Number of deployed sensors / Number of

grid cells). If sensors in the network are evenly distributed, a will be at the minimum. If the sensors are not evenly distributed, a will increase. To avoid uncertainty in sensor deployment, a should not be too small, but this may slightly impact packet delay due to longer transmission cycle/frame.

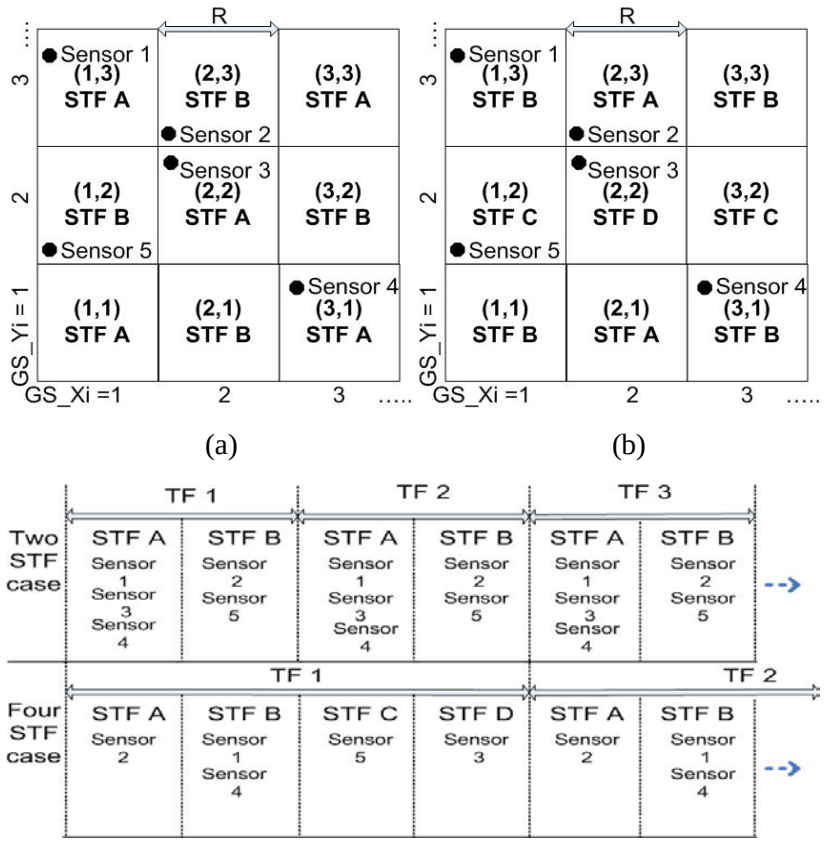

Figure 5-5 (a) Network with Two STFs configuration (b) Network with Four STFs configuration (c) Comparison of STF examples

3) Time Slots Assignment

After sensors discover their GS and STF, the next step is to determine a time slot for the transmission state of each sensor. We use *Latin Squares* (LS) to assign time slots for sensors, thereby avoiding collisions between neighbors. First, each sensor performs neighborhood

discovery to prepare for time slots scheduling. The neighborhood discovery requires all sensors to broadcast their information about GS and STF to one-hop neighbors. In this way, every sensor is aware of its neighbors and maintains a neighbor table which records neighbors' ID, distance/hop count, GS and STF. Furthermore, sensors need to keep complete and accurate neighbors information within their grid cells (local data) so each sensor must broadcast newly-received data and update its neighbor table. Sensors adopt the data aggregation, CSMA broadcast and ACK techniques to avoid fine-grained and failed broadcasts. Because the side length of all grid cells is 2.1r, the maximum distance for a sensor to convey data within a grid cell is 3 hops. In other words, the sensor needs 2 or 3 broadcast messages to announce itself and to discover neighbors' presence within a grid cell if none of the messages is lost.

Next, sensors utilize the given information about STF to generate a *Latin Squares Matrix* (LSM) for time slots assignment. LSM for m time slots of a STF is an $m \times m$ array, where each cell of the array contains one of a set of m symbols. Each symbol occurs only once in each row and once in each column [75]. An LSM with immediate sequential symbols can easily be constructed. One method of building a $2k \times 2k$ LSM is explained next and shown in Figure 5-6 [87].

1. Number the $2k$ symbols successively from 1 to n.
2. Assign successively the integers from 1 to n to the n cells in the first row by proceeding from left to right entering only cells in odd-numbered columns, then reversing direction and filling in the cells in even-numbered columns.
3. In each column, starting with the number already entered in the top cell, proceed downward, entering in each cell the integer immediately following the one in the cell above it, except that the integer n is followed by the integer 1.

	TS1	TS2	TS3	TS4	TS5	TS6
Sen1	1	6	2	5	3	4
Sen2	2	1	3	6	4	5
Sen3	3	2	4	1	5	6
Sen4	4	3	5	2	6	1
Sen5	5	4	6	3	1	2
Sen1	6	5	1	4	2	3

Figure 5-6 Example of a Latin Squares Matrix

Accordingly, sensors can build an LSM of any size. We define rows of the LSM to represent each local sensor's transmission and columns of LSM to represent time slots of the STF (see in Figure 5-6). Each sensor selects the local sensors of its LSM by choosing the sensors with the same GS and STF in the neighbor table. The selected local sensors are sorted by ascending order of their IDs in the LSM rows. When *Value of a cell of Latin Squares Matrix* (VLS (i, j)) is equal to 1, the corresponding sensor i of the cell is allowed to transmit in its corresponding time slot j. For example, Sensor 5 is set to transmit its data in time slot 5 according to the LSM shown in Figure 5-6. The rest of the time slots are in either receive or idle states. Note, that sensors can configure the time slots to the receive state using the information of one-hop neighbors' time slots assignment. The rest of the time slots are in the sleep state for energy savings. After the time slot of a sensor is determined using LSM, the sensor broadcasts the information of its time slot and neighbor table to one-hop neighbors using the CSMA and ACK techniques.

There is no guarantee that the generated LSM rows can be completely assigned to the local sensors. When the number of local sensors is less than the size of LSM, some sensors, e.g.,

sensor 1 in Figure 5-6, are asked to access channel more frequently in order to use bandwidth efficiently, but channel access fairness becomes an issue. We adopt the rotating procedure that arranges local sensors in extra rows of the LSM to give fair channel access to all the sensors inside the grid cell. If the number of local sensors is more than the size of LSM, some sensors' operations are omitted temporarily based on the rotating procedure. Such a situation reveals an over-congested grid cell. In other words, network resources are poorly and unfairly distributed. With the procedures above, local sensors can create an identical LSM that ensures the same transmission schedule is shared by all the sensors in the grid cell if the sensors perform their neighborhood discovery correctly. The whole process is independent and distributed for every sensor.

With the LS function, we enable non-overlapping time slots assignment inside each grid cell. However, it is still possible that collisions will occur between transmissions near the intersection of any four grid cells because sensors from different grid cells may use an identical STF. To address this challenge, we devised a function, called *Collision Avoidance near Intersection of Grid Cells* (CAIG) shown in Figure 5-7. This function is initiated when a sensor with even GS_Yi finds that its time slot overlaps the time slots of its neighboring sensors that are within two-hops. In this case, the sensor updates its time slot and broadcasts the new neighbor table using the CSMA and ACK techniques. The sensors with even GS_Yi are chosen to perform the update since collisions occur near intersections of the grid cells with the same STF. Thus, it is sufficient to avoid all of the collisions by monitoring partitions of the network. This design indirectly reduces computation of the reassignment of conflicting time slots. Regarding the process of updating a conflicting time slot, the sensor chooses the smallest available time slot from the time slots not occupied by the sensor and its neighbors within two-hop, so it reduces the

chance of exceeding the length of STF. If the length of STF is too short to include the required amount of time slots, some sensors will be forced to turn their transmission states off, resulting in a gap in the WSN. We can avoid this problem by adjusting the a parameter.

```
/*Collision Avoidance near Intersection of Grid function*/
/*Given neighbor information from the LSM broadcast*/
if GS_Yi of this sensor i = even number &&
   time slot of this sensor i =
   time slot of its 1-hop or 2-hop neighboring sensor
/*Available time slots in STF = time slots not used by
   the sensor i and its 1-hop and 2-hop neighbors*/
      if Available time slots in its STF = true
            Sensor i sets the overlapping time slot to
            a minimum time slot in the available time slots;
            Sensor i broadcasts its new neighbor table;
     else
            Sensor i stops the transmission state;
else if GS_Yi of 1-hop neighbor of the sensor i =
        even number &&
        time slot of 1-hop neighbor of the sensor i
        in current grid = time slot of 1-hop neighbor
        of the sensor i in other grid
      Sensor i broadcasts its new neighbor table;
/*End*/
```

Figure 5-7 Pseudocode of Collision Avoidance near Intersection of Grid Cells Function

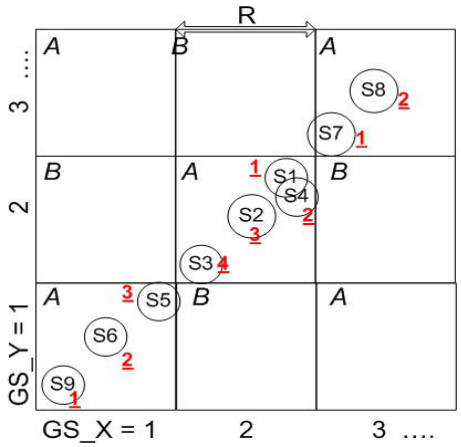

Figure 5-8 Case Study

We use an example to demonstrate the CAIG function. Given the network shown in Figure 5-8, *A* and *B* denote the STF, sensors are denoted by the letters in circles and an underlined red number next the sensor is the time slot of the sensor (derived from the LSM technique). In the case study, we assume that every sensor already knows the information about its neighbors in the same grid cell because of local neighborhood discovery. A sensor broadcasts the updated neighbor table after determining a time slot using LSM, so that the sensors located at the boundary of other grid cells can discover potential collisions. For instance, nodes S1 and S7 are one-hop apart and located in different grid cells. After node S7 broadcasts its neighbor data, node S1 will know that they share the same time slot. Node S1 thus starts the reassignment of its time slot (time slot 5) and then broadcasts the updated neighbor data. Note, that the assignment of a new time slot involves searching for the smallest available time slot in the sensor's two-hop neighborhood, i.e., the two-hop graph coloring problem [80] [90]. For Node S1, time slots 1, 2, 3 and 4 are used by nodes S7, S8, S2 and S3 respectively. So the next smallest time slot is time slot 5. Similarly, node S4 learns about the collision between itself and node S8. Therefore, node S4 locally reassigns and broadcasts its new time slot (time slot 6). An instance of the hidden terminal problem is between nodes S2 and S5. They belong to different grid cells and are two-hops apart. So the broadcast message from one is not received by the other. However, when node S3 hears the broadcast message of node S5, it finds that its neighbor node S2, shares the same time slot 3 with another neighbor, node S5. Node S3 thus broadcasts its updated neighbor data to help node S2 know of the possible collision. Node S2 reassigns its time slot to time slot 2 and broadcasts it. Thus, CAIG alleviates possible collisions by providing distinct time slots to different sensors in any two-hop neighborhood.

After the time slot assignment schedule is set (supported by the LS and CAIG) sensors run the transmission, receive or sleep mode in time slots by following this schedule. In static networks, transmission of data should be conflict-free and need no ACK message, but this protocol still adopts the ACK function in data delivery for higher layers management, e.g., the re-generation of time slots allocation for excessive colliding packets.

In this chapter, the spatial reuse of channel assignment is based on the TDMA technology on a single frequency. The channel (time slot) assignment of GLASS can be converted into a frequency channel or an orthogonal spread spectrum code with no changes whatsoever. We note here that if time slots are replaced by a set of frequency channels or orthogonal codes, this will imply that the entire PM transmission occurs during the same time. The sensors will occupy the frequency channels or use the spreading codes with a given probability.

5.3 GLASS ANALYSIS

In this section, we analyze the correctness and the overhead complexity of the protocol.

5.3.1 Correctness of the time slots schedule

To test the validity of the time slots schedule generated by the GLASS, we first define what a conflicting time slot is. Based on the two-hop graph coloring problem, there is a conflict with the time slot, when the time slot of a sensor is same with the time slot of another that is within two-hops of the sensor [80] [90]. If we satisfy the condition that no conflicting time slots

exist between any two sensors from any one grid cell and from any two different grid cells, we will prove that the generated time slot schedule for transmission is conflict-free.

Theorem 5.1: There is no conflicting time slot assignment between any two sensors within any grid cell when the protocol converges.

Proof: To prove Theorem 5.1, it is sufficient to prove that no two sensors within two-hops of each other share the same time slot in any grid cell. Given the side length of a grid cell is 2.1*r*, the maximum distance between any two points within a grid cell is *Diagonal* (D), which is 2.98*r*.

$$D = 2.1 \times 2^{0.5}\, r \bullet 2.98r \tag{5-3}$$

To cover such a distance, a three-hop transmission is required. Our neighborhood discovery scheme covers the neighbors up to three-hops away within the grid cell. This ensures that every sensor discovers all of its neighbors within its grid cell for the correct time slots assignment. Next, we apply the LS characteristic to guarantee distinctive time slots for all the sensors located within a given grid cell. Under the assumption of correct neighborhood discovery, local sensors use the LS generation algorithms [75] [87] to create an identical LSM. Such LSM ensures every local sensor the same time slots assignment schedule as every other sensor that prevents overlapping time slots assignment within the grid cell (seen Figure 5-6). If the situation where a sensor's time slot conflicts with its neighbor's time slot occurs, then the CAIG function is initiated. This situation will not impact the accuracy of the time slots assignment in any two-hop neighborhood because the CAIG follows the two-hop graph coloring concept. We accordingly guarantee that all sensors select a time slot, which is different from the time slots of its neighbors within two-hops, in the grid cell.

Theorem 5.2: There is no conflicting time slot assignment between any two sensors from any two different grid cells when the protocol converges.

Proof: To prove Theorem 5.2, it is enough to prove two points: (i) there are no conflicting time slot assignments between any two sensors that belong to different grid cells and use different STFs and (ii) there are no conflicting time slot assignments between any two sensors that belong to different grid cells but use the same STF**.** We refer these to the fact that any two neighboring grid cells share either an identical STF or different STFs in this GLASS protocol. To prove point (i), in the Transmission Frame Assignment phase we interleave STFs in non-adjacent grid cells as shown in Figure 5-5 (a) and (b) so transmissions, i.e., scheduled time slots, from the grid cells with different STFs never overlap because of *temporal* separation. The first point therefore is validated. Concerning the point (ii), chances of conflicting transmissions, namely overlapping time slots take place either at a common receiver in between, (i.e., a hidden terminal problem) or around intersections of any four grid cells, i.e., diagonally neighboring grid cells. With the two STFs setup, the distance between any two grid cells with an identical STF is the side length of a grid cell, 2.1r, except at the intersection of four grid cells. Such a distance prohibits the sensors from these two grid cells to communicate directly if the sensors are not in the intersection region. The sensors are also unable to find a common receiver to relay data because the transmission distance between each other is over two-hops (2.1r). Therefore, a common receiver that uses overlapping time slots to receive data from both the sensors does not exist. The proposed CAIG function is devised to address the conflicting time slots in the region of intersections. Using collected neighbor information from other grid cells, a sensor near the border of its grid cell can examine the assigned time slots to exclude potential collisions. It re-assigns itself a distinctive time slot that is different from the time slots used by its two-hop

neighborhood if a conflicting time slot is discovered. As a result, the concerns with the hidden terminal problem and the collision around intersections of any four grid cells are alleviated. Taking into consideration the proofs for the points (i) and (ii), we guarantee that there is no conflicting transmission between any two sensors from any two grid cells.

Theorem 5.3: There is no conflicting time slot assignment between any two sensors when the protocol converges.

Proof: According to Theorems 5.1 and 5.2, there is no conflicting time slot assignment within any grid cell as well as between any two grid cells. So, the time slots assignment schedule with the two STFs configuration is proved to be conflict-free. Besides, the time slot assignment schedule with the four STFs configuration is also conflict-free based on Theorem 5.1 and point (i) of Theorem 5.2.

These results regarding the behavior of GLASS are based on the spatial and temporal relationships between different sensors. In this chapter, we do not consider the effects of radio propagation or interference. We do incorporate the two-hop graph coloring problem into the design of GLASS to support conflict-free time slot scheduling. The hops indicate radio connectivity rather than any particular propagation model.

5.3.2 Overhead complexity

The overhead of GLASS occurs during neighborhood discovery and the message complexity depends on the area of local neighborhood namely the grid cell. Thus, the value of R has significant impact on the overhead cost. R ranges between $2r$ and $2.1r$ as shown in Equation (5-1). We set R to be larger than $2r$ because of the alleviation of the hidden terminal problem (see the proof of Theorem 5.2) and less than $2.1r$ because we try to minimize the overhead

messages by limiting the maximum hop count, 3 hops, inside a grid cell (see the proof of Theorem 5.1). In other words, we configure the R in such a way to enhance the transmission reliability while minimizing the neighborhood discovery cost. To achieve efficient spatial reuse of the available bandwidth, the smaller the value of R, intuitively the better is the spatial reuse of all sensors. Meanwhile, we take into account the effect of radio irregularity [81] between transmissions so we keep a buffer distance for reducing such effect. We set the default of R as $2.1r$ to preserve the buffer, i.e., 10% of r, avoiding transmission collisions while considering the spatial reuse factor, the transmission reliability and the overhead cost.

After neighborhood discovery is completed, each sensor derives the time slots schedule in a distributed and self-organized way with one or more broadcast messages. These depend on the degree of local contention. Its complexity remains $O(x)$ where x is the size of local contending neighbors.

5.4 PERFORMANCE VALIDATION

5.4.1 Simulation Configuration

We implemented GLASS in ns-2 [73] and evaluated transmission efficiency, overhead complexity, impact of changing topology and scalability. We compare the GLASS protocol with the IEEE 802.15.4 CAP mode (CSMA/CA) [11] and DRAND [80]. The comparison with 802.15.4 is the benchmark of this study, and DRAND serves as an example of an advanced access-scheduling approach. DTA [84] and NAPT [85] are not included in this comparison study because the DTA is not a distributed scheme and the NAPT does not perform as well as DRAND

in terms of transmission efficiency. We set the channel data rate to 250 Kbps and the sensor transmission range to 15 meters. The packet size is 70 bytes. Four network topologies are tested in simulation as shown in Figure 5-9. The first topology (Figure 5-9 (a)) is a random dense network. It includes 20 sensors randomly placed in a 63×63 m^2 flat area with a BS, and all sensors intend to report sensed data to the BS. We place the BS in two different locations to demonstrate different aspects of the GLASS protocol. The first BS location is near an *Intersection of Grid Squares* (IGS), e.g., node 0, and the second location is *Not near an Intersection of Grid Squares* (NIGS), e.g., node 20. The average 2-hop neighborhood size in this topology is 12.5 sensors. It reflects a densely populated network with challenging hidden terminal problems and multi-hop data delivery to the BS. The second to fourth topologies are tree network topologies with different node densities. They include 20, 40 and 80 nodes in a 126×126 m^2 flat area with a BS in center. The system model as in Section 5.1 is followed here. We assume that each sensor always has pending data ready for transmission, so the simulations represent a data intensive traffic scenario. For the radio channel propagation model, a two-ray path loss model was chosen and fading was not considered in the simulations. The reported simulation results are averaged over 30 runs. Simulations run for 400 seconds of simulation time. Mobile scenarios are discussed later.

We evaluate the network performance through these metrics:

Throughput: Amount of the successful data arrived at the BS per second.

Success rate: Ratio of the number of transmitted packets that reach the BS successfully to the total number of generated packets from the application layer.

Average number of control messages per sensor: Number of transmitted control messages per sensor per cycle of time slot generation.

Variation ratio of the packet loss rate: A measure of dispersion between the packet loss rate at the 100th second and the packet loss rate afterward. The network topology has no changes until 100 seconds. Packet loss rate = (1 – success rate).

Average number of cumulative overhead messages per sensor: Number of transmitted control messages per sensor at the end of all time slot recoveries. The time slot recovery is designed to update a time slot schedule for all sensors.

Probability of conflict-free time slot schedule in the new two-hop neighborhood: Probability that a sensor's time slot does not conflict with those of its neighbor's within a two-hop distance after the sensor moves to a new location.

Average delay of successful packets: The average time for a packet to successfully reach the BS.

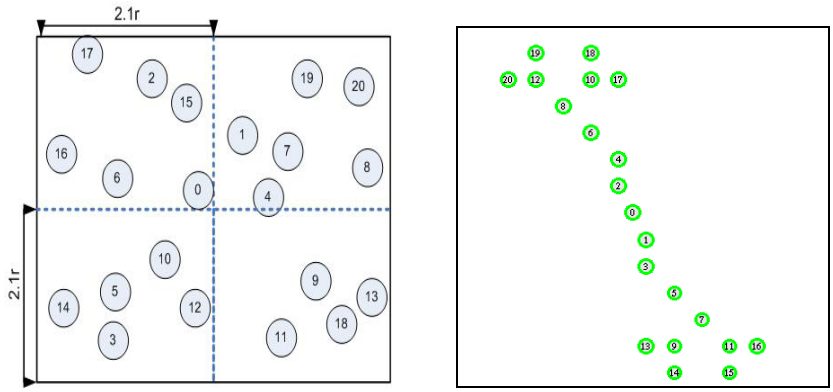

(a) (b)

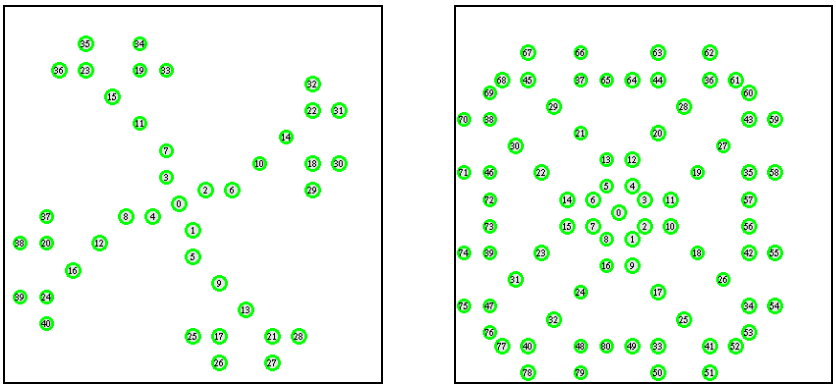

(c) (d)

Figure 5-9 Network Topologies: (a) Random Dense Network (b) Sparse Network (c) Medium Sparse Network (d) Large Dense Network

5.4.2 Analysis of Results

A. Transmission Efficiency

To show the transmission efficiency at different levels of network loads, we vary the number of simultaneous senders from 1 (low contention) to 20 (high contention) in the random dense network. These simultaneous senders are selected around the BS for each run. Furthermore, we configure all sensors in the network as simultaneous senders and program them to deliver CBR packets in different data generation rates, i.e., (packet/second/node).

We utilize two metrics to demonstrate the transmission efficiency: throughput and success rate (Figure 5-10). We notice that transmission efficiency of the CSMA is unacceptable for high contention scenarios. On the other hand, transmission efficiency of the DRAND is satisfactory for all traffic loads. In Figure 5-10 (a) and (b), the GLASS protocol is not equipped with the CAIG function. It shows poorer performance than the DRAND protocol, but significantly outperforms the CSMA. Since collisions still occur near intersections of grid cells,

the DRAND protocol is better than the GLASS protocol without the CAIG function. Overall, the performance with NIGS is higher compared to the case of IGS, since with NIGS the BS is not near the high contention area. The success rate of GLASS-IGS between 8 to 20 senders has a concave shape: more data are lost with more than 15 senders. Next, the GLASS protocol with the CAIG function is tested under stringent conditions: 20 simultaneous senders and different data generation rates. Figure 5-10 (c) shows that the GLASS and DRAND protocols are comparable in the success rate metric while the CSMA performs worse because of high channel contention and retransmission. Accordingly, it is apparent that the CAIG function indeed maintains collision resolution around intersections of grid cells, and the complete GLASS protocol matches the DRAND protocol in transmission efficiency in different traffic loads.

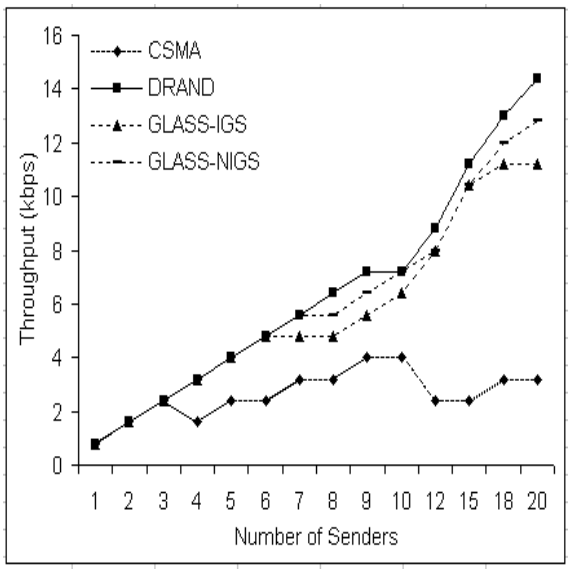

(a)

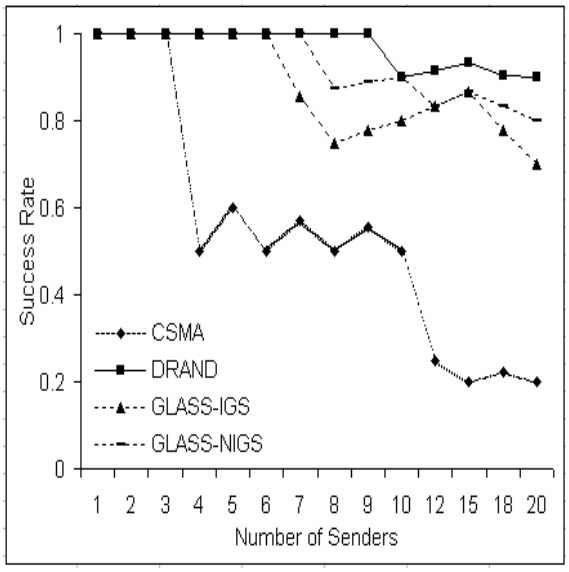

(b)

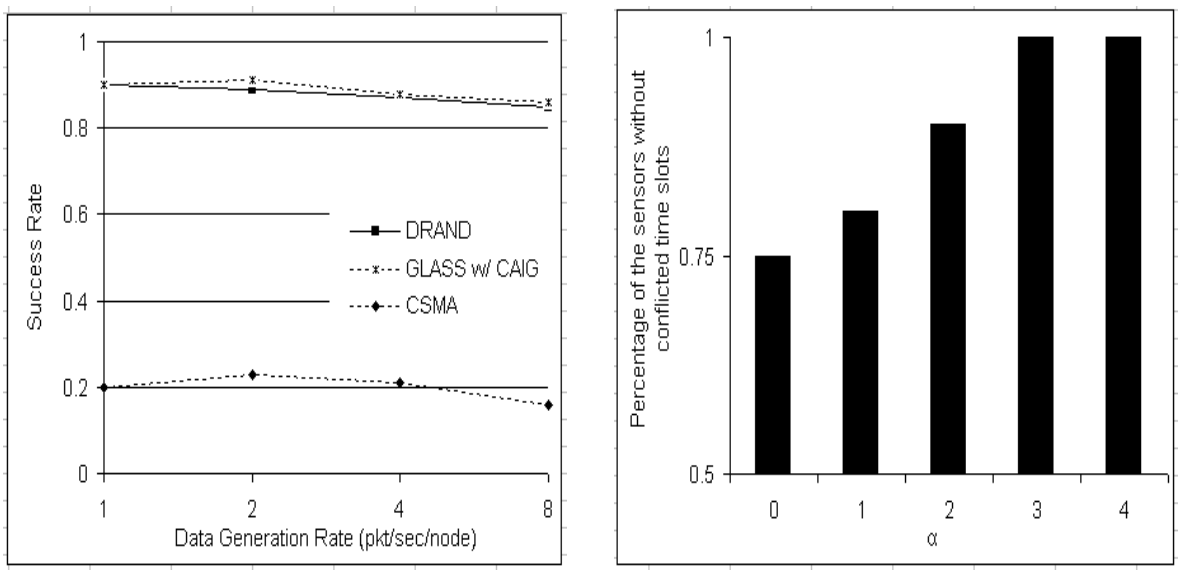

(c) (d)

Figure 5-10 Transmission Efficiency in Random Dense Network Topology (a) Effect of CAIG on Throughput Performance (b) Effect of CAIG on Packet Success Rate Performance (c) Transmission Reliability Comparison given • = 3 (d) Effect of • on Collision Avoidance

Tuning the a parameter can influence the tradeoff between collision avoidance and packet delay. Figure 5-10 (d) shows the collision effect while the delay effect is demonstrated in the next results. We use the percentage of sensors without conflicting time slots as a metric of collision avoidance. In the random dense network, we observe that collision avoidance improves with an increase in a . The optimal value of a depends on network topology. For the topology in Figure 5-9 (a), an optimal a from simulation is 3.

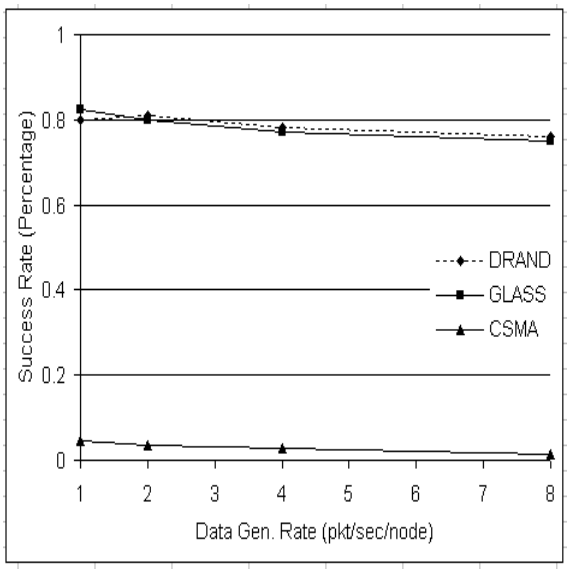

(a)

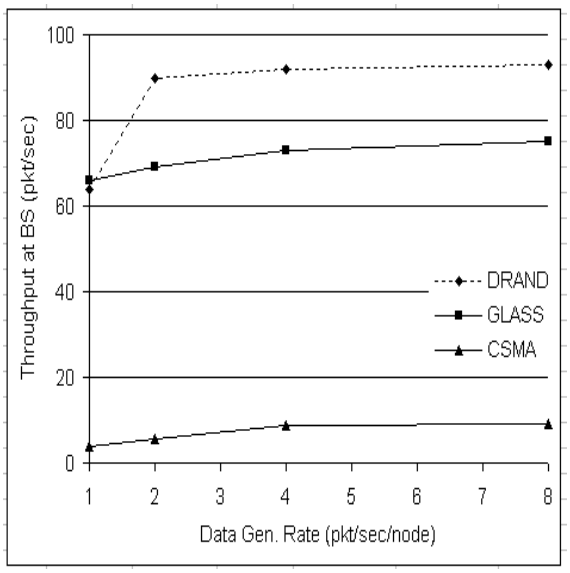

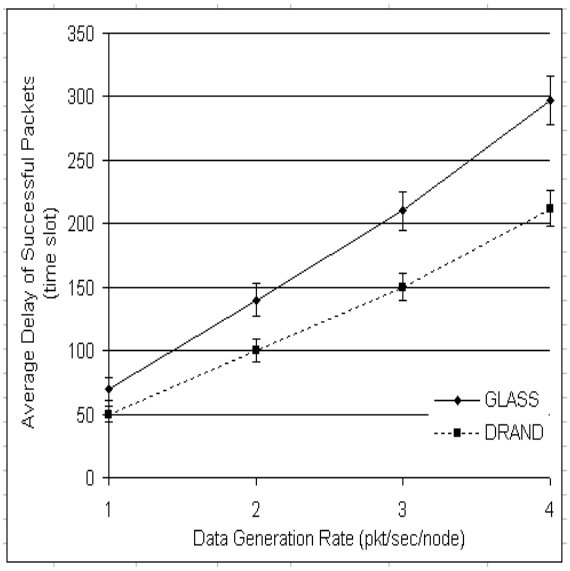

(b) (c)

Figure 5-11 Performance in Large Dense Network Topology (a) Packet Success Rate Performance Comparison (b) Throughput Performance Comparison (c) Packet Delay Performance Comparison

B. Scalable Network

We compare performances of the considered schemes in the large dense network (80 nodes). Figure 5-11 (a) displays the success rate of packets. Both GLASS and DRAND are consistently reliable because of their conflict-free time slots assignment schedules. In contrast,

CSMA is poor. The CSMA presents an even lower success rate than that of the random dense network (see Figure 5-10 (c)) because more multi-hop transmissions in scalable networks increase the probability of conflicting transmissions. Figure 5-11 (b) shows the throughput of the CSMA is much lower than that of the DRAND and GLASS protocols. This is because the CSMA is inefficient in the network with higher channel contention. Both the DRAND and GLASS protocols are designed to overcome challenges of data intensive traffic scenarios and so their performance is better. DRAND and GLASS results are comparable under low traffic loads, e.g., 1 pkt/sec/node. As the traffic load increases, the DRAND protocol shows higher throughput compared to the GLASS protocol, since its Transmission Frame (TF) is shorter. Both of the techniques face a bottleneck at the BS in this topology. Their throughputs thus remain flat at higher traffic loads. Figure 5-11 (c) displays the latency performance of GLASS and DRAND. Because of the shorter length of DRAND's TF, the average delay of a successful DRAND packet is shorter than that of a successful GLASS packet. We previously mentioned that the a parameter influences the length of TF. With a longer TF, average packet delay is affected as shown in Figure 5-11 (c). Thus, the selection of a needs to consider the described tradeoff.

C. Overhead Evaluation

For scheduling based approaches like GLASS and DRAND, the control overhead occurs in both of Neighborhood Discovery phase (ND) or Time Slots Schedule and Dissemination phase (TSSD). For CSMA, no control message is used since the RTS/CTS mechanism is not applied. For a fair comparison, both of the GLASS and DRAND protocols adopt the broadcast method to exchange the control messages.

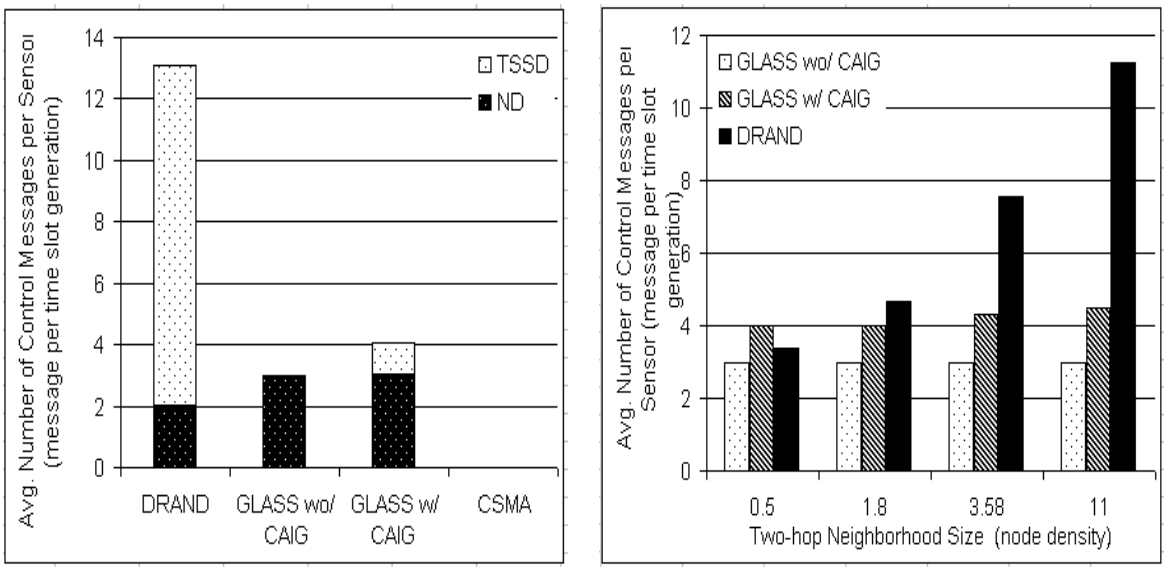

(a) (b)

Figure 5-12 Comparison of Control Overhead (a) Overhead Cost in Random Dense Network Topology (b) Effect of Node Density on Overhead Cost

Figure 5-12 (a) shows comparative overhead costs in the random dense network. DRAND has higher overhead than GLASS due to extensive messages exchanged for the time slot assignment. GLASS, relying on local sensor computations outperforms DRAND 3-to-1. We also explored the effect of network density on control overhead. We performed experiments with network topologies by varying the average number of two-hop neighborhoods from 0.5 to 11 nodes. The neighborhood size of the network is changed by varying the numbers of nodes from 20 to 160 within a 150×150 m^2 flat area. Figure 5-12 (b) shows that control overhead with DRAND increases proportionally as the network density increases. The overhead with GLASS is almost independent of the network scale and node density. In addition, we note that the overhead cost, contributed by the CAIG function, does not overwhelm the system because the CAIG function only involves conflicting sensors in the local level rather than in the global level.

D. Impact of Sensor Mobility

In mobile WSNs, the topology may change because of sensors relocation. Sensor mobility may result in degrading transmission efficiency and/or increasing overhead cost. Here, we investigate the impact of sensor mobility and changing network topology on GLASS compared to DRAND.

First, we conduct three sets of experiments in the random dense network with different topology update frequencies resulting in time slot recovery, i.e., 1, 2 and 4 times. We randomly select 5 mobile nodes moving to random locations. The node relocations and time slot recovery occur evenly within the simulation duration. We use the metric called *Variation ratio of the packet loss rate* to demonstrate (i) the effect of changed topology on transmission efficiency and (ii) the improvement after time slot recovery. Figure 5-13 (a) illustrates that the changed topology constantly results in an increase in packet loss until the time slot recovery. For instance, GLASS and DRAND with 1 TS recovery (red lines) show continuous increases of the metric until 375 seconds when the time slot recovery occurs. We observe a step trend in the variation ratio increase, since some node relocations do not impact network performance. For example, with GLASS, the performance does not change much from 300 to 350 seconds. More frequent time slot recovery reduces variations in the packet loss rate enhancing transmission efficiency. Thus, the degrading influence of the changed topology is alleviated (as shown by the blue and green lines). In other words, a regular update of time slots helps sensors overcome the impact of changed topology. The overhead cost caused by the time slot recoveries, however, results in a tradeoff because transmission of control messages consumes energy and bandwidth [29]. Figure 5-13 (b) displays this tradeoff for GLASS and DRAND. GLASS considerably out-performs DRAND (3-fold decrease in the overhead cost).

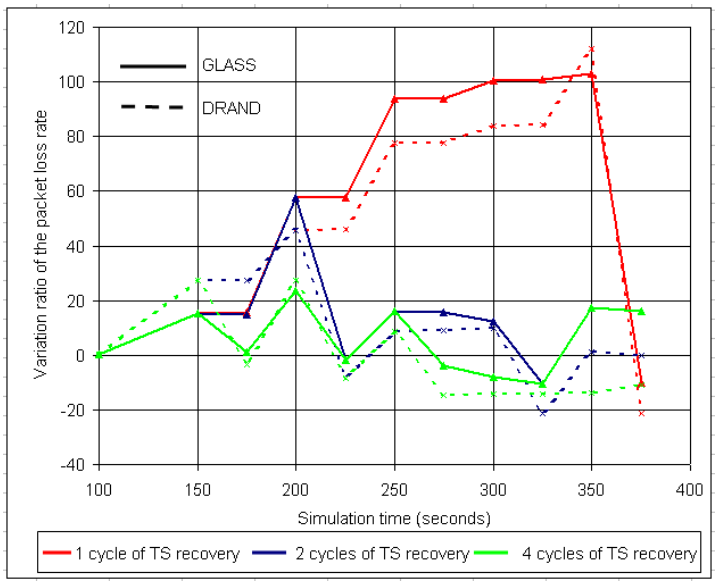

(a)

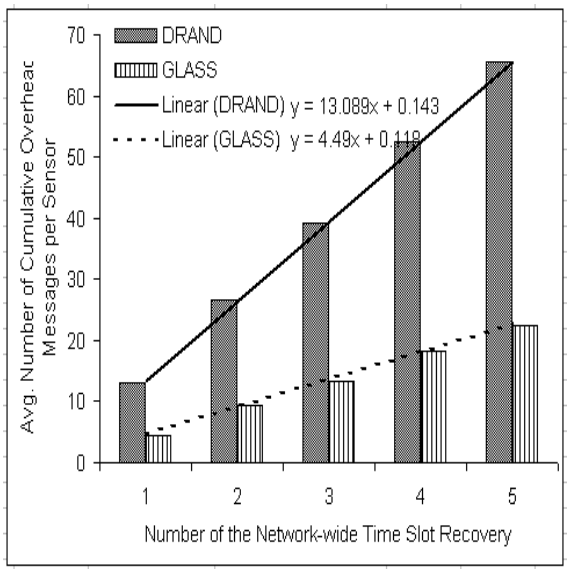

(b)

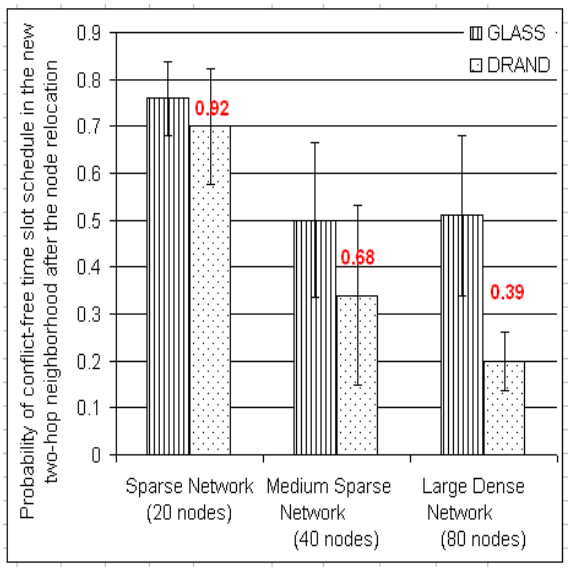

(c)

Figure 5-13 Influence of the Changed Topology between GLASS and DRAND (a) Transmission Efficiency in Dynamic Networks with Time Slot Recovery (b) Overhead Cost of Time Slot Recovery (c) Robustness Against Changing Topology

Note, that some time slot recovery may not enhance network utility if the network is not changing frequently. Meanwhile, the overhead cost is added anyway.

Figure 5-13 (c) shows the robustness of the considered schemes with respect to the changing topology in different networks. Here, we assume that the time slot is not updated after relocation of a node. We set up an experiment that randomly selects a node with a random location in the network. After that, we check if the current time slot of the node is conflicting with the time slots of its new two-hop neighbors after the relocation. If it does, this node is in a possible collision area and its time slot schedule is not conflict-free. This is repeated 10 times (i.e., we consider 10 randomly moving nodes) in each experiment. Ten trials are run for each network topology, i.e., Figure 5-9 (b), (c) and (d), with 95% confidence intervals represented by error bars. To capture variation of results, we calculate the percentage of similarity between the average results showed by a red number above the DRAND column in Figure 5-13 (c). In the sparse network, because of low node density, both DRAND and GLASS are comparable, with 92% similarity, and their probabilities of conflict-free time slot schedule after relocation are both around 0.7. As more nodes join the network (resulting in medium sparse and large dense networks), we observe that performance of both techniques degrade, but degradation with DRAND is more considerable than that with GLASS (only 39% similarity in the large dense network). In the large dense network, GLASS adapts better to changing topology according to the statistical results. This is because the GLASS protocol adopts the two STFs configuration and the grid concept. In the case of GLASS, there is 50% chance that a node moves to a new location and finds a different temporal domain, i.e., different STF, so potential collision is avoided. DRAND does not support such a feature and it is more vulnerable to sensor mobility and changing network topology.

E. Discussion

GLASS efficiently mitigates high data loss in mobile data intensive sensor networks. We demonstrated that GLASS considerably outperforms the IEEE 802.15.4 CAP mode and matches DRAND in terms of transmission efficiency. Meanwhile, GLASS is much more efficient in adapting to sensor mobility and changing network topology. At the same time, it provides a distributed and scalable channel access.

The GLASS performs channel access using sensor location information. In general, the precision of location determination techniques may be an issue. Recently, this issue has been partially resolved via the advancement of intelligent and inexpensive positioning techniques [78] [91]. In addition, our protocol is not sensitive to the location-based errors since the designs of STF and CAIG function provide both temporal and spatial collision prevention techniques.

The length of TF is an important factor. It affects bandwidth utilization and packet delay. GLASS and DRAND both adopt the two-hop graph coloring to assign time slots and so the protocols try to minimize the length of TF. Because of the two STFs configuration in GLASS, it may trade small amounts of throughput and packet delay to reduce collisions, control overhead and degradation due to changing topology which are important for resource-constrained WSNs. Due to the low complexity and small overhead characteristics in GLASS, the cost of time slots recovery is considerably lower compared to DRAND. Finally, the GLASS performance is less susceptible to the changing topology.

5.5 EFFECT OF THE CHANGED TOPOLOGY

We have demonstrated that sensor mobility makes some changes in a network topology and results in varying degrees of performance degradations, depending on channel access

protocols (see Figures 3-11 and 5-13). Meanwhile, the overhead cost of recovering from a changed topology is considerably different between different access schemes. These reasons motivate us to investigate the effect of the changed topology on the proposed protocols in this dissertation. This section will present a simulation-based comparison study among the considered channel access schemes, e.g., DTA, DRAND, CPT, NAPT_2hc, GLASS, and IEEE 802.15.4 CSMA/CA.

First, we evaluate the effect of the changed topology on transmission efficiency of all the considered protocols. We choose the random dense network (shown in Figure 5-9 (a)) as the representative network with mobile sensors. Five selected sensors moving to random locations are configured in this experiment. These sensors sequentially move to random locations in the topology and then setup new routes to the BS. There is no time slot recovery until the end of the simulations. We again use the *Variation ratio of the packet loss rate* metric to demonstrate the effect of changed topology on transmission efficiency and the improvement after time slot recovery.

Figure 5-14 illustrates that the changed topology may result in an increase in packet loss until the time slot recovery. This outcome is almost not applicable to the random channel access schemes, like CPT and 802.15.4 CSMA/CA, since their channel accesses are independent of local network changes, e.g., added or deleted nodes in networks have no impact on channel access. With CSMA/CA or CPT, a sensor accesses the network using instant channel monitoring or a random transmission probability. Thus, the network topology is not a significant factor for the channel access. In the case of DTA, a centralized scheduling access protocol, it is obviously opposite to that of the random access protocols because considerable packet loss is generated by inaccurate DTA transmission schedules in mobile networks. DTA is designed to derive collision-

free query schedules in static networks. Its optimizer calculates new schedules, which include start time of transmission, the amount of pending data, and the next hop node, for all sensors in the network. If some sensors relocate their locations, the original transmission schedules cannot guarantee conflict-free data delivery because the time slots of new neighbors may be conflicted or the next hop node may be out of the sensor's transmission range. In this experiment, the schedule update is belated so that the sensor relocations are not considered in the transmission schedules causing inefficient transmission results.

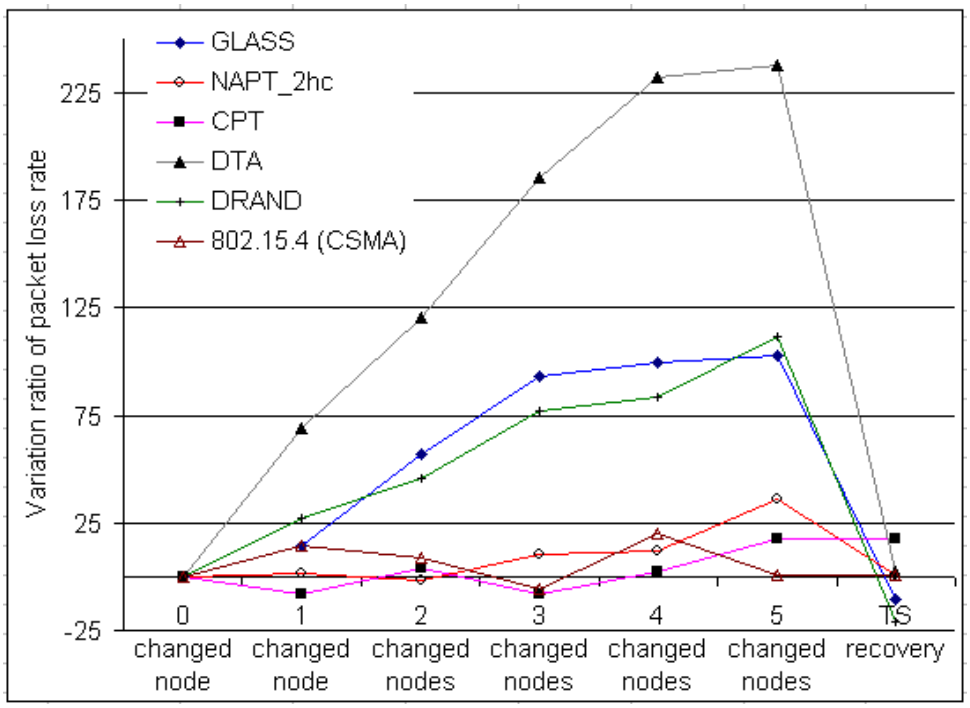

Figure 5-14 Effect of the Changed Topology on Transmission Reliability

A similar trend is observed with the distributed scheduling access protocols, e.g., GLASS, DRAND, and NAPT_2hc, albeit with fewer numbers of dropped packets (2-fold decrease). The distributed scheduling access schemes exchange control messages, which take into consideration the radio connectivity among neighboring sensors (i.e., design of the two-hop graph coloring) or limited local information (i.e., hop count to the sink), facilitating setup of

access schedules. Thus, transmission performance is only limited by accuracy of time slots assignment in mobile networks. Consequently, they are less susceptible to ineffective transmissions, compared with the DTA. Overall, we can clearly recognize that the random access is the most effective approach against the changed topology while the centralized and cross-layer scheduling technique, i.e., the DTA, is the worst among the considered protocols. We propose the next experiment to further investigate transmission performances of the GLASS, DRAND, and NAPT_2hc protocols with the changed topology. Note that the results of Figure 5-14 do not reflect the transmission reliability of the protocols. Instead, they demonstrate the effect of changed topology on all the considered protocols in general.

Figure 5-15 shows the robustness of the distributed scheduling access schemes with respect to the changing topology in different networks. The configuration of this experiment is same as that of Figure 5-13 (c). Here, we assume that the time slot is not updated after relocation of a node. We set up an experiment that randomly selects a node with a random location in the network. After that, we check if the current time slot of the node is conflicting with the time slots of its new two-hop neighbors after the relocation. If it does, this node is in a possible collision area and its time slot schedule is not conflict-free. This is repeated 10 times (i.e., we consider 10 randomly moving nodes) in each experiment. Ten trials are run for each network topology, i.e., Figure 5-9 (b), (c) and (d), with 95% confidence intervals represented by error bars. In the sparse network, because of low node density, all of the compared protocols, namely DRAND, GLASS, andNAPT_2hc, are comparable and their average probabilities of conflict-free time slot schedule after relocation are around 0.70. As more nodes join the network (resulting in medium sparse and large dense networks), we observe that performance of all techniques degrade, but degradations with DRAND and NAPT_2hc are more considerable than that with GLASS. In the large dense

network, GLASS adapts better to changing topology according to the statistical results. We attribute the robustness of GLASS to the two STFs configuration and the grid concept in the GLASS scheme. DRAND and NAPT_2hc do not support such features – so they are prone to be affected by sensor mobility and changing network topology.

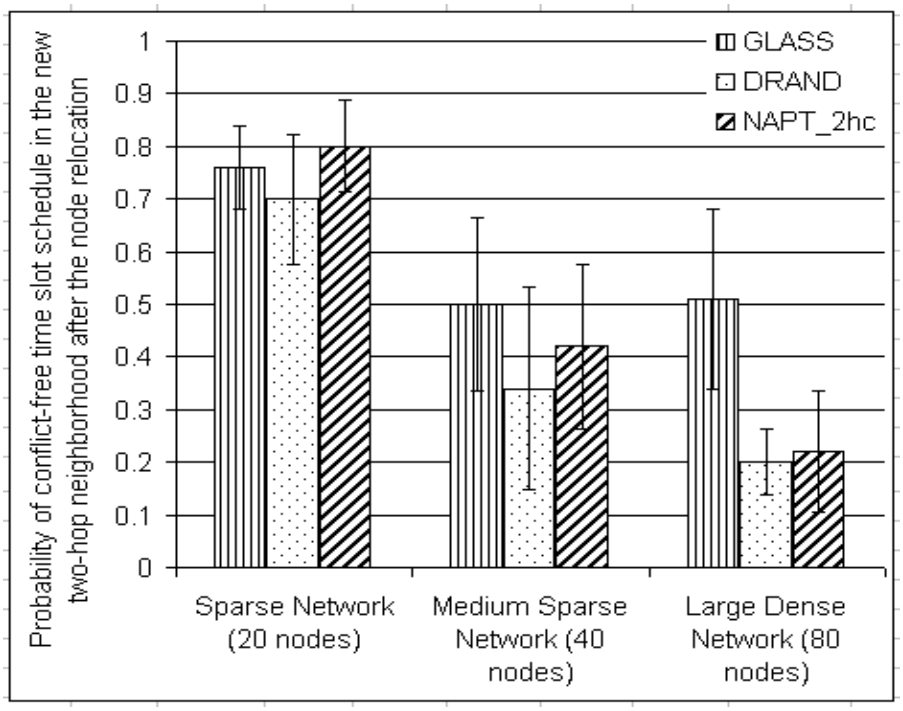

Figure 5-15 Effect of the Changed Topology on GLASS, DRAND, and NAPT_2hc

We have illustrated that moving nodes in a WSN can degrade transmission performance. To cope with this challenge, scheduling protocols normally adopt a cyclic time slot recovery method, which includes a topology update and calculations of time slots assignment, ensuring effectiveness of transmission schedules. The overhead cost caused by the time slot recovery, however, results in a tradeoff because transmission of control messages consumes energy and bandwidth. The control messages increase linearly when a mobile WSN maintains high transmission reliability by running frequent time slot recoveries (see Figure 5-13 (b)). Thus, we

compare the overhead cost of all the considered protocols to understand this tradeoff. In the experiment, the CSMA/CA method is used to deliver control messages in the TSSD phase while reliable broadcast is used in the ND phase. Figure 5-16 displays the average number of control messages per sensor per cycle of time slots generation in varying network topologies, i.e., 20, 40, 80, and 160 nodes within a 150×150 m^2 area. IEEE 802.15.4 CSMA/CA and CPT do not employ any control message in every topology because of their designs in channel access. GLASS and NAPT_2hc consume small amounts of overhead, 3 ~ 6 control messages per sensor, and the network topology or the node density almost has no effect on their overhead consumption. DRAND's overhead cost strongly depends on the node density resulting in considerable increases in overhead cost as more sensors join the network. Overhead result of DTA is more complex. DTA is a centralized optimization technique, which collects local information from every sensor to derive an optimal transmission schedule and then relays the schedule back to every sensor. Thus, it is obvious that the amount of control messages, utilized by the DTA, increases in a global order, instead of in a local order, e.g., distributed approaches. In sparse networks (e.g., 20 nodes and 40 nodes topologies), the DTA's overhead cost is light because the networks are so sparse that some local sensors can not find forwarding routes to communicate with optimizer (Base Station). As we increase the network density, the control messages in DTA increase exponentially and out-perform all the considered protocols. Note that, the overhead cost of DTA in the 160 nodes network is slightly less that that in the 80 nodes network. This is because of two reasons: (1) the network is highly congested and loaded with global traffic causing the wireless medium to be constantly busy. Therefore, some nodes are forced to remain in a backoff state for channel access and eventually give up trying to access the channel (given the maximum access retry of CSMA/CA is 4 in this experiment). (2) With more nodes (i.e., 160

nodes) in a large scale network, the average number of control messages *per sensor* is less than that of the 80 nodes network, because more nodes participate in producing smaller amounts of control messages due to the fact that some nodes have no chance to transmit due to the high channel contention.

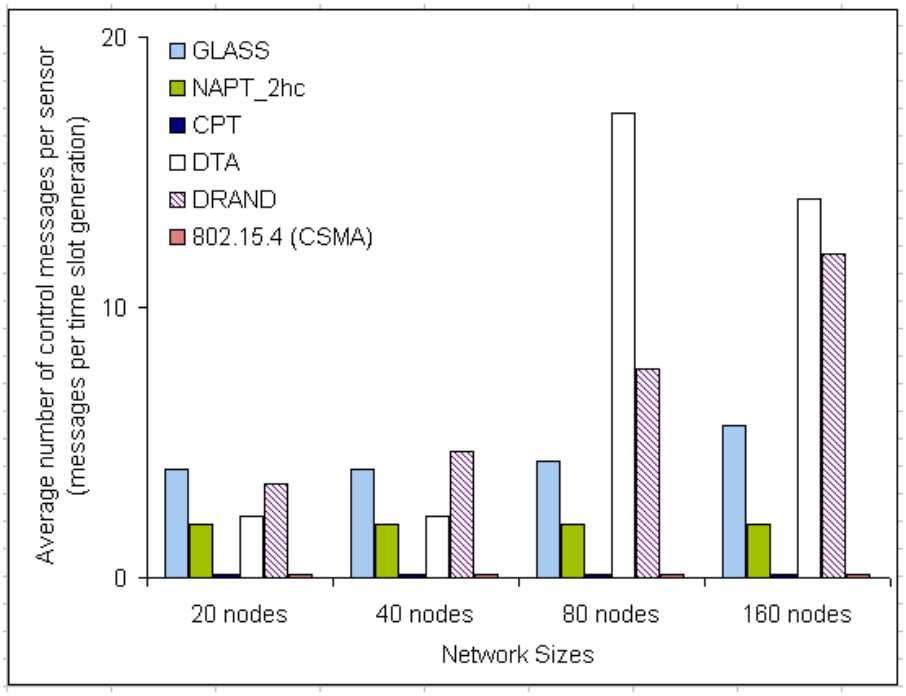

Figure 5-16 Overhead Cost of Considered Protocols at Different Networks

5.6 CONCLUSION

We have proposed a novel grid-based scheduling access technique called GLASS that utilizes Latin Squares to mitigate the significant performance degradation in data intensive sensor networks with minimal control overhead. We analytically prove that GLASS efficiently eliminates conflicting time slots in transmission schedules. In particular, our simulation-based study demonstrated that GLASS has about 33% of the DRAND overhead in each generation of

time slots schedules with comparable transmission reliability. Our approach is especially suitable for a mobile data intensive sensor network with frequently changing topology, compared to other scheduling protocols.

In this chapter, we also verify the effect of changed topology on all the considered protocols in this dissertation. Our finding indicates that the random access schemes, e.g., 802.15.4 CSMA/CA and CPT, are very robust to the changing topology and consume no overhead. Their transmission efficiency in DISNs however is not desirable. The centralized scheduled access scheme, like DTA, performs reliable data transmission in static networks, but its overhead cost and transmission efficiency raise a concern when the network is dynamic. Finally, the distributed scheduled access schemes, e.g., DRAND, GLASS, and NAPT_2hc, present acceptable transmission efficiency in DISNs and maintain low overhead cost. In the network with mobile sensors, GLASS performs best in adapting to the changing topology.

6.0 ADAPTABLE PROBABILISTIC TRANSMISSION FRAMEWORK

So far, this dissertation discussed benefits and concerns of fundamental access approaches (i.e., random access and scheduling access), and then presented a suite of hybrid access protocols for DISNs ranging from a randomized transmission scheme (i.e., CPT) to a decentralized access scheduling scheme (i.e., NAPT or GLASS). The work aims at addressing the significant performance degradation issue with DIAs, and provides different degrees of network utility's enhancement. For example, GLASS is apt at performing highly reliable communication while CPT is not, but CPT's performance changes little in a mobile network. Because of such reasons, in this chapter, we consider the resolution of the network performance issue in a DISN from a different perspective. Instead of designing an explicit communication protocol to meet certain objectives (see Section 1.1), we propose tuning the channel access mechanism in an adaptable way so that the access framework is able to handle different sensor application's requirements. It is also beneficial from an economical and flexibility standpoint since the channel access framework uses simple tuning efforts to achieve adjustable channel access functionality meeting specific objectives of sensor applications.

We emphasize two performance objectives, *Energy* and *Delay*, in the tuning process of this chapter. Minimizing sensor query response time is crucial in mission-critical sensor networks. At the same time, minimizing energy consumption per query is equally crucial for battery-powered sensors. In general, the time/energy trade-offs involve energy and time

gains/losses associated with specific channel access techniques. Note that performance objectives can be expanded beyond energy and delay. This chapter only considers these two problems. Consideration of multi-performance objectives (i.e., more than 2 objectives) is left as something for future work.

Several techniques have been proposed to address the problems above at the network level such as location-based routing and access methods [83] [86] [88] [89]. Sensor data management research has also utilized graph theory to design channel access strategies reducing the query response time and energy consumption [80] [86] [90]. With the same goal in mind, our research makes an effort to fuse methods and techniques currently used in the two different areas of location-based networking and graph theory-based data management. In this chapter we propose an adaptable transmission approach for properly tuning the delay and energy utilities in a DISN.

Maintaining acceptable query response time and energy efficiency is a *Multi-objective Optimization Problem* (MOP) [92]. In general, MOP aims at minimizing the values of several objective functions *f1* … *fn* under a given set of constraints. In most cases it is unlikely that different objectives would be optimized by the same choice of parameters (i.e., vectors). To choose between different vectors of the optimization objectives, an optimizer utilizes the concept of *Pareto optimality* [92]. Informally, an objective vector is said to be Pareto optimal if all other feasible vectors in the objective space have a higher value for at least one of the objective functions, or else have the same value for all objectives. Typically, there is more than one Pareto optimal vector (Pareto points) reflecting the trade-offs between different objectives. For example, if the following set includes feasible solutions for bi-objectives MOP: {(5, 1), (2, 2), (2, 3), (4, 4), (3, 4), (1, 5), (5, 3)}, then the *Pareto optimal set* (also called *Pareto front*) is {{(5, 1),

(2, 2), (1, 5)} (see Figure 6-1). Our adaptable transmission approach follows the concept of Pareto optimality while considering the tradeoffs between energy and delay objectives in a DISN.

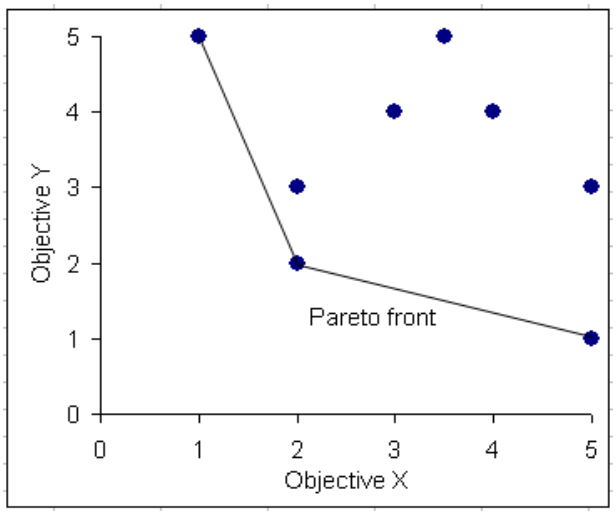

Figure 6-1 Example of the Pareto front: The points represent feasible choices, and smaller values are preferred to larger ones. Point (2, 3) is not on the Pareto front because it is dominated by point (2, 2).

To cope with the situation of Pareto optimality, we propose an access scheme called *Adaptable Probabilistic Transmission* framework (APT). APT is an extension of *Cyclic Probabilistic Transmission* (CPT) protocol [85] that performs data transmissions based on predefined probabilities. In a manner similar to CPT, APT maintains a *Transmission Probability Matrix* (TPM), each cell of which holds a probability of data transmission of a sensor within a given time slot. The TPM specifies one "network transmission cycle" where every sensor knows its own transmission probabilities in fixed time slots and repetitively uses the same TPM preserving distributed nature of processing and transmissions. In addition, similar to the GLASS protocol considered in Chapter 5, location information is used to improve channel access. Sensors divide the monitoring area into a virtual grid. Then each sensor associates itself with one

virtual grid cell or sector using geographical data. This design allows neighboring sensors to maintain *spatial* and *temporal* separation between potentially colliding packets while keeping channel access scalable. Finally, APT utilizes *Latin Squares* characteristics (LS) [75] to tune the probabilities in the TPMs of sensors enabling trade-offs between our objectives for optimization. We demonstrate the feasibility of our technique using analysis and simulations. The analytical model captures the characteristics of the DISN with APT while the simulation study validates the analysis and the performance in different networking environments. In particular, the simulation results show that the overhead cost with APT is minimal because only local inquiry is involved. We note that the network performance depends on the objective of the sensor application. Note that APT assumes that each node in a DISN is aware of its geographic location[4]. While location-based approaches have been adopted in routing mechanisms [88] [89], to the best of our knowledge they are rarely utilized for optimizing channel access.

6.1 SYSTEM MODEL

We assume the following system model:

1. Initially, sensors are evenly deployed in a field. Each sensor is aware of geographical data (e.g., approximate coverage and location) associated with the monitored area.

2. We adopt a quasi-periodic traffic model as it is more appropriate for Data Intensive Applications (DIAs). This model also presents a challenging scenario in terms of channel access

[4] We note that using global positioning system (GPS) is not always possible in WSNs because of energy and location precision constraints. WSNs commonly utilize ad hoc localization methods based on nodes, calculating their coordinates using special beacon nodes whose positions are known. Further consideration of this subject is beyond of the scope of this dissertation.

due to the large numbers of concurrent data transmissions within a short period of time. Collisions occur when a sensor receives more than one transmission simultaneously from different parties.

3. Every sensor transmits or receives on a common carrier frequency. It transmits in assigned time slots (using probabilistic transmission) and idle-listens or receives otherwise. A sensor can transmit a packet at the beginning of a time slot and complete the transmission, including receiving an ACK message, within the same time slot (which is 7 ms given a 250 kbps data rate). All sensors transmit at the same power that covers a limited footprint. Sensors are stationary, uniquely identified, and equipped with omni-directional antennas.

4. Time synchronization is managed by a Base Station (BS) using beacons. Note that sensors may lose beacon messages and there may be clock drift between synchronizations. Hence, sensors are designed not to transmit during the first ms of every time slot. This provides a slack time for synchronization errors and prevents collisions at the boundary of time slots.

6.2 DESCRIPTION OF APT FRAMEWORK

The APT framework is a data transmission mechanism, which utilizes heuristics (including LS, virtual grid network, and probabilistic transmission) to tune channel access to meet a variety of application objectives. Consider two Pareto optimal objectives (*Energy Factor* (EF) and *Delay Factor* (DF)), where EF and DF, as the application's bi-objectives for this chapter, are set to be between 0 and 1 (a higher value of the objective is equal to a higher priority in its respective concern.). Thus, every application is associated with a combination of (EF, DF). In order to determine the preferred goal of a sensor application (i.e., energy or delay), we define

a tuning parameter, *K*, which is equal to the ratio EF/DF, to show the orientation of such sensor applications. *K* is a weight measurement between the two objectives. If *K* is larger than 1, the objective of the application inclines to energy conservation. Otherwise, the objective of the application tends to be delay-sensitive. For example, sensor applications define following combinations of the targeted objectives: {(0.9, 0.3), (0.5, 0.5), (0.09, 0.9)}, consequently, their *K* values are 3, 1, and 0.1, which represent energy-oriented objective, non-specific objective, and delay-oriented objective respectively. We will apply this *K* parameter in the tuning algorithms presented next.

The tuning process of APT includes three phases: Grid Partition, Latin Squares Matrix, and Probabilistic Tuning. Sensors follow these steps to deliver data to their next hops cooperatively. The protocol is completely decentralized as well as scalable. Note that the first phase of APT borrows from the *Grid-based Latin Squares Scheduling Access* protocol (GLASS) described in Chapter 5.

1) Grid Partition

We use the *Grid Searching* (GS) algorithm from the previously proposed protocol GLASS [86] to assign sensors in the monitoring area to grid cells. We assume that the monitoring area consists of virtual grid cells where their shapes and sizes are uniform (see Figure 6-2). *R* is the length of one edge of any grid cell, and it is 2.1*r* or 2.1 times the sensor's transmission range. Such a value for *R* is critical for alleviation of collisions and overhead. Please refer to Section 5.3 for more details. In addition, each grid cell is identified by a sole Identification (ID), associated with its location, i.e., a pair of coordinates (GS_Xi, GS_Yi). GS_Xi and GS_Yi represent the vertical and horizontal coordinates of the grid cell respectively. Every sensor applies the GS algorithm, presented in Figure 6-3, to determine the ID of the grid

cell using its location information. Here (xi, yi) is the location of Sensor i and (X', Y') defines the area covered by a DISN. Using spatial relationships between the sensor and the monitoring area, the sensor independently calculates the ID of the grid cell. If a sensor is located on a border between two grid cells, namely the value of *Z* (i.e., the *x* and *y* coordinates in units of the length *R* of the side of a grid cell – see Figure 6-3) is an integer, this sensor will randomly choose a grid cell's ID that is between these two grid cells.

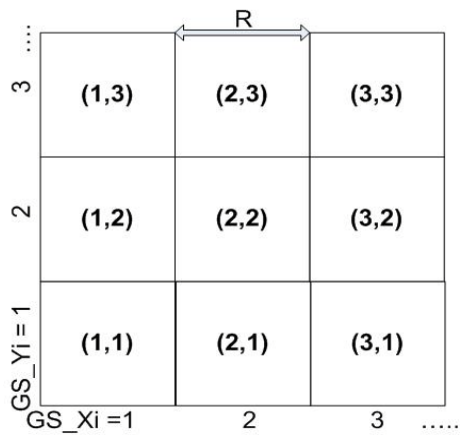

Figure 6-2 Virtual Grid Network

```
/* Given the 2 dimensional monitoring area = (X', Y')
          the location of sensor i = (xi, yi)
To find the grid  cell location of Sensor i:                    */
if xi ≤ X' and yi ≤  Y'
      Z= (xi ÷ R)
         if Z is an integer
           select a random number between 0 and 1
             if the number >0.5
               GS_Xi = Z
             else
               GS_Xi = Z+1
         else if Z is a number with decimal
               GS_Xi = ⌈Z⌉
else
       disable Sensor i /*Outside the monitoring area*/
Repeat the same steps above to solve GS_Yi
End
The Grid cell location of Sensor i = (GS_Xi, GS_Yi)
```

Figure 6-3 Pseudocode of Grid Cell Search

After a sensor locates its grid cell, it proceeds with the *Transmission Frame* assignment (TF). We define a TF as a group of continuous time slots. The TF structure repeats to manage sensors' transmit, idle or receive states. The TF can be divided into multiple equal *Sub Transmission Frames* (STFs). In this chapter, we use a configuration with two STFs: A and B. Figure 6-4 (a) describes the algorithm for assigning an STF for a sensor. The sensor uses the GS result to independently assign itself an STF (either A or B). As a result, sensors in adjacent grid cells operate with different STFs, reducing the potential for collisions. We can also configure four STFs using the algorithm shown in Figure 6-4 (b), which is similar to the algorithm in Figure 6-4 (a).

```
Given the grid cell location of Sensor i = (GS_Xi, GS_Yi)
To find the Sub Transmission Frame of Sensor i:

if GS_Yi is odd and GS_Xi is odd
    STF of Sensor i = A
else if GS_Yi is odd and GS_Xi is even
    STF of Sensor i = B
else if GS_Yi is even and GS_Xi is odd
    STF of Sensor i = B
else if GS_Yi even and GS_Xi is even
    STF of Sensor i = A
```

(a)

```
Given the grid cell location of Sensor i = (GS_Xi, GS_Yi)
To find the Sub Transmission Frame of Sensor i:

if GS_Yi  is odd and GS_Xi is odd
    STF of Sensor i = B
else if GS_Yi  is odd and GS_Xi is even
    STF of Sensor i = A
else if GS_Yi  is even and GS_Xi is odd
    STF of Sensor i = C
else if GS_Yi  is even and GS_Xi is even
    STF of Sensor i = D
```

(b)

Figure 6-4 Pseudocode of Assigning the Sub Transmission Frame for the Sensor i (a) Two STF Scenario (b) Four STF Scenario

Figure 6-5 presents examples of STF assignments. There is a network with 9 grid cells and 5 nodes with two different STF scenarios (see Figure 6-5 (a) and (b)). Each node uses the algorithm to find its STF as shown in Figure 6-5 (c). Thus, collisions of transmissions, for

example, from Sensors 2 and 3 are avoided due to temporal separation. With the four STFs configuration (see Figure 6-5 (b)), this scheme extends sensors' transmissions over more STFs and intuitively guarantees collision-free inter-grid transmissions in the network. But it may result in worse bandwidth utilization and higher packet delay compared with the two STFs configuration because of the reduction in concurrent transmissions by sensors. Therefore, we pick the two STFs configuration for the rest of this chapter.

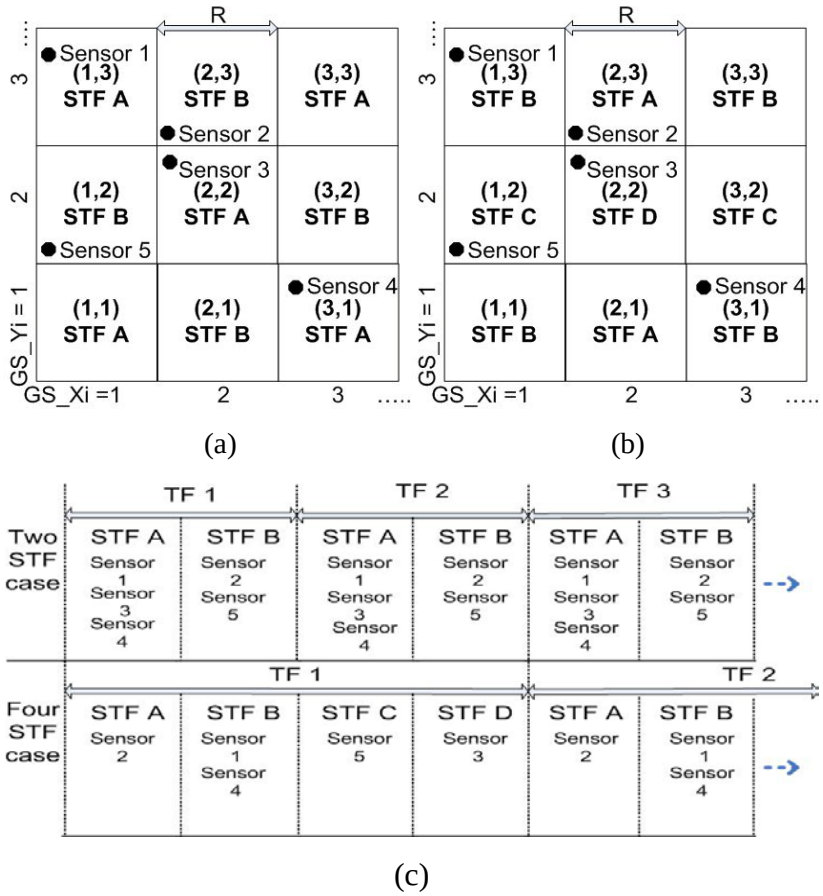

Figure 6-5 (a) Network with Two STFs configuration (b) Network with Four STFs configuration (c) Comparison of STF examples

In the two STFs case, the length of TF is configured differently for different sensor location distributions:

Length of TF = 2 * STF

$$= 2 * \left(\left\lceil \frac{\text{Number of deployed sensors}}{\text{Number of grids in the network}} \right\rceil + \alpha \right)$$

The number of deployed sensors and number of grid cells are known in the pre-deployment stage. The parameter a is an adjustable variable between zero and (number of deployed sensors / number of grid cells). If sensors' positions in the network are evenly distributed, a will be at the minimum. If the sensors are not evenly distributed, a will increase. To avoid uncertainty in sensor deployment, a should not be too small, but this may slightly impact packet delay due to longer transmission cycles/frame [86].

2) Latin Squares Matrix

After sensors discover their GS and STF, the next step is to derive *Latin Squares Matrixes* (LSM) for setup of the adaptable transmission. As we have already introduced the LSM in GLASS, the generation of the LSM in APT is slightly altered. First, each sensor performs neighborhood discovery to prepare for generation of LSMs. The neighborhood discovery requires all sensors to broadcast their information to one-hop neighbors. In this way, every sensor is aware of its neighbors and maintains neighbor tables which record neighbors' ID, distance/hop count, GS and STF. Furthermore, sensors need to keep complete and accurate neighbors information within their grid cells (local data) so each sensor must broadcast newly-received data and update its neighbor tables. There are two types of the neighbor tables, N1 and N2, in this algorithm. N1 records a list of the neighboring sensors that share the same grid cell's ID while N2 records a list of the neighboring sensors that have different grid cell's ID but identical STF. In these neighbor tables, the information of GS, STF, distance/hop count, and order (descending order of a sensor's ID in its grid cell) of neighbors is stored. Sensors adopt the data aggregation, CSMA broadcast and ACK techniques to avoid fine-grained and failed

broadcasts. Because the length of a side of any grid cell is 2.1r, the maximum distance for a sensor to convey data within a grid cell is 3 hops. In other words, the sensor needs 3 or more broadcast messages to announce itself in a grid cell, to discover neighbors' presence, and to broadcast its order information.

Next, sensors utilize the given information about STF to generate a LSM. LSM for m time slots of a STF is an $m \times m$ array, where each cell of the array contains one of a set of m symbols. Each symbol occurs only once in each row and once in each column [75]. An LSM with immediate sequential symbols, e.g., integers, can easily be constructed. One method of building a $2k \times 2k$ LSM is explained next and shown in Figure 6-6 [87].

1. Number the $2k$ symbols successively from 1 to n.
2. Assign successively the integers from 1 to n to the n cells in the first row by proceeding from left to right entering only cells in odd-numbered columns, then reversing direction and filling in the cells in even-numbered columns.
3. In each column, starting with the number already entered in the top cell, proceed downward, entering in each cell the integer immediately following the one in the cell above it, except that the integer n is followed by the integer 1.

	TS1	TS2	TS3	TS4	TS5	TS6
Sen1	1	6	2	5	3	4
Sen2	2	1	3	6	4	5
Sen3	3	2	4	1	5	6
Sen4	4	3	5	2	6	1
Sen5	5	4	6	3	1	2
Sen1	6	5	1	4	2	3

Figure 6-6 Example of a LSM

Accordingly, sensors can build an LSM of any size. We define a row of the LSM to represent a local sensor's transmission and a column of the LSM to represent the time slot of the STF (see Figure 6-6). Each sensor selects the local sensors of its LSM by choosing the sensors from N1. The selected local sensors are sorted by ascending order of their IDs in the LSM rows.

There is no guarantee that the generated LSM rows can be completely assigned to the local sensors. When the number of local sensors is less than the size of LSM, some sensors, e.g., sensor 1 in Figure 6-6, are asked to access the channel more frequently in order to use bandwidth efficiently, but channel access fairness becomes an issue. We adopt a rotating procedure that arranges local sensors in extra rows of the LSM to give fair channel access to all the sensors inside the grid cell. If the number of local sensors is more than the size of the LSM, some sensors' operations are omitted temporarily based on the rotating procedure. Such a situation reveals an over-congested grid cell. In other words, network resources are poorly and perhaps unfairly distributed. With the procedures described above, local sensors can create identical LSMs that ensure the same adaptable channel access is shared by all the sensors in the grid cell if the sensors perform their neighborhood discovery correctly. The whole process is independent and distributed for every sensor. Note that the size of LSMs of all grid cells is uniform because we intend to alleviate the difficulty of synchronization and overhead cost of maintaining an updated LSM.

3) Probabilistic Tuning

After sensors form their LSMs, the next step is to setup the adaptable probabilistic transmission using a TPM. Before explaining how to tune a TPM in detail, we will re-visit the concept of TPM that was discussed in Chapter 4. We assume that delivery of every data frame is based on the tuned probabilities derived from the APT framework. Thus, for a sensor node *i* the

probability of transmission in a time slot t is P(i, t)**.** If the sensor i intends to transmit a frame at time slot t, it will compare P(i, t) to a random value between 0 and 1 (i.e., probabilistic process). In case that P(i, t) is larger than the random value, the pending frame is transmitted. Otherwise, this probabilistic process for the frame transmission is repeated in the next (N-1) time slots if necessary, where N is the size of a local TPM (see in Figure 6-7). For the purpose of fair access opportunity to every MAC frame, we retry the probabilistic process of frame transmission up to N times, to ensure that the frame is sent. The probability that a frame is sent is close to one because there is at least one high probability in every row of a TPM according to the LSM and the tuning probability function described next.

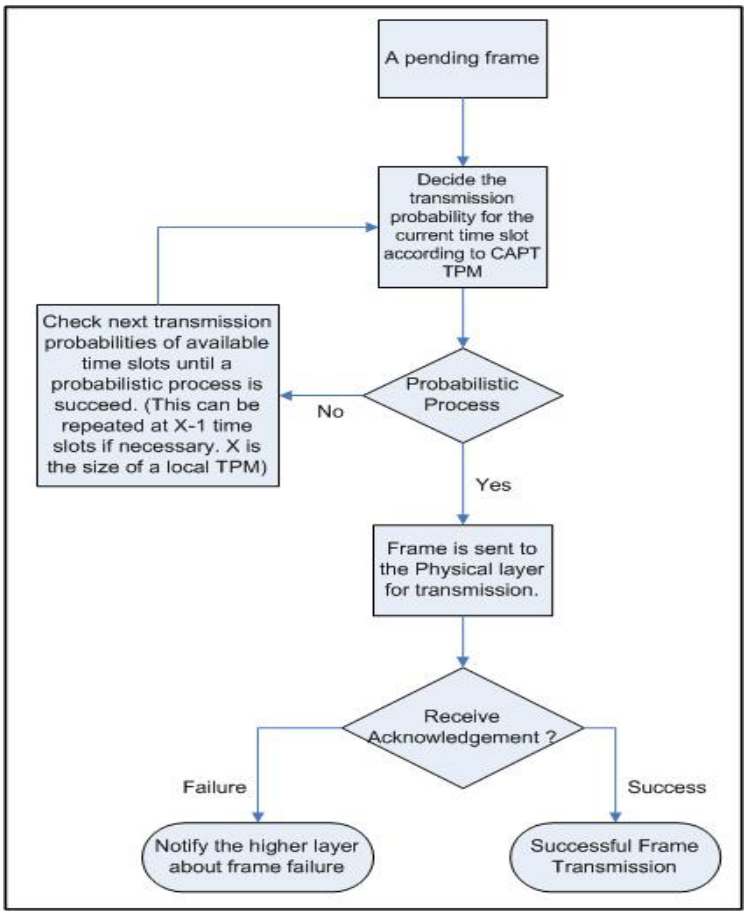

Figure 6-7 Data Frame Flow Chart of APT

Similar to the CPT protocol, the APT framework maintains an $N \times N$ TPM, where each row corresponds to a transmission of a local sensor while each column represents the time slot for the transmission. The size of a TPM is equal to the size of the LSM because they originally depend on a configuration of the STF. Each cell of the TPM holds a probability P(i, t) of the data transmission of the sensor i to occur within a given time slot t. An individual sensor only needs to know its transmission probabilities in N time slots and these probabilities repeat periodically. Figure 6-8 illustrates the concept of TPM. Figure 6-8 (a) corresponds to a serial data delivery where each transmission is deterministically assigned to one time slot. This is reflected with each row having P(i, t) = 1 for one time slot and = 0 for the rest of them. Figure 6-8 (b) assigns some non-zero probabilities for each transmission to occur in each time slot. The second matrix has higher degree of concurrency of data delivery, as well as higher probability of collisions. In the example of transmissions from *N3* and *N5* at time slot *1* in Figure 6-8 (b), the Prob. Trans case shows the concurrency chance of the transmissions is 0.45 while the concurrency chance of Serial Trans is 0. By adjusting the probabilities in the TPM we can tune the concurrency/collision tradeoffs. Proper tuning of this tradeoff is the primary objective of the APT framework.

Prob.Trans.	1	2	3	4	5	6
N1	1	0	0	0	0	0
N2	0	1	0	0	0	0
N3	0	0	1	0	0	0
N4	0	0	0	1	0	0
N5	0	0	0	0	1	0
N6	0	0	0	0	0	1

(a)

Prob.Trans.	1	2	3	4	5	6
N1	0.3	0.5	0.8	0.4	0.9	0.1
N2	0.6	0.3	0.9	0.3	0.1	0.7
N3	0.9	0.7	0.3	0.5	0.3	0.1
N4	0.3	0.3	0.1	0.8	0.7	0.9
N5	0.5	0.5	0.2	0.7	0.9	0.1
N6	0.1	0.2	0.5	0.6	0.4	0.9

(b)

Figure 6-8 Transmission Probability Matrix (TPM): (a) Serial Transmission (b) Random Probabilistic Transmission

```
/*Given the bio-objective (EF, DF), N1, N2 and derived
LSM of the node i*/
VLS(i, t) = (0, 1, 2, 3 ...) /*cell value of LSM*/
K = (EF / DF)
O_x = Descending order of the node x in its grid cell
i ∈ N1
t ∈ STF

If (K < 1)                  /*Delay-oriented application*/
        P(i, t) = e^(-K*VLS(i, t));
Else If (K = 1)             /*Non-specific application*/
        P(i, t) = e^(-K*VLS(i, t));
Else If (K > 1)             /*Energy-oriented application*/
        If (GS_Yi of the node i is even && O_i = O_j
        j ∈ N2 && VLS(i, t) = 0)
        P(i, t) = K^-1;    /*Reduce the chance of inter grid
        cells collision*/
        Else
        P(i, t) = e^(-K*VLS(i, t));
/*End*/
```

Figure 6-9 Pseudocode of Adaptable Probabilistic Transmission

To tune a TPM such that it meets the bi-objective, we devise a LS-based probabilistic transmission method as shown in Figure 6-9. This algorithm uses the given information, e.g., bi-objective parameters, tables N1 & N2, and the derived LSM, in a tuning probability function, namely an exponential decay function, in order to generate adaptable probabilities for the TPM. The decay function, $P(i, t) = e^{(-K * \mathrm{VLS}(i, t))}$ (we explain the parameters below), is used to derive probabilities for the elements of the TPM while the application objective is delay-oriented or non-specific. In addition, this function can be applied in an energy-oriented application if a sensor is not threatened by a colliding transmission of a neighboring grid cell. In the case where a sensor, with the energy-oriented application, is interfered by a neighboring node, $P(i, t)$ will be equal to K^{-1} to reduce the chance of data collision. The principles behind this are motivated by the *Collision Avoidance near Intersection of Grid Cells* function (CAIG) previously discussed in Section 5.2. Note that a sensor, with an energy-oriented application, determines the existence of

an interfering neighbor using the order information in the N2 table since two sensors with an identical order in different TPMs result in the same sequence of probabilities making them easily interfere with each other (this is based on the possibility that the two sensors are separated within 2-hop distance and share the same STF type in different grid cells.).

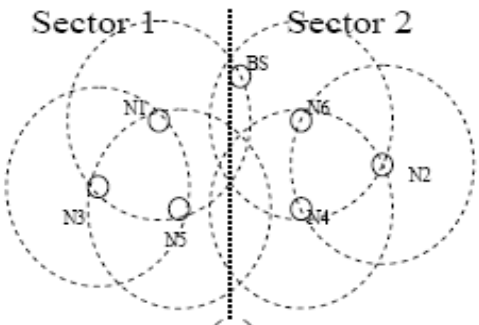

(a)

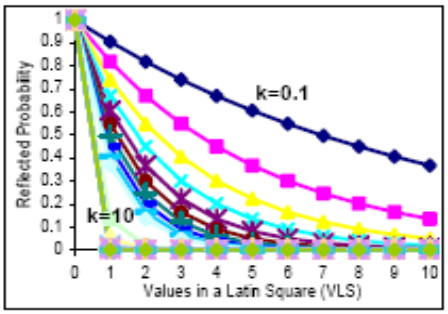

(b)

Two Sectors	1	2	3	4	5	6
N1	0. 14	1	0.37	0.14	1	0.37
N2	0.37	1	0.14	0.37	1	0.14
N3	1	0.37	0.14	1	0.37	0.14
N4	0.14	0.37	1	0.14	0.37	1
N5	0.37	0.14	1	0.37	0.14	1
N6	1	0.14	0.37	1	0.14	0.37

(c)

Single Sector	1	2	3	4	5	6
N1	1	0.37	0.14	0.05	0.02	0.01
N2	0.37	0.14	0.01	1	0.05	0.02
N3	0.14	0.01	0.02	0.37	1	0.05
N4	0.01	0.02	0.05	0.14	0.37	1
N5	0.02	0.05	1	0.01	0.14	0.37
N6	0.05	1	0.37	0.02	0.01	0.14

(d)

Figure 6-10 (a) Simple Network Topology (b) LS-based Tuning Probability Function with Different *K* Parameters (c) Tuning TPM with 2 sectors with *K* = 1 (d) Tuning TPM with single sector with *K* = 1

The decay function includes two parameters, *Cell Value of LSM* (VLS(i, t)) and *K*, to tune probabilities. Given a set of values for VLS(i, t), we can manipulate the *K* parameter of the decay function creating variations between sets of tuning probabilities (see Figure 6-10 (b)). In general, a large *K* parameter corresponds to larger differences between a high probability and other low probabilities. Using different *K* parameters to generate multiple sets of the TPM results in trade-offs between concurrent transmission and data collision in these TPMs. This phenomenon will be illustrated in Section 6.3.

We use the topology (shown in Figure 6-10 (a)) to demonstrate tuning probabilities in a network. The elements in the TPM, which considers a topology with a single virtual grid cell, are displayed in Figure 6-10 (d). Supposing there are six elementary transmissions in the network, using cell values from a 6×6 LSM and the decay function with $K = 1$, the derived TPM presents one high probability, i.e., 1, in each row and in each column. This result is derived from the Latin Squares characteristic and achieves alleviation of transmission collisions in the network.

If the network is divided into multiple virtual grid cells, the derived LSM and TPM will be considerably changed and result in a different network performance. First, the usual concerns, e.g., scalability and overall overhead, are reduced in a network with multiple sectors, compared to those in a network with a single grid cell. This is because our APT framework divides the network into sectors using the grid partition method. As a result, local neighborhood discovery is constrained to be within the sector, instead of the whole network, making the channel access scalable and the overhead cost less expensive. Figure 6-10 (c) shows the tuning TPM for the network with two grid cells (Figure 6-10 (a)). Sensors in both of the sectors create a 3×3 LSM after the grid partition and the neighborhood discovery. They next generate a TPM, which includes two high probabilities, i.e., 1, in each row and in each column. Consequently, this

changes the degrees of concurrent transmission opportunity and data collision probability. We will investigate and discern the effects of *K* and network partition on these two parameters in an analytical study next. We will also validate the analytical assessment by simulations.

So far, we described the steps of the adaptable probabilistic transmission in a DISN. To summarize briefly, at first sensors obtain the given information, e.g., application objective (EF, DF), location-aware functionality, and coverage, prior to deployment. These conditions are commonly accepted in most sensor networks. Next, the sensors are deployed into a field and automatically (locally) generate an appropriate TPM following the procedures of the APT. The whole process is self-organized and decentralized. Meanwhile, channel access is distributed.

6.3 TPM ANALYSIS AND EVALUATION

In the APT framework, we derive a TPM, in which, the probabilities that make up its elements are adaptable according to the sensor application. To evaluate the feasibility of a derived TPM for an application, we propose the following analytical metrics, i.e., data collision degree and concurrent transmission degree. These metrics provide us insight into the network performance and can be used to evaluate the application's objectives. We will show the feasibility of the metrics by following the analysis with simulations.

$$CD\ of\ TPM = \frac{\sum_{CollidedPair \in CG,\ t \in Ts} P(CollidedPair, t)}{Number\ of\ CollisionPairs\ in\ a\ Network} \tag{6-1}$$

$$BCD(t) = \frac{\sum_{i \in A\ set of\ Nodes\ of\ TPM} P(i, t)}{Number\ of\ Nodes\ in\ a\ Network} \tag{6-2}$$

$$BCD\ of\ TPM = \frac{\sum_{t \in TS} BCD(t)}{Number\ of\ Time\ Slots\ of\ TPM} \tag{6-3}$$

Equation (6-1) defines *Data Collision Degree* (CD) associated with a TPM. The probability of colliding transmissions depends on the probabilities that make up the elements of the TPM and the spatial relationships between sensors. We thus set the CD to be a cumulative probability that is normalized over the total number of colliding transmission pairs (the value of CD is therefore in the range of (0, 1).). A colliding pair represents transmissions of two different sources that are within 2-hops of one other and it belongs to a set of Collided Pair Groups (CG). Here *t* denotes a time slot and belongs to a set of Time Slots of a TPM (TS). Note that the CD is an *approximate metric* of potential occurrence of packet collisions in a network. Later, we will demonstrate that the CD metric provides a reasonable approximation for transmission reliability. In Appendix A we discuss the issue of the dependence of the CD on previous transmission attempts as in Chapter 4 (Section 4.4) and present additional analysis. In addition, Equations (6-2) and (6-3) represent the *Blind Concurrent Transmission Degree* (BCD) associated with a TPM. We capture the degree of concurrent transmissions possible by using the average transmission probability since the average transmission probability using a TPM corresponds to the amount of concurrent transmissions/senders. In other words, the BCD shows how enthusiastically sensors of the entire network intend to deliver their data regardless of the chance of *blind* concurrent transmissions, namely, assuming that collisions may happen between the concurrent transmissions.

With the CD and BCD metrics, we can analytically evaluate the TPMs based on different *K* parameters (i.e., different objectives). For the example that considers the topology in Figure 6-10 (a), taking into account the factors of network partition and *K*, we study two sets of TPMs that

are derived for the networks - with a single grid cell and with two grid cells. Figure 6-11 illustrates results of these metrics (straight lines represent TPMs with a single LSM/sector (SLS) and the dashed lines represent TPMs with two LSMs/sectors (TLS)). We also vary the *K* parameter between 0.1 and 10 to show different decay degrees of the probability impacting relative values of transmission probabilities in different TPM cells. From Figure 6-11, we make the following observations:

1. Effect of the blind concurrent transmission in a network with more grid cells is stronger no matter what value of *K* is used. It indicates that a network with multiple sectors indeed enhances the probability of concurrent data delivery, compared to a single sector network. In addition, the value of *K* linearly affects the average probability in the TPM so the blind concurrent degree follows this trend.
2. The negative effect of colliding transmissions is stronger in a network with multiple sectors when *K* is small. As *K* increases, the negative effect of colliding transmission in both the single sector and multiple sectors networks is mitigated. So the value of *K* is able to considerably change the occurrence of data collisions in a network.

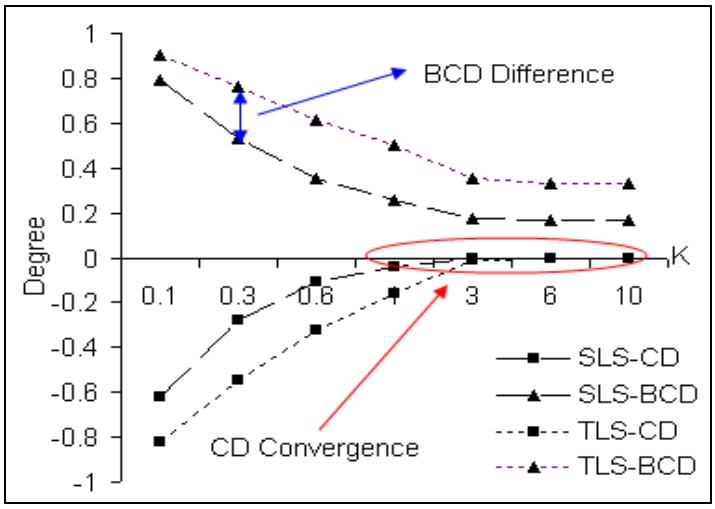

Figure 6-11 Analytical Evaluation with the Effects of the *K* parameter and the network partition

Next, we perform an extensive study of CD and BCD in a more complex network topology, a Random Dense Network. This network includes 20 nodes placed in a 63 × 63 m^2 flat area with a BS (see Figure 6-12 (a)). The average 2-hop neighborhood size in this topology is 12.5 nodes. This reflects a densely populated network with challenging hidden terminal problems and multi-hop data delivery to the BS. In addition, positions of the nodes in the topology are altered to introduce potential data collisions near intersections of grid cells. Three topologies, i.e., unfortunate network, average network (Figure 6-12 (a)), and fortunate network, are thus generated and evaluated here. The unfortunate network includes a high chance of conflicting transmissions near intersections of grid cells (i.e., sensors near the intersections have the same order of TPMs.) while the fortunate network represents the opposite situation.

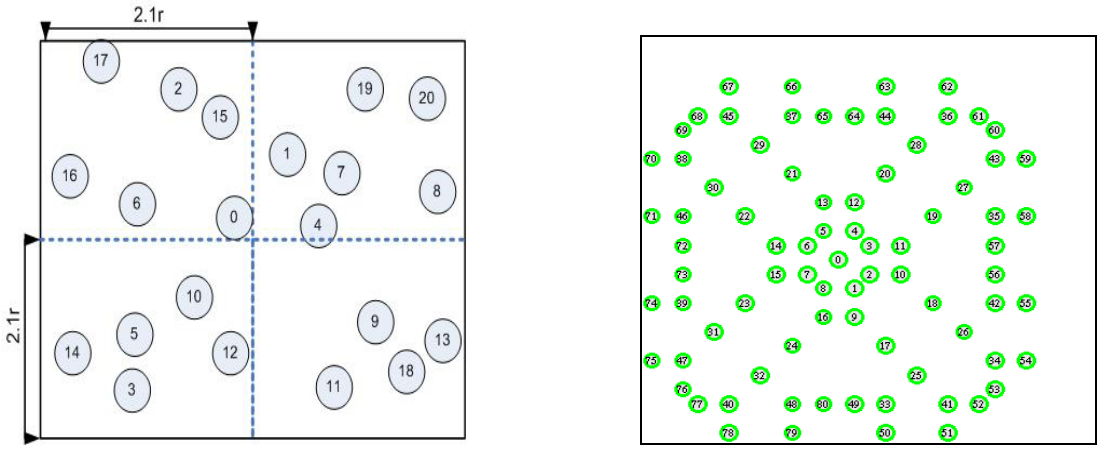

(a) (b)

Figure 6-12 (a) Random Dense Network (Average Network) (b) Large Dense Network

In Figure 6-13, results of CD vs. BCD of the random dense network are presented. The network is divided to 4 sectors using the grid partition. The *K* parameter is varied (i.e., set to 0.1, 0.3, 0.6, 1, 3, and 6) with the different topologies. We find that the results here reinforce the

previous observations of the simple network, namely, an increasing *K* parameter reduces CD and BCD. Meanwhile, the APT is almost not influenced by changes in network topology, i.e., fortunate, average and unfortunate networks, because it has taken into consideration the collision issue near intersections of grid cells. In addition, the TPM of the CPT protocol [85], Random Probabilities (RP), is assessed in Figure 6-13. It shows medium results for CD and BCD, which are optimized for neither metrics. Note that the distribution of the metrics follows a trend of Pareto points. With different *K* values, the trade-off between CD and BCD exists. We expect that such trade-offs will reflect on the network performance and test this hypothesis next by running simulation-based evaluations.

In summary, the analytical model points out that the method of network partition enhances the chance of concurrent transmissions while the *K* parameter affects the occurrence of data collision in a network. Therefore, our APT framework adopts the grid partition and the LS-based probability tuning satisfying the bi-objective with respect to the requirements of sensor applications in a DISN.

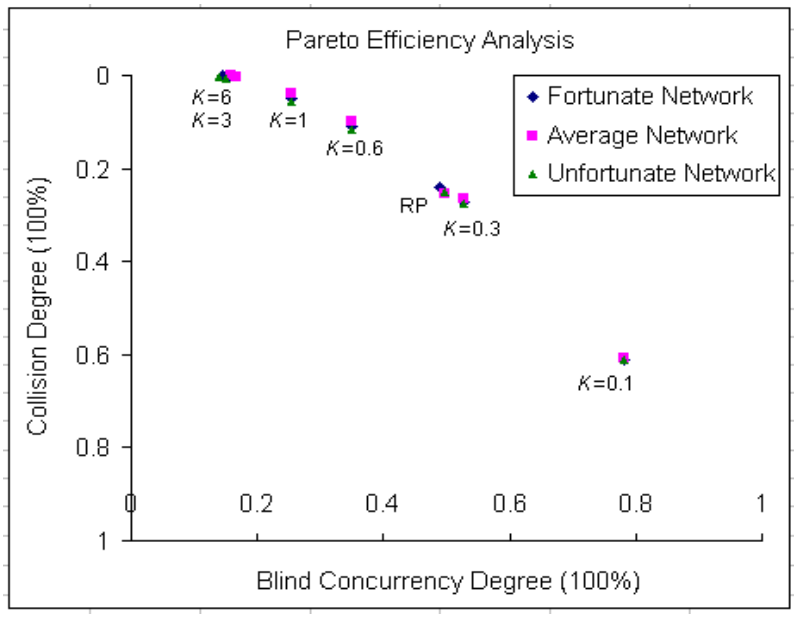

Figure 6-13 Analysis of the TPM in Random Dense Network

6.4 EXPERIMENTAL RESULTS

In this section we have following goals: 1) we verify the analysis in Section 6.3. 2) We test the APT in the large dense network. 3) We evaluate the overhead of APT.

6.4.1 Simulation Setup

We implemented the TPM in ns-2 [73] and evaluated transmission efficiency, overhead complexity, scalability, energy efficiency, and average packet delay. We set the channel data rate to 250 Kbps and the sensor transmission range to 15 meters. The packet size is 70 bytes. Two network topologies are tested in simulation as shown in Figure 6-12. The first topology (Figure 6-12 (a)) is the random dense network as described earlier. The second topology (Figure 6-12 (b)) is a large tree network that includes 80 nodes in a 126 × 126 m^2 flat area with a BS. The

system model as in Section 6.1 is followed here. We assume that each sensor always has pending data ready for transmission, so the simulations represent a data intensive traffic scenario. For the radio channel propagation model, a two-ray path loss model was chosen and fading was not considered in the simulations. We applied the energy cost model from [74], where the transmit power is 17 mW, receive power is 35 mW and idle power is 0.71 mW. The reported simulation results are averaged over 30 runs with a 95% confidence interval presented by error bars. Simulations run for 400 seconds of simulation time.

We evaluate the network performance through these metrics:

Throughput: Number of the successful packets to reach the BS.

Packet success rate: Ratio of the number of transmitted packets that reach their next hop successfully to the total number of transmitted packets from all nodes. Loss rate = 1 – Packet success rate.

Average number of control messages per sensor: Number of transmitted control messages per sensor per TPM generation.

Response time of packets: Average number of time slots for a packet to successfully reach the BS.

Energy consumption of a successfully received packet at BS (ECSP): A measure of the energy efficiency that is defined as the total energy consumed in the network per second divided by the number of packets received at the BS.

6.4.2 Analysis of Results

A. Validation of Analysis

Previous analysis for the simple network and the random dense network is evaluated here. First, we test the effect of *K* (i.e., adaptable transmission) and the network partition in the simple network. We assume that every time slot has pending data for transmission. As the value of *K* increases, the average probability of elements in the TPM decreases. The number of transmitted packets in a network thus is decreased according to the results shown in Figure 6-14 (a). This demonstrates that the *K* parameter strongly affects the aggressiveness of sensors' transmission. In addition, we note that a sectored network (TLS) always delivers more packets than a single sector network (SLS). So partitioning a network indeed augments the blind concurrent data transmission.

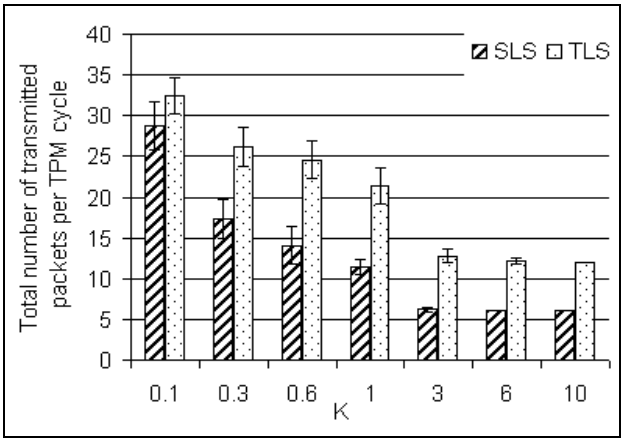

(a)

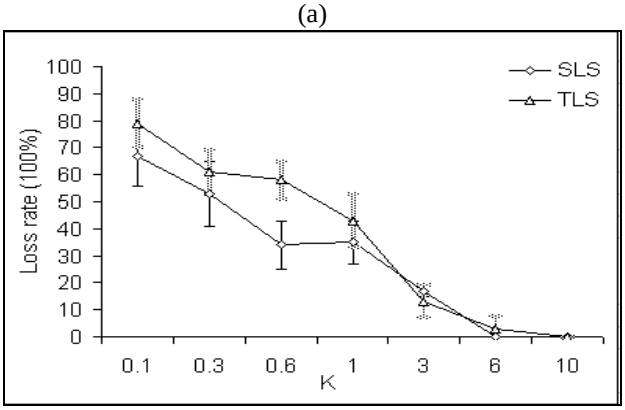

(b)

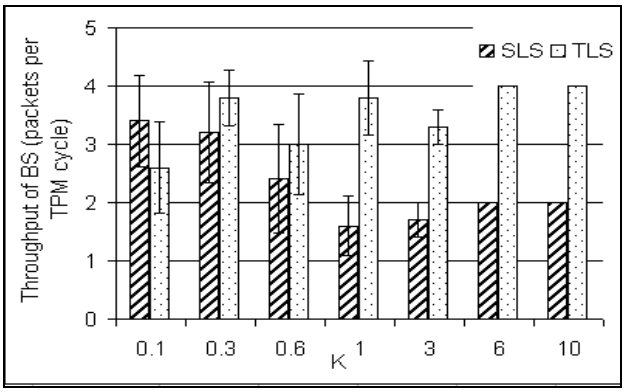

(c)

Figure 6-14 Simulation Evaluation of the Simple Network Topology: (a) Number of Transmitted Packets (b) Loss Rate (c) Throughput at BS

Figure 6-14 (b) shows the packet loss rates with different *K* values. It indicates that a larger *K* promotes better packet delivery reliability no matter if a network is sectored or not. When the loss rate is low, it not only translates into reliable data delivery but also shows improved energy efficiency because of energy saving from fewer lost packets.

Figure 6-14 (c) presents the performance of throughput. In most cases, the throughput of the two sector network is higher than that of the single sector network, so the network partition method better supports a network with a higher traffic load. In conjunction with a large *K*, the throughput of the two sector network increases even more. The throughput of the single sector network presents a concave result: When *K* is small, aggressive transmissions result in a higher throughput, but many packets are lost. As *K* increases, the aggressiveness is not sufficient to compensate for the lost packets initially. As *K* increases even further, packet losses due to collisions reduce increasing the throughput at the BS. Note that the throughput of a single sector network outperforms that of a two sector network while *K* is 0.1. This phenomenon is contributed to by a higher loss rate in the sectored network when *K* is small.

Next, we evaluate the network performance of APT in the random dense network. We perform the simulations with various network loads with data generation rates of 1, 2, and 4 packets/second/node. The simulation limits the loads to 4 packets/second since we observed the limitation (bottleneck) of network utility with high loads in Sections 4.5 and 5.4. Such a trend is again shown in the following results (see Figure 6-16). The data rate of 4 packets/second is thus adequate to mimic the situation of the performance bottleneck in DISNs. Figure 6-15 (a) shows the packet success rate with different *K* configurations and traffic loads. Here, the effect of *K* is identical to that of the simple network, namely, an increasing *K* improves transmission reliability of a network. As the traffic load of the network increases, the performance of packet success rate is almost not affected. Figure 6-15 (b) shows the trade-off between energy and delay while using the APT. As the *K* parameter is tuned, energy efficiency of the whole network is improved but the network pays a considerable price in packet delay, and vice versa. Energy efficiency is improved with a large *K* parameter because failed transmissions are reduced in the network. Meanwhile, an efficient TPM that reduces colliding transmission using large *K* results in increased packet delay. It is because the local TPM runs like a serial transmission schedule (BCD is reduced). As *K* becomes smaller, the packet response time also gets shorter since more packets are set to transmit early increasing the chance of a packet to reach the BS earlier. However, only small numbers of the transmitted packets reach the BS. A lot of the energy resource is wasted in collided packets. This finding demonstrates the applicability of using *K* to tune the bi-objective: energy and delay. In addition, the effect of traffic load is investigated here. Figure 6-15 (b) shows that traffic load has a small effect in the delay performance but considerable effect in the energy performance (because more data delivery reduces the average ECSP).

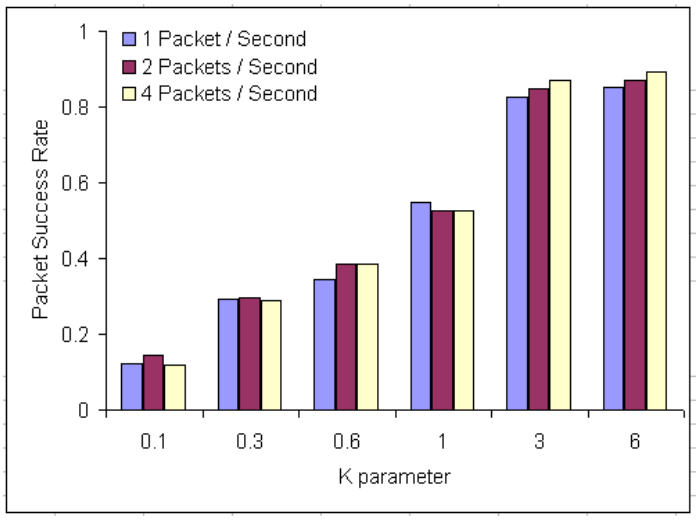

(a)

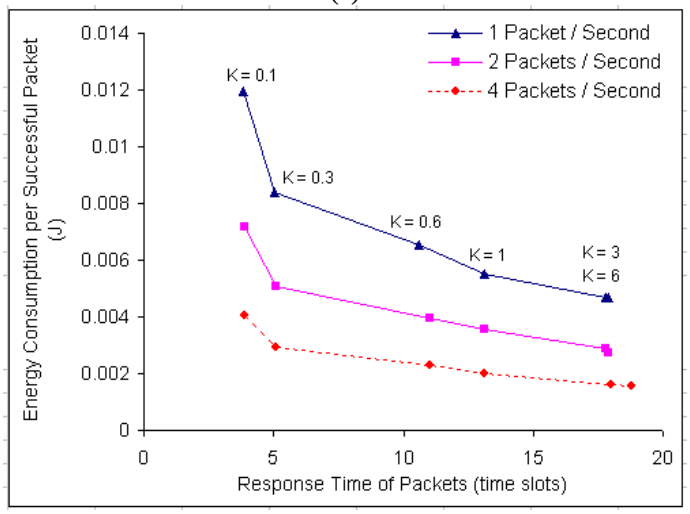

(b)

Figure 6-15 Simulation Evaluation of the Random Dense Network Topology: (a) Packet Success Rate (b) Trade-off between Energy and Delay

So far, the simulations have tested the network performance in simple and random dense networks. The results closely match the predictions from analysis. In particular, CD is proved to be an effective metric for transmission efficiency (see Figure 6-11, Figure 6-13, Figure 6-14 (b), Figure 6-15 (a)), which helps us estimate the energy efficiency in a DISN (Good transmission reliability conserves energy as shown in Figure 6-15 (b).). BCD is a metric that estimates the efficient bandwidth usage of sensors' transmission in a network (see Figure 6-11, Figure 6-13,

Figure 6-14 (a)). We note that change in *K* collaboratively transforms BCD and response time of packets (see Figure 6-15 (b)) so there is a decisive link between them. Overall, the analytical model approximately captures the essence of the network performance. Meanwhile, the simulation results show that an adaptable *K* parameter in APT is useful to meet the bi-objective in a DISN.

B. Validation of the Large Dense Network

We compare network performance of the APT in the large dense network (80 nodes) where average node density and degree of multi-hop transmission are higher than that of the random dense network. Figure 6-16 (a) displays the packet success rate. The results shares trends that are similar to those in the random dense network (Figure 6-15 (a)) except for slightly lower packet success rates. Such degradation is caused by a more complex network topology. In particular, the performance degradation with a small *K* is more severe since the degrading effect from unreliable probabilistic transmission and node interference is increased in the course of longer multi-hop delivery. Packet success rate becomes stable when *K* is 3 or larger. It is the outcome of reliable serial transmission schedules from local TPMs. Figure 6-16 (b) shows the trade-off between energy and delay in the large dense network. In general, the trend of this result is similar to that of the random dense network (Figure 6-15 (b)), namely, the tuning parameter, *K*, shapes the network performance. As the traffic load increases (e.g., 2 and 4 packets/second), variation of the ECSP is not as high as that of the random dense network because more nodes/packet are involved in sharing the energy cost, thus reducing the variation. In addition, ECSPs of the 2 packets/second generation rate and the 4 packets/second generation rate are approximately overlapping when *K* is 0.1, 0.3, 0.6, or 1. This result, where packet success rates are lower at 4 packets/second traffic load than at 2 packets/second traffic load causes a smaller

variation between their throughputs at the BS, thus reducing the difference in the ECSPs. Response time of packets is also considerably different from that of the random dense network. First, the average delay of packets is 2 or 3 times longer due to longer delivery paths. Next, at K = 3 or 6, the delay increases exponentially with a high traffic load, like 4 packets/second generation rate. This is contributed to by the limited channel capacity (250 kbps) and the bottleneck around the BS.

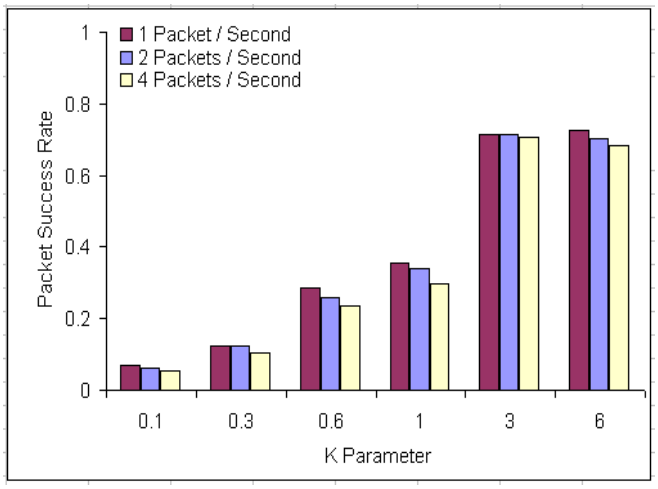

(a)

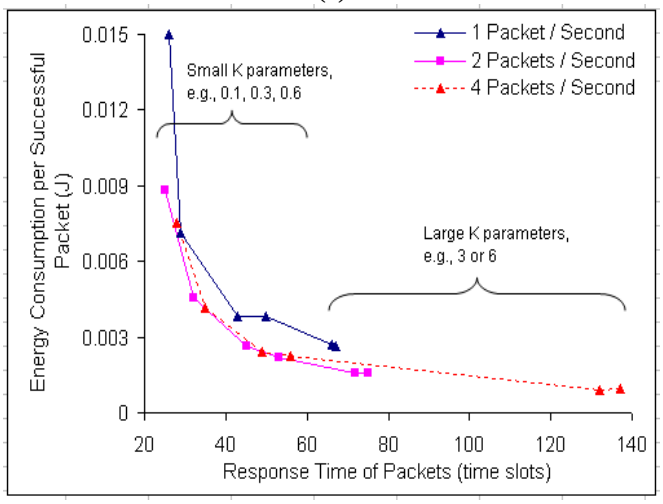

(b)

Figure 6-16 Simulation Evaluation of the Large Dense Network Topology: (a) Packet Success Rate (b) Trade-off between Energy and Delay

C. Overhead Evaluation

Some access control mechanisms may exchange control packets to establish channel access including APT. Such control packets hold no application data and consume energy and bandwidth resources, so we regard these packets as overhead. We applied reliable broadcast to exchange the control messages and explored the effect of network density on control overhead. We performed experiments with network topologies by varying the average number of two-hop neighborhoods from 0.5 to 11 nodes. The neighborhood size of the network is changed by varying the numbers of nodes from 20 to 160 within a 150×150 m^2 flat area. Figure 6-17 shows that control overhead with APT is almost independent of the network scale and node density because APT derives its TPM by inquiring local information in a sensor's grid cell and the computing complexity of APT is scalable. Such a procedure is similar to the GLASS protocol so their control overhead is acceptable and scalable. Overhead cost of dense networks is slightly higher than that of sparse networks because additional control messages are exchanged to mitigate increasing channel contention in congested areas.

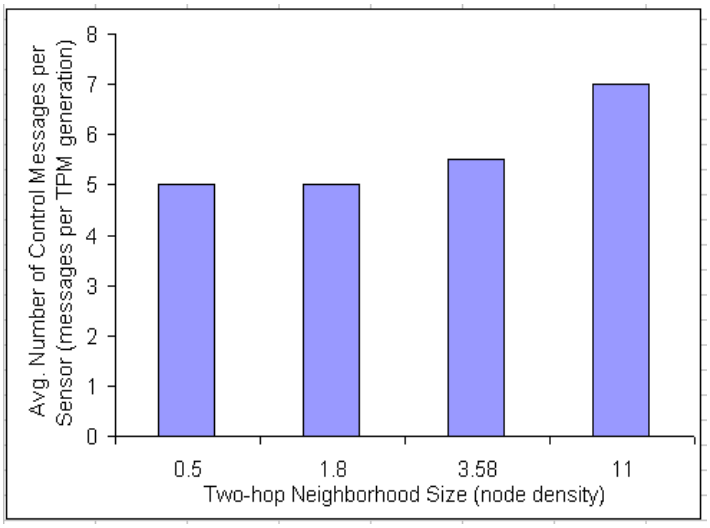

Figure 6-17 Control Overhead with Different Node Densities

D. Discussion

The APT framework has demonstrated potential for adaptable channel access that achieves Pareto optimality in our bi-objective problem. It adopts the heuristics of Latin Squares, virtual grid network, and probabilistic transmission tuning data. As a result, network objectives, e.g., energy and delay, are adjustable by controlling a tuning parameter, *K*, which is based on a given objective combination, (EF, DF), in every sensor. We use analysis and simulation to evaluate TPMs generated by the APT, in particular, with the metrics of transmission reliability, energy efficiency, and packet delay. The simulation results have proved the feasibility of the proposed analytical model while validating the benefits provide by the APT framework, such as adaptability, low overhead complexity, and scalability.

The APT framework is tested in various network topologies. Their results all illustrate a similar trend, Pareto front, between energy objective and latency objective, as the *K* parameter varies. When *K* is ether considerably large or considerably small, the results of all topologies shows optimal performances for the energy-oriented application or the delay-oriented application respectively. So, the design of adaptable transmission, based on *K*, provides an efficient way to facilitate the objective-based data transmission. CPT provides a middle of the road performance as expected and is a robust scheme.

Some networking conditions, e.g., bottleneck around the BS, bandwidth limitation, long multi-hop delivery, traffic load etc, present some challenges to the targeted performance objective as shown in Figure 6-16 (b). To address these concerns, we may add extra heuristics (e.g., load-balancing) into the APT. This will need more research efforts to complete and so we consider it as a part of the future work. If a system administrator intends to support more than two objectives in sensor applications, how does the APT respond to this? It is a common

question that needs to be answered. Maybe we utilize a multi-dimensional LSM for such question. Please refer this to Section 7.2. Overall, this chapter presents a preliminary study on how to tune probabilistic transmission to meet different performance objectives in a DISN. So far, we look at this as a bi-objective problem and run some experiments to validate the adaptable data transmission scheme. In order to fully understand its complexity, limitation and efficiency, more work is necessary.

6.5 CONCLUSION

This chapter takes a novel view of probabilistic transmission by considering it to be comprised of both Latin Squares feature and a virtual grid in data intensive wireless sensor networks. We developed a heuristic-based probabilistic transmission scheme ATP to tune channel access, meeting various demands in network performance (Energy vs. Delay). Meanwhile, the proposed framework consumed reasonable overhead. We also proposed an analytical model to assess the network performance. The significant benefits of APT are illustrated through extensive simulations.

7.0 CONCLUSION

There are performance deficiencies, like collisions, retransmissions, and excessive control messages, that hamper the deployment of Data Intensive Sensor Networks. To address this issue, this dissertation has examined the limitations and benefits of current approaches (random access and scheduling access) and proposed a suite of novel channel access schemes to mitigate concerns of existing protocols, like IEEE 802.15.4 CSMA/CA, DTA, and DRAND, in DISNs. In this chapter, the major contributions of this dissertation are summarized in Section 7.1 and possible future research directions are discussed in Section 7.2.

7.1 CONTRIBUTIONS

We have considered the problem of significant performance degradation issue in data intensive sensor networks. As we have reviewed in Chapter 2, current access protocols in the literature either do not support high bandwidth needs for data transmission with DIA, or incur considerable overhead in terms of control messages and computing complexity to setup scalable and distributed access for sensors, thus resulting in inapplicable network utility. To fill the holes of these protocols, we have applied the concept of probabilistic transmission and heuristic scheduling to manage data transmission of sensors in a network. Specifically, major contributions of this dissertation consist of the following:

1. This research is a comprehensive study of channel access management for DISNs. We first investigate and discern the quality of existing techniques and then propose a set of suitable access methods. Traditionally, channel access techniques of wireless sensor networks are classified into two approaches: random access and scheduling access. In order to evaluate feasibility of the existing approaches, we developed a simulation-based case study that performed comparison between the algebraic cross-layer optimization scheme DTA (scheduling access) and the IEEE 802.15.4 CSMA/CA (random access) for intensive data delivery in wireless sensor networks. We demonstrated that, in most cases, DTA considerably outperformed CSMA/CA. In particular, the percentage of transmitted packets reaching the sink node improves at least by 20% and the overall packet delay with DTA increases linearly unlike with CSMA/CA with corresponding increases in the network traffic load. Nevertheless, the scalability and complexity of deriving a DTA schedule in a large network remains a concern. Sensor mobility further aggravates this concern.
2. Take into consideration the issues of CSMA/CA and DTA, we have proposed a novel hybrid access approach that combines the advantages of both random access and scheduling access. The devised hybrid transmission schemes, CPT and NAPT, are decentralized and scalable, and based on random probabilistic access and a distributed scheduling algorithm using limited neighbor information. As a result, they mitigate the impact of performance degradation of high traffic load in sensor networks while maintaining minimal overhead. We devised an analytical model to characterize the performance of our hybrid access schemes and verify the analytical results using simulations. We also tested our protocols with various network topologies with

increasing traffic loads. The simulation results demonstrate the considerable utility of the CPT and NAPT protocols with minor overhead. In particular, our protocols over-perform the IEEE 802.15.4 CSMA/CA protocol in terms of transmission reliability, throughput and energy efficiency. NAPT compares favorably with DRAND in terms of low overhead cost and features high network utility. Some concerns undesirably come along with the hybrid access protocols. For example, the transmission performance of CPT is unreliable due to lack of intelligence for collision alleviation. NAPT also presents a small concern with conflicting transmissions, namely data delivery is not completely conflict-free. This is because of limited coordination among local sensors during setup of channel access. Note that we designed the hybrid access protocols to be light-weight and scalable, reducing the overhead, perhaps at the cost of some transmission reliability.

3. We next proposed a decentralized channel access technique with high utility. It fills the gaps of early hybrid access protocols while conserving their positive contributions. The devised protocol, GLASS, runs like a distributed access scheme that alleviates transmission collisions by applying a virtual grid in a network and adopting Latin Squares features to transmission schedules. The design of a virtual grid network spatially divides the sensors within collision range to avoid potential collisions. The Latin Squares function is used to facilitate the assignment of time slots for transmission among sensors within a grid cell, thus reducing the number of colliding transmissions further. We analytically proved the conflict-free transmission feature of GLASS and its high efficiency in saving overhead. A systematic evaluation using simulations is also conducted, and it considers the factors, such as traffic load,

network scale/density, and sensor mobility, in the simulations. We demonstrated acceptable transmission efficiency in DISNs. Furthermore, it efficiently handles the effect of changing topology with low overhead cost.

4. We have developed an extension of CPT to efficiently adjust the network performance and make the proposed channel access framework APT adaptable to different sensor application's requirements. Two performance objectives, energy and delay, were considered for tuning channel access. The ideas of a grid network, Latin Squares, and probabilistic access were employed to tune the channel access scheme. The Latin Square algorithm is used to locally tune transmission probabilities of sensors in the time domain while the design of a grid network eases management of sensor's scalability. The tuning process for the transmission probabilities results in different tradeoffs between data collisions and concurrency opportunities, or in other words, different tradeoffs between transmission efficiency, energy efficiency, and latency. The whole access process is light-weight, distributed, and scalable. We proposed an analytical model to capture the characteristics of the network performance and validated the analytical results using simulations. The benefits of APT are illustrated through extensive simulations, e.g., controllable energy and delay performance, acceptable overhead cost, and easy tuning process.

7.2 FUTURE WORK

This dissertation has addressed the challenges of a DISN and the issues of current access techniques by using techniques, e.g., neighborhood awareness, smart heuristics, and probabilistic

access, to facilitate the channel access management. Their results showed a graceful performance degradation as a traffic load increases. Meanwhile, the proposed protocols are scalable and light-weight. During the research, some topics were noticed for potential improvement, as described below.

We devised a distributed grid-based access scheduling scheme (GLASS) to enhance network utility in DISNs and also presented an idea of adaptable transmission (APT) to meet different performance objectives of sensor applications. The design of a virtual grid network is used in both of the GLASS and the APT. It was shown to be an effective and simple method to cluster local sensors, improving network scalability, but its operation depends on location-aware sensors. To avoid such assumption, we can apply clustering techniques [23] [24] [26] [93] to group local sensors, instead of using grid cells. The cluster approach enables sensors to select neighbors by building a local communication cluster. Afterward, the sensors run the processes of transmission frame assignment and time slots assignment according to GLASS. The difference between the original GLASS and this extension is on the methods of the cluster formation and the transmission frame assignment. Consequently, we can think of different degrees of trade-offs in control message overhead since increasing the complexity of clustering techniques or cluster coverage is an important factor to be considered and needs investigation. Note that the concept of clustering is not novel and already adopted in ad hoc routing research [23] [24]. We can try to extend existing clustering techniques for substituting the grid network in GLASS and APT protocols. Such a plan needs more effort and time to verify its feasibility. Thus, the topic of GLASS with distributed clustering is considered as a part of future work.

Another interesting topic is to further expand the study of APT. Open questions include the investigation of different combinations of bi-objectives in APT, expanding the selection of

APT's performance objectives beyond two choices, the potential of dynamic *K* parameters in sensors, and the comprehensive performance evaluation. So far, the APT study in this dissertation considers energy efficiency and delay efficiency as performance objectives. It will be interesting to learn if the same framework is applicable to a different set of bi-objectives, like throughput vs. energy or throughput vs. delay. In addition, some sensor networks support multiple objectives in their application profile; so it is possible that there are more two performance objectives that APT needs to tune. The current APT framework is restricted to handling two objectives only. We have to extend the APT in three areas: newly defined tuning parameters, generation of a multi-dimensional LSM, and a new probability tuning function to accommodate multiple objectives. In the existing APT work, all sensors calculate a uniform *K* parameter for tuning process, namely, the whole WSN works toward achieving a single objective. If we assume that nodes in the WSN support bi-objectives (i.e., different applications) simultaneously, we can allow any individual sensor to tune the *K* parameter based on its resource conditions, e.g., energy, and then perform sensor networking accordingly. For example, assuming that a sensor is originally configured to be delay-sensitive ($K < 1$), the sensor switches to be energy-conservative ($K > 1$) after the remaining energy of the sensor is below a defined threshold. This enables sensors to efficiently manage resources while executing their assigned tasks. Benefits of such approach include better resource management (i.e., consideration of sensor conditions), concurrent support for the bi-objectives, and extending lifetime of sensors while the concerns, such as utilization of dual channels and coverage of sensor networks, are raised. Finally, the current APT results are based on a preliminary investigation. There is room for further understanding of its benefits and limitations. For example, we can conduct a comparison study between the APT and other access protocols (DTA, DRAND, or IEEE

802.15.4). The effect of changing topology with APT is not discussed yet. We can add extra heuristics (e.g., load-balancing thresholds) to avoid an overloaded network. Overall, these gaps need more time and effort to complete and they will be considered as parts of future work.

In order to further validate the functionality of CPT, NAPT, GLASS, and APT beyond simulation, implementation of these schemes in real sensor networks is reasonable for evaluation of their performances on test-bed networks. Given the availability of SunSpot sensors and Mote sensors, which allows modifications in sensor's software, our schemes can be implemented. Promising results from investigation in real test-bed networks will confirm the benefits of the proposed schemes while any unforeseen results will offer a better understanding of the protocols and enable designers to make necessary modifications.

The wireless channel presents a time-varying characteristic, where, sensors observe different network conditions that can vary with time. In this study, the impact of such time-varying characteristic is not fully considered. Future work should investigate a method to capture good channel conditions improving the network utility in DISNs.

APPENDIX A

ANALYSIS FOR SUCCESSFUL TRANSMISSION OF PACKETS WITH APT

The design of data transmission with APT follows the probabilistic transmission based on the elements of a TPM. In APT, the transmission process adopts the retry policy of *Probabilistic Process* (PP) (see Figure 6-7). We recall that a sensor is permitted to run the PP up to *N* times in consecutive time slots (*N* is the size of local TPM) to generate a packet transmission, ensuring a fair chance of transmission for each packet. If the packet is correctly received by its destined node, the sending node will stay in idle mode and wait for next pending events (e.g., transmission and receipt). Otherwise, the sending node will notify upper layers about the unsuccessful delivery without re-transmitting the packet. There are no retransmissions if a packet collides in a time slot. Overall, the chance of a packet transmission in a sensor thus depends only on the probability values (elements of a TPM) and conditional probabilities between successive PPs in time domain. For example, given the TPM shown in Table A-1, *node 1* has a probability 0.4 to transmit a packet if the packet is ready for delivery in *time slot 1*. If the PP for *node 1* in *time slot 1* is not successful, the PP will be repeated again in *time slot 2* according to the retry policy of PP and the conditional probability of the transmission now is (1-0.4) × 0.3 = 0.18. Similarly, with a pending delivery of a packet from *node 1* in *time slot 2*, the probabilities of

transmission in *time slot 2* and the following time slot are 0.3 and 0.28 respectively (Shade of Table A-1 covers a cyclic TPM). The average probability of transmission for *node 1* in any time slot using this TPM is (0.4+0.18+0.3+0.28)/4 = 0.29. Therefore, we can calculate the amount of transmitted packets from a sensor, given the information related to the traffic load, e.g., data generation rate of a sensor.

Table A-1 TPM of Two Nodes Topology

	time slot 1	*time slot 2*	*time slot 3*	*time slot 4*
node 1	0.4	0.3	0.4	0.3
node 2	0.1	0.6	0.1	0.6

Next, take into consideration the discussion above and the radio connectivity among neighboring sensors, we can derive probabilities of conflict-free transmissions for sensors. Here, the definition of a conflict-free transmission complies with the concept of the two-hop graph coloring problem: given the two nodes topology, i.e., *node 1* and *node 2* within one hop of each other, transmission of *node 1* is not interfered by that of its neighbors if and only if *node 1* is transmitting while *node 2* and its one hop neighbors are not transmitting in the same time. Therefore, if both *node 1* and *node 2* have pending packets for delivery at *time slot 1*, the probability of successful transmission of *node 1* in *time slot 1* will be 0.4 × (1-0.1) = 0.36 while the probability of successful transmission of *node 1* in *time slot 2* will be (1-0.4) × 0.3 × [1-((1-0.1) × 0.6)] = 0.0828. In summary, this analysis has briefly illustrated the interaction between the conditional probabilities that need to be considered for analysis of successful transmissions. This analysis is more refined compared to the BCD and CD calculations. As part of future work, we

plan to derive a mathematical model, which can evaluate network utilities in terms of packet reliability, supported traffic capacity of sensors, and packet latency.

BIBLIOGRAPHY

[1] The MEMS and Nanotechnology Exchange. http://www.memsnet.org/

[2] N. Xu, S. Rangwala, K.K. Chintalapudi, D. Ganesan, A Broad, R Govindan, and D Estrin. "A wireless sensor network for structural monitoring". Proc. of the 2nd ACM Conference on SENSYS 2004.

[3] The Intel Research Sensor Nets / RFID. http://www.intel.com/research/exploratory/heterogeneous.htm/

[4] The IBM Zurich Research Laboratory - Sensor Networks Project. http://www.zurich.ibm.com/sys/communication/sensors.html/

[5] J. Cox, "Wireless sensor networks grabbing greater attention," NetworkWorld.com, 09/27/2004. http://www.networkworld.com/news/2004/092704sensors.html?page=1/

[6] S. Kuchinskas, "The future looks bright for M2M market," Internetnews.com, 05/10/2004. http://www.internetnews.com/wireless/article.php/3352021/

[7] FocalPoint Group, "M2M White paper: the growth of device connectivity," White Paper, 2003.

[8] Stephanie vL Henkel, "Tiny radio broadcasts from your insides," sensors, 03/01/2005. http://wireless.sensorsmag.com/sensorswireless/article/articleDetail.jsp?id=279765/

[9] S. Chatterjea, L.F.W. van Hoesel, P.J.M. Havinga, "AI-LMAC: An Adaptive, Information-centric and Lightweight MAC protocol for Wireless Sensor Networks," Proceedings of the DEST International Workshop on Signal Processing for Sensor Networks, 2004.

[10] IEEE 802.11 Working Group. Wireless LAN Medium Access Control (MAC) and Physical Layer (PHY) Specifications: Higher-Speed Physical Layer Extension in the 2.4 GHz Band, 1999.

[11] IEEE P802.15.4/D18, "Low Rate Wireless Personal Area Networks," draft std., Feb. 2003.

[12] Bluetooth Special Interest Group, "Specifications of the Bluetooth System, vol.1, v.1.0B 'Core' and vol.2 v1.0B 'Profiles'," December 1999.

[13] ANSI/IEEE Std. 802.3, "Carrier Sense Multiple Access with Collision Detection," 1985.

[14] C. Schurgers, O. Aberthorne, and M. Srivastava, "Modulation Scaling for Energy Aware Communication Systems," Proceedings of International Symposium on Low Power Electronics and Design, Aug. 2001.

[15] A. Wang, S. Cho, C. Sodini, and A. Chandrakasan, "Energy Efficient Modulation and MAC for Asymmetric RF Microsensor Systems," Proceedings of International Symposium on Low Power Electronics and Design, Aug. 2001.

[16] R.X. Gao and P. Hunerberg, "CDMA-based wireless data transmitter for embedded sensors," Proceedings of 18th IEEE Instrumentation and Measurement Technology Conference, volume 3, pp. 1778-1783, 2001.

[17] C. Chien, I. Elgorriaga and C. McConaghy, "Low-power direct sequence spread spectrum modem architecture for distributed wireless sensor networks," Proceedings of International Symposium on Low Power Electronics and Design, Aug. 2001.

[18] E. Johnson, H. Lam, L. Katafygiotis, J. Beck, "The Phase I IASC-ASCE Structural Health Monitoring Benchmark Problem using Simulated Data," ASCE Journal of Engineering Mechanics, 130(1), 2004.

[19] N. Xu, S. Rangwala, K.K. Chintalapudi, D. Ganesan, A. Broad, R. Govindan, and D. Estrin, "A wireless sensor network for structural monitoring," Proceedings of the 2nd ACM Conf. on SENSYS 2004.

[20] C. E. Jones, K. M. Sivalingam, P. Argrawal and J-C Chen, “A survey of energy efficient network protocols for wireless networks,” Wireless Network 7, pp. 343-358, 2001.

[21] C. Intanagonwiwat, R. Govindan, and D. Estrin, “Directed Diffusion: A scalable and robuts communication paradigm for sensor networks,” Proceedings of the MOBICOM 2000

[22] C. E. Perkings, Ad Hoc Networking, Addison-Wesley, 2001

[23] F. Ye, H. Luo, J. Cheng, S. Lu, and L. Zhang, “A TwoTier Data Dissemination Model for Largescale Wireless Sensor Networks, “ Proceedings of the MOBICOM, 2002

[24] W. R. Heinzelman, A. Chandrakasan, and H. Balakrishnan, “Energy-Efficient Communication Protocol for Wireless Microsensor Networks, “ Proceedings of the IEEE Hawaii International Conference on System Sciences, Hawaii, 2000

[25] S. Ikiz and V. Ogale, “Coordinated energy conservation for ad hoc networks,” Department of Electrical and Computer Engineering, University of Texas at Austin.

[26] J. C. Cano and P. Manzoni, “A low power protocol to broadcast real-time data traffic in a clustered ad hoc network,” Proceedings of the IEEE GLOBECOM, pp. 2916, 2001.

[27] I. Stojmenovic and X. Lin, “Loop-free Hybrid Single-Path/Flooding Routing Algorithms with Guaranteed Delivery for Wireless Networks,” IEEE Trans. ParallelDist. System, vol. 12, no. 10, 2001, pp. 1023–32.

[28] F. Kuhn, R. Wattenhofer, and A. Zollinger, “Worst-Case Optimal and Average-Case Efficient Geometric Ad Hoc Routing,” Proc. 4th ACM Int’l. Conf. Mobile Comp. and Net., 2003, pp. 267–78

[29] C. Siva Ram Murthy and B. S. Manoj, Ad Hoc Wireless Networks – Architectures and Protocols, Prentice Hall Communication Engineering Series, 2003, pp. 230.

[30] C. E. Jones, K. M. Sivalingam, P. Argrawal and J-C Chen, “A survey of energy efficient network protocols for wireless networks,” Wireless Network 7, pp. 343-358, 2001.

[31] M. Stemm and R. H. Katz, “Measuring and reducing energy consumption of network interfaces in hand-held devices,” IEICE Transactions on Communications, vol. E80-B, no. 8, pp. 1125-1131, Aug. 1997.

[32] L. M. Feeney and M. Nilsson, “Investigating the energy consumption of a wireless network interface in an ad hoc network environment,” Proceedings of the IEEE INFOCOM, pp. 1548, 2001

[33] R. Kravets and P. Krishnan, “Power management techniques for mobile communication,” Proceedings of the ACM International Conference on Mobile Computing and Networking, Dallas, TX, 1998.

[34] M. J. Lee and J. Zheng, “Will IEEE 802.15.4 Make Ubiquitous Networking a Reality? A Discussion on a Potential Low Power, Low Bit Rate Std,” IEEE Communication Magazine, June 2004.

[35] I. F. Akyildiz, W. Su, Y. Sankarasubramaniam, E. Cayirci, Wireless Sensor Networks: a survey, Computer Networks, Elsevier Science, vol. 38, no. 4, 2002, pp. 393-422.

[36] V. Zang, M. Lombardi, L. Nelson, A. Novick, “Time and Frequency Measurements Using the Global Positioning System,” The International Journal of Metrology, September 2001.

[37] C. Coutras, S. Gupta, and N. B. Shroff, “Scheduling of real-time traffic in IEEE 802.11 Wireless LANs,” Wireless Networks. Vol.6, no.6, p. 457 2000.

[38] Wei Ye, John Heidemann, and Deborah Estrin, “An energy-efficient MAC protocol fro wireless sensor network,” IEEE INFOCOM, 2002.

[39] Juan-Carlos Cano and Pietro Manzoni, “Evaluating the energy-consumption reduction in a MANET by dynamically switching-off network interfaces,” IEEE, 2001.

[40] S. Singh and C. S. Raghavendra, “PAMAS – Power aware multi-access protocol with signaling for ad hoc networks,” Computer Communication Review 28(3), 1998.

[41] M. Liu and M. T. Liu, “A power-saving scheduling for IEEE 802.11 mobile ad hoc network,” Proceedings of the international conference on computer networks and mobile computing (ICCNMC’03), 2003.

[42] E-S Jung and N. H. Vaidya, “An Energy efficient MAC protocol for wireless LAN,” IEEE INFOCOM, 2002.

[43] C. Schurgers, V. Tsiatsis, S. Ganeriwal, and M. Srivastava, “Topology Management for Sensor Networks: Exploiting Latency and Density,” In ACM MobiHoc June 2002.

[44] N. Vaidya, M. Miller, "A MAC Protocol to Reduce Sensor Network Energy Consumption Using a Wakeup Radio," IEEE Trans. Mobile Computing, vol.4, no. 3, May/June 2005.

[45] H. Yin, H, Liu, "Distributed rate adaptive packet access (DRAPA) for ulticell wireless networks," IEEE Trans. Wireless Commun., vol.3, no.2, pp. 432-440, 2004/03.

[46] J. Sarker and S. Halme, "Auto-controlled algorithm for slotted ALOHA," IEEE Proc. Commun, Val. 150, No.1. February, 2003.

[47] H. Zhang, H. Shen and H. Kan, "Distributed Tuning Attempt Probability for Data Gathering in Random Access Wireless Sensor Networks," Proceedings of the 20th International Conference on Advanced Information Networking and Applications (AINA'06), 2006.

[48] A. Karnik and A. Kumar, "Distributed Optimal Self-Organization in a Cass of Wireless Sensor Networks," Proceedings of the IEEE INFOCOM 2004.

[49] K. M. Sivalingam, J-C Chen, P. Agrawal and M. B. Srivastava, "Design and analysis of low power access protocols for wireless and mobile ATM," Wireless Network 6, pp. 73-87, 2000.

[50] L.F.W. van Hoesel and P.J.M. Havinga, "A lightweight medium access protocol (LMAC) for wireless sensor networks: Reducing Preamble Transmissions and Transceiver State Switches," First International Conference on Networked Sensing Systems, Tokyo, 2004.

[51] S. Chatterjea, L.F.W. van Hoesel, P.J.M. Havinga, "AI-LMAC: An Adaptive, Information-centric and Lightweight MAC protocol for Wireless Sensor Networks," Proceedings of the DEST International Workshop on Signal Processing for Sensor Networks, 2004.

[52] M.H. Ammar and D.S. Stevens, "A Distributed TDMA Rescheduling Procedures for Mobile Packet Radio Networks," Proceedings of IEEE International Conference on Communications (ICC), pp. 1609-1613, Denver, CO, June 1991.

[53] F.N. Ali, P.K. Appani, J.L. Hammond, V.V. Mehta, D.L. Noneaker, and H.B. Russell, "Distributed and Adaptive TDMA Algorithms for Multiple-Hop Mobile Networks," Proceedings of MILCOM, 2002.

[54] N. Trigoni, Y. Yao, A. Demers, and J Gehrke. Wave Scheduling: Energy-efficient data dissemination for sensor networks, Proceedings of the Data Management for Sensor Networks (DMSN), 2004.

[55] S. Madden, M.J. Franklin, J.M. Hellerstein, and W. Hong. The design of an acquisitional query processor for sensor networks. Proceedings of the ACM SIGMOD 2003.

[56] S. Madden, M.J. Franklin, J.M. Hellerstein, and W. Hong. TAG: A Tiny Aggregation service for Ad-hoc sensor networks, OSDI 2002.

[57] Y. Yao and J. Gehrke. Query Processing in Sensor Networks. In Conference on Innovative Data Systems Research (CIDR) 2003.

[58] Yu-Chee Tseng, Chih-Shun Hsu and Ten-Yueng Hsieh, "Power-saving protocols for IEEE 802.11-based multi-hops ad hoc networks," Proceedings of the IEEE INFOCOM, 2002.

[59] R. Zheng, J. C. Hou and L. Sha, "Asynchronous wakeup for ad hoc networks," Proceedings of the Mobicom, Annapolis, Maryland, USA, 2003.

[60] H. Garcia-Molina and D. Barbara, "How to assign votes in a distributed systems," Journal of the ACM, vol. 32, pp. 841-860, Oct. 1985.

[61] I. Anderson, "Combinatorial design and Tournaments," chapter 2., Oxford University Press, 1998.

[62] V. Zadorozhny, P. Chrysanthis, P. Krishnamurthy, "A Framework for Extending the Synergy between MAC Layer and Query Optimization in Sensor Networks," Proceedings of the DMSN, 2004.

[63] V. Zadorozhny, D. Sharma, P. Krishnamurthy, A. Labrinidis. "Tuning query performance in sensor databases," Proceedings of the MDM, 2005.

[64] B.P. Crow, I. Widjaja, L.G. Kim and P.T. Sakai, "IEEE 802.11 Wireless Local Area Networks," IEEE Communications Magazine, Vol. 35, No. 9, p.p. 116-126, September 1997.

[65] V. Zadorozhny, D. Sharma, P. Chrysanthis, A. Labrinidis. 2005. "Data Transmission Algebra for Collision-Aware Scheduling in Sensor Networks," In L.Kalinichenko (ed.) Formal Methods in Compositional infrastructures of Heterogeneous Distributed Information Systems, Russian Academy of Science Publ., 2005.

[66] S.Nahar, S. Sahini, and E.Shragowitz. 1986. "Simulated annealing and combinatorial optimization," 23rd Design Automaton Conference, pp. 293-299, 1986.

[67] Y.E. Ioannidis, Y.Kang. "Randomized algorithms for optimizing large join queries," ACM SIGMOD 1990.

[68] S.Kirkpatrick, C.D. Gellatt, M.P. Vecchi Jr. "Optimization by simulated annealing," In Science, May 1983.

[69] The CMU Monarch Project. The CMU Monarch Project's Wireless and Mobility Extensions to NS, 1998.

[70] A. Boukerche, R. Werner, N. Pazzi and R. Araujo, "A Fast and Reliable Protocol for Wireless Sensor Networks in Critical Conditions Monitoring Applications," MSWiM'2004, Venezia, Italy.

[71] H. Zhang, H. Shen, "Reliability-latency Tradeoffs for Data Gathering in Random-access Wireless Sensor Networks," GCC2005, China.

[72] A. Arora and Hongwei Zheng. "Reliable Bursty Converge-cast in Wireless Sensor Networks." MobiHoc'05, May, 2005.

[73] ns-2 --- The Network Simulator, http://www.isi.edu/nsnam/ns, 2006.

[74] B. Bougard, F. Catthoor, D. Daly, A. Chandrakasan, and W. Dehaene, "Energy Efficiency of the IEEE 802.15.4 Standard in Dense Wireless Microsensor Network: Modeling and Improvement Perspectives," Proceedings of the conference on Design, Automation and Test in Europe, 2005.

[75] Charles F. Laywine and Gary L. Mullen, Discrete Mathematics Using Latin Squares, John Wiley & Sons, 1998.

[76] S.M. Cherry, "The Wireless Last Mile," IEEE Spectrum, Vol. 40, No. 9, p.p. 18-22, Sep. 2003.

[77] G. J. Pottie and W.J. Kaiser, "Wireless integrated network sensors," Communications of the ACM, Vol. 43, No. 5, p.p. 51-58, May 2000.

[78] N. Bulusu, J. Heideann and D. Estrin, "GPS-less low-cost outdoor localization for very small devices," IEEE Personal Communications, Vol. 7, No. 5, p.p. 28-34, Oct. 2000.

[79] Y. E. Sagduyu and A. Ephremides, "The Problem of Medium Access Control in Wireless Sensor Networks," IEEE Wireless Communications Journal, Dec. 2004.

[80] I. Rhee, A. Warrier, J. Min and L. Xu, "DRAND: Distributed Randomized TDMA Scheduling for Wireless Ad Hoc Networks," Proceedings of MobiHoc 2006, Florence, Italy.

[81] G. Zhou, T. He, S. Krishnamurthy, and J. A. StanKovic, "Impact of radio irregularity on wireless sensor networks," Proceedings of MobiSys 2004, New York, USA.

[82] I. Rhee, A. Warrier, M. Aia, and J. Min, "Z-MAC: a Hybrid MAC for Wireless Sensor Networks," Proc. ACM SenSys, November 2005.

[83] D. Sharma, V. Zadorozhny, and P. Chrysanthis, "Timely Data Delivery in Sensor Networks using Whirlpool," Proceedings of the 2nd International VLDB Workshop on Data Management for Sensor Networks, Trondheim, Norway, 2005.

[84] C-k Lin, D. Sharma, V. Zadorozhny, and P. Krishnamurthy, "Efficient Data Delivery in Wireless Sensor Networks: Algebraic Cross-layer Optimization Vs. CSMA/CA," International Journal on Ad hoc and Sensor Wireless Networks, Vol. 4, No. 1-2, pp. 149-174, 2007.

[85] C-k Lin, V. Zadorozhny, and P. Krishnamurthy, "Efficient Hybrid Channel Access for Data Intensive Sensor Networks," the 3rd IEEE Workshop on Heterogeneous Wireless Networks (HWISE) in conjunction with AINA, 2007.

[86] C-k Lin, V. Zadorozhny, and P. Krishnamurthy, "Grid-based Access Scheduling for Mobile Data Intensive Sensor Networks," the 9th International Conference on Mobile Data Management (MDM), 2008.

[87] J. V. Bradley, "Complete counterbalancing of immediate sequential effects in a Latin square design," Journal of the American Statistical Association, Vol. 53, No. 284, December 1958.

[88] Y. Xu, J. Heidemann and D. Estrin, "Geography-informed energy conservation for ad hoc routing", Proceedings of the 7th ACM/IEEE International Conference on Mobile Computing and Networking (ACM Mobicom), Rome, Italy, 2001.

[89] F. Kuhn, R. Wattenhofer and A. Zollinger, "Worst-case optimal and average-case efficient geometric ad-hoc routing", Proceedings of the 4th ACM International Symposium on Mobile ad hoc networking & computing, Annapoils, USA, 2003.

[90] T. Herman and S. A. Tixeuil, “A distributed TDMA slot assignment algorithm for wireless sensor networks”, Proceedings of the Workshop on Algorithmic Aspect of Wireless Sensor Networks (AlgoSensors), pp. 45-58, 2004.

[91] L. Doherty, K. S. J. Pister, and L. E. Ghaoui, “Convex position estimation in wireless sensor networks”, Proceedings of the IEEE INFOCOM, pp. 1655-1663, Alaska, 2001.

[92] K. Miettinen, Nonlinear Multiobjective Optimization, Kluwer Academic Publisher, 1999.

[93] O. Younis and S. Fahmy, “Distributed clustering in ad-hoc sensor networks: A hybrid, energy-efficient approach”, Proceedings of the INFOCOM, 2004.

[94] Theodore S. Rappaport, Wireless Communications: Principles and Practice, Prentice Hall, 1996.